Norwegian University of Life Sciences

Master's Thesis 2019 60 ECTS
Faculty of Chemistry, Biotechnology and Food science.

YthA - a lone ranger or team player in the cell envelope stress response of *Lactococcus lactis* IL1403?

Pelle Sandhaug Mikkelsen
Master of Science - Molecular Microbiology

Acknowledgements

The work in this master`s thesis was conducted at the Laboratory for Microbial Gene Technology at the Norwegian University of Life Sciences in Ås.

I am very thankful to my supervisors Prof. Dzung B. Diep and Associate Prof. Morten Kjos, not only for sharing their vast knowledge and technical experience, but also for their continued encouragement and support throughout the year.

I would also like to direct a special thanks to Dr. Beatriz Martínez and Esther Sánchez-Llana at IPLA in Spain, Dr. Saulius Kulakauskas and Christine Péchoux at INRA in France and Dr. Torstein Tengs at NMBU for their collaboration on this project and for sharing their knowledge and results.

To the rest of my colleagues at the Laboratory for Microbial Gene Technology, thank you for making this year such a pleasant one, and a special thanks to Amanda Morken Andersen and May Britt Hovet for their positive attitude and all their help.

I thank my dear family for their ongoing support!
Lastly, I want to thank Kristina Severine Stenløkk and the rest of my fellow students at the Norwegian University of Life Sciences for these past five years.
They have been truly enjoyable!

13.05.2019
Ås

Pelle Mikkelsen

Abstract

Considering the increasing problem of antibiotic-resistant pathogens emerging world-wide, research into novel antimicrobial substances that can become clinically relevant is now of the utmost importance. The small antimicrobial peptides known as bacteriocins, may represent a valid option. Lactic acid bacteria produce several well-known bacteriocins, including the newly discovered garvicin KS, whose mechanism of action is still not understood. Previous work has identified strains of *Lactococcus lactis* IL1403 that show increased resistance to garvicinKS, attributed to a mutation in the *pspC*-homologue *ythA*. Efforts to unravel the role of YthA in the garvicin KS mechanism of action, has led to the development a working model hypothesizing that YthA is involved in activation of the cell envelope stress regulatory system CesSR. In this thesis, previously isolated resistant mutants were characterized with respect to antimicrobial resistance and by microscopy approaches. To further understand this mechanism, quantitative PCR was used to relatively quantify expression levels of key genes in *ythA* mutants. Based on our results, we cannot conclude to what extent mutations in *ythA* affects the expression levels of CesSR. However, we show that stress in the form of sublethal doses of garvicin KS induces the expression of the *yth*-operon as well as genes associated with CesSR in wild type *L. lactis* IL1403. A positive correlation between dose and upregulation was also observed. This strongly suggests involvement of the *yth*-operon in the stress response mechanism of *L. lactis.* In further work, it will be necessary to confirm interactions between YthA and constituents of CesSR to better understand this stress response and how YthA is involved. The research presented here expand our knowledge of bacteriocins and their mechanisms, which is necessary for the development of novel, clinically relevant bacteriocins.

Sammendrag

Det stadig økende problemet med antibiotikaresistente patogener på verdensbasis nødvendiggjør forskning på nye antimikrobielle stoffer med potensiale for klinisk bruk. Et lovende alternativ er de små antimikrobielle peptidene produsert av bakterier, kjent som bakteriociner. Melkseyrebakterier produserer flere kjente bakteriociner, inkludert det nyoppdagede garvicin KS, som ikke enda har en kartlagt virkemekanisme. Tidligere arbeid har identifisert stammer av *Lactococcus lactis* IL1403 med økt resistens mot dette bakteriocinet, som en følge av mutasjon i *pspC*-homologen *ythA*. Arbeidet med å forstå hvilken rolle YthA har i resistensmekanismen mot garvicin KS, har resultert i en hypotese om at YthA aktiverer *cell envelope stress response system*, CesSR. Resistente mutant-stammer ble karakterisert med hensyn på resistens mot ulike antimikrobielle forbindelser og ved mikroskopi. For å forstå denne mekanismen ytterligere ble kvantitativ PCR brukt til å relativt kvantifisere ekspresjonsnivåer av gener forbundet med CesSR i *ythA*-mutanter. Basert på resultatene kan vi ikke med sikkerhet si at mutasjoner i *ythA* påvirker uttrykksnivåene av CesSR. Derimot fant vi at stress, i form av subletale doser av garvicin KS, induserer ekspresjonen av *yth*-operonet, samt gener som er assosiert med CesSR i villtype *L. lactis* IL1403. Det ble også observert en positiv korrelasjon mellom dose og oppregulering. Dette antyder en sammenheng mellom *yth*-operonet og CesSR i *L. lactis* IL1403 under stress. Det vil videre være nødvendig å bekrefte interaksjoner mellom YthA og bestanddelene i CesSR på proteinnivå for å få en bedre forståelse av denne stressresponsmeksnismen og av hvordan YthA er involvert. Denne type forskning er nødvendig for å forbedre våre kunnskaper om bakteriociner og deres mekanismer, som er nødvendig for utviklingen av klinisk relevante bakteriociner.

Table of contents

1 - Introduction

In 2014, the World Health Organization proclaimed the expanding problem of antibiotic resistant pathogens as one of the biggest challenges human society will face in the coming decades (World Health Organization 2014). As of 2015, it is estimated that approximately 33.000 people die every year in Europe alone, as a direct result of pathogens resistant to antibiotics (Cassini, Hogberg et al. 2019). The overuse and misuse of antibiotics, and the lack of novel antimicrobial pharmaceuticals being developed are the main reasons behind this increasing problem. Although development and approval of pharmaceuticals in general is a slow and expensive process, a solution is the development of novel antimicrobial substances that can supplement or replace conventional antibiotics. One potential candidate that has shown a lot of promise is the group of antimicrobial peptides produced by bacteria referred to as bacteriocins.

With a long history of safe use within the field of biotechnology, lactic acid bacteria (LAB) are producers of most of the bacteriocins currently implemented or under development. They are therefore uniquely positioned to further advance our understanding of the mechanisms associated with bacteriocins, and to accelerate the development of new applications. As it is estimated that upwards of 99 % of all bacteria produce at least one type of bacteriocin, these peptides represent a huge and diverse group of antimicrobials, with potentially lifesaving capabilities in the future (Riley and Wertz 2002).

1.1 - Bacteriocins and garvicin KS

Contrary to conventional antibiotics, which are synthesized through complex multi-enzyme pathways, bacteriocins are ribosomally synthesized antimicrobial peptides (Clardy, Fischbach et al. 2009, Hassan, Kjos et al. 2012). These peptides display extensive heterogeneity and as such, multiple classification schemes exist. An

agreement on which to use has been the source of much debate for many years (Tagg, Dajani et al. 1976, Oscariz and Pisabarro 2001), and although the classifications have changed, the most common approach is to classify bacteriocins based on mechanism of action, mode synthesis and size. Bacteriocins produced by the Gram-positive LAB are now classified in three different classes (Alvarez-Sieiro, Montalban-Lopez et al. 2016). Class I comprises small peptides with a high degree of post-transcriptional modification, and as such they are divided in subclasses according to what modified amino acids they contain. Class II consists of small and heat stable unmodified peptides, subdivided according to several criteria such as size, shape and whether it consists of one or more peptides. Class III is made up of larger and heat liable peptides, subdivided based on their ability to cause cellular lysis or not.

Lately, there has been a growing interest in bacteriocins, both as food preservatives and more recently as a possible means to combat antibiotic-resistant pathogens (Corr, Li et al. 2007, Yang, Lin et al. 2014). They are of high interest because they often show a high degree of specificity, and some are so specific as to only be effective against a single species (Miljkovic, Uzelac et al. 2016). This is often species closely related to the producer strain, as their role *in vivo* is thought to be part of a strategy to compete for nutrients in ecological niches. There also exist several wide spectrum bacteriocins, like the widely used nisin or the newly discovered garvicin KS (GarKS) (Ovchinnikov, Chi et al. 2016).

Bacteriocins are known for being efficient at killing or inhibiting growth at very low concentrations, in the pico- to nanomolar range, especially those that are highly specific (Hassan, Kjos et al. 2012, Mathur, Field et al. 2017). As opposed to conventional antibiotics, which often function as enzyme inhibitors, bacteriocins usually interact with specific receptors on the target cell membrane where they facilitate the formation of pores resulting in cytoplasmic leakage (Martinez, Bottiger et al. 2008, Ovchinnikov, Chi et al. 2016). These receptors have functions that are important to the cells survivability, for example involvement in key processes in the cells metabolism. An example is the mannose phosphotransferase system (Man-PTS), a four-domain membrane complex involved in the uptake of sugars in bacteria. Two of these domains, IIC and IID, are involved in the binding to several bacteriocins, such as the lactococcins, among others (Diep, Skaugen et al. 2007). Additionally, because

of this receptor mediated inhibition, and thus different mechanisms of action, common resistance mechanisms against conventional antibiotics will most likely be ineffective against bacteriocins, allowing the use of these against multi-resistant pathogens (Ghodhbane, Elaidi et al. 2015).

These receptors are also under a strong selective pressure to perform their normal function to maintain fitness, in addition to confer resistance to any bacteriocins the cell may be exposed to. This could explain why resistance against some bacteriocins are not often observed to evolve as quickly as for conventional antibiotics (Kumariya, Garsa et al. 2019). In fact, despite being used as a food preservative for several decades, no report on the development of resistance to nisin has been published for food related wild type strains (Perez, Zendo et al. 2014, Martinez, Alvarenga et al. 2016). Indeed, their proteinaceous nature means they can be degrades by proteases, resulting in non-existent traces in the environment. Combined with a fast acting mechanism at low concentrations, these factors may be beneficial to avoid the development of resistance, as no natural selection for resistance occurs in uncontrolled environments.

The loss of function due to proteolytic activity also introduces challenges with large scale utilization of novel bacteriocins in the preservation of food. In these cases it is important that inhibitory concentrations of the bacteriocin is maintained in the food substrate during the entire shelf life of the product (Silva, Silva et al. 2018). The clinical use of bacteriocins give rise to even more challenges, like maintaining optimum serum concentration of the antimicrobial peptide necessary for effective treatment in an environment hostile to foreign peptides (Levison and Levison 2009, Chikindas, Weeks et al. 2018). They are also often very expensive to produce, and for that reason a widely-used approach to this day is to inoculate foods with bacteriocin-producing strains of LAB. In recent years, the discovery of new bacteriocins, and the continually growing interest in them has warranted research towards potential applications in the future (Chikindas, Weeks et al. 2018). As of 2018, only two bacteriocins are commercially used as a preservative in the food industry. Pediocin PA1 (Microgard^{TM}) and nisin, commercially known as Nisaplin®, which is currently the most widely used and is approved in over 50 countries (Silva, Silva et al. 2018). Bacteriocins are used extensively in the dairy industry, as food-grade LAB are producers of several relevant

bacteriocins that have been well studied, like the aforementioned nisin that targets lipid II during PG synthesis (Egan, Field et al. 2016). The same level of research is needed for promising bacteriocins that have yet to become commercially relevant.

One such promising bacteriocin is the newly discovered GarKS that was isolated from a strain of *Lactococcus garvieae* (Ovchinnikov, Chi et al. 2016). This bacteriocin consists of three separate peptide chains, two chains of 34 and one of 32 amino acid residues, encoded by *gakABC* (protein sequences are included in the Appendix, section A.6). What makes this bacteriocin particularly interesting is the activity it displays against a wide selection of bacterial genera, several of which are important human pathogens, like *Bacillus, Enterococcus, Listeria, Staphylococcus* and *Streptococcus (Telke, Ovchinnikov et al. 2019).* Combined with the newly discovered method for large scale production, the potential for practical applications in the future is incontrovertible. This makes GarKS a high priority candidate for further study, as the disclosure of the hitherto unknown mechanism of action is necessary before any practical applications can be achieved.

1.2 - The model organism *L. lactis* IL1403 and general stress response mechanisms

L. lactis is a Gram-positive LAB that is commonly used in the dairy industry worldwide (Song, In et al. 2017). Humans have utilized LAB in the making of dairy products for centuries, and as such most of them are generally regarded as safe by the American Food and Drug Agency (Silva, Silva et al. 2018). In addition *L. lactis* has been used extensively in scientific research as a model organism, resulting in it being the first genetically modified organism that was used alive to treat human disease, where the human interleukin-10 gene was cloned into *L. lactis*, which was used to treat patients with Crohn´s disease (Braat, Rottiers et al. 2006). As previous work at the Laboratory for Microbial Gene Technology (LMG) has uncovered *L. lactis* IL1403 strains that are resistant to GarKS (Chi 2018), this presented us with an ideal model organism for the study of the mechanism of action for GarKS.

Gram-positive bacteria are characterized by a thick outer cell wall, which mainly consists of a three-dimensional heteropolymer known as peptidoglycan (PG). Chains of alternating *N*-acetylglucosaminyl-β-1 (NAG) and 4-*N*-acetylmuramoyl (NAM) residues are cross-linked by short peptide chains, and anchored to the lipid membrane by teichoic acids, to form what is called the PG sacculus (Vollmer, Blanot et al. 2008). This macromolecule surrounds the cell and provides protection against the high osmotic pressure differences between the cytoplasm and environment, as well as giving the cell a defined shape. As the outermost part of the cell, this protective barrier is heavily involved in sensory functions, and as such it is the target of several antimicrobial substances like the beta-lactams and muramidases (Ballal, Veiga et al. 2015). For example, the common beta-lactam penicillin G binds to penicillin binding proteins located within the PG sacculus. These proteins catalyse trans-peptide linkage formation between neighbouring NAG-NAM-chains at the C3 position of NAM residues. Binding of penicillin G inhibits the synthesis of PG by steric hindrance of the cross-linking process (Yocum, Rasmussen et al. 1980). The mammalian muramidase lysozyme is also active against the cell wall, but instead of hindering synthesis it catalyses the hydrolysis of 1,4-beta-glycosidic bonds between N-acetylmuramic acid and N-acetyl-D-glucosamine residues (Chapot-Chartier and Kulakauskas 2014).

As bacteria have little control over changes in their environment, they depend on their ability to sense and effectively respond to these changes. Bacteria can become stressed if they experience environmental changes such as sudden drought, extreme temperatures, unfavourable pH or salt concentrations, to mention a few. Signal pathways that activate the use of alternative sigma factors allow the bacteria to alter their expression pattern in response to these changes, resulting in the cell making appropriate modifications in response to the type of stress it is subjected to (Boor 2006). As such, the numerous and complex stress response mechanisms found in bacteria show a high degree of diversity and versatility (Guo and Gross 2014). Modification of the lipid composition in the cell membrane, expression of various shock proteins and upregulation of efflux pumps to combat high cytosolic concentrations of deleterious substances are just a few examples (Liu, Wang et al. 2016, Zhu and Dai 2018)

A common strategy for Gram-positive bacteria is to chemically modify their PG sacculus in several different ways (Yadav, Espaillat et al. 2018). One of these ways is the O-acetylation of NAM-residues, which increases the cells resistance to hydrolysis (Clarke and Dupont 1992). This O-acetylation is performed by the enzyme O-acetyltransferase, encoded by *oatA* in *L. lactis*. This enzyme catalyses the reaction in which an acetyl group is attached to the 6-carbon of N-acetylmuramic acid, forming N,6-O-diacetylmuramic acid, see **Figure 1.1** for a schematic overview. Homologues of this enzyme have been found in several different bacteria, such as *Listeria monocytogenes* (Aubry, Goulard et al. 2011) and *Staphylococcus aureus* (Bera, Herbert et al. 2005). In both these organisms, and several others, O-acetylation of PG is associated with an increase of resistance to the mammalian muramidase lysozyme. O-acetylation directly inhibits lysozyme, by steric hindrance of key residues near the catalytic site of the enzyme (Kikuchi, Yamamoto et al. 1988)

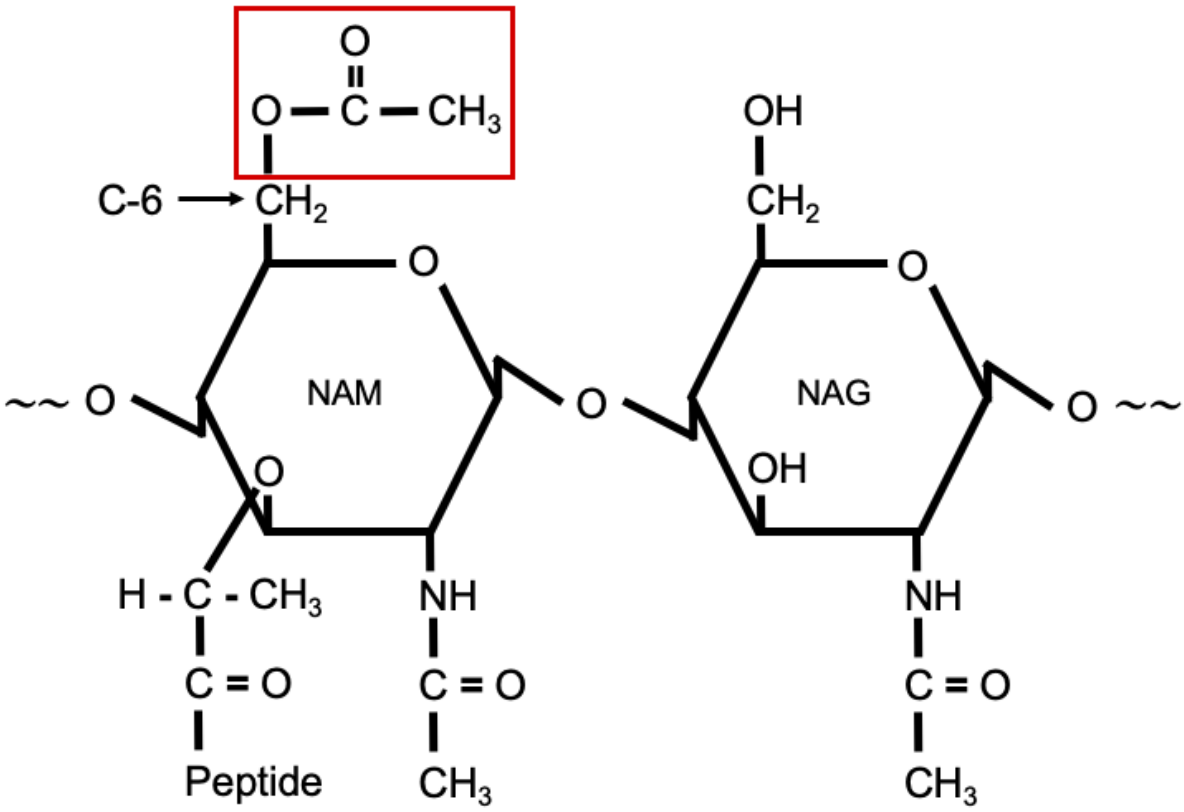

Figure 1.1: Illustration of the structure of the glycan portion of the repeating subunit of O-acetylated peptidoglycan. The presence of an acetyl moiety, marked with a red box, at C-6 of the N-acetylmuramic acid residue results in steric hindrance for the binding of lysozyme (Clarke and Dupont 1992, Pfeffer, Strating et al. 2006).

1.3 - The phage shock protein C and its homologue in *L. lactis*, YthA

As mentioned, the upregulation of different shock proteins is another common response in cells under stressful conditions. The phage shock response in bacteria has been extensively studied in organisms such as *Escherichia coli* and *Yersinia enterocolitica (Darwin 2007, Flores-Kim and Darwin 2012).* As part of the conserved extra cytosolic stress response mechanism in Gram-negative bacteria, the inner membrane bound phage shock protein C (PspC) is significantly upregulated in response to external stress factors such as extreme heat, ethanol or osmotic shock (Flores-Kim and Darwin 2012). This upregulation results in an elevated ability to maintain a structurally sound bacterial envelope, and an increased effort to maintain the proton motive force (Kleerebezem, Crielaard et al. 1996, Fallico, Ross et al. 2011). In *L. lactis* IL1403*, ythA* is a homologue to the *pspC* gene in the PspC family, which includes proteins with the presumed 60 amino acid residue PspC-domain thought to be a transcriptional regulator. As studies have shown that *yhtA* is upregulated in cells under stressful conditions, it raises the question of how YthA is involved in the stress response of *L. lactis* IL1403 (Wu, Liu et al. 2018).

YthA is involved in the mechanism of action associated with resistance against GarKS (Chi 2018). The initial hypothesis was that YthA functions as the receptor of GarKS, and that strains with a mutation in *ythA* are resistant to GarKS due to conformational changes in receptor. This was hypothesized to affect the binding affinity of GarKS to YthA, resulting in increased resistance. A similar mechanism has been established for the pediocin-like bacteriocin lactococcin A (LcnA) (Kjos, Nes et al. 2009). LcnA binds to the mannose phosphotransferase system and causes pore formations that result in the leakage of solutes from the cytoplasm and eventually cell death. It has been experimentally shown that immunity protein binds to Man-PTS forming a complex that hinders Lactococcin A from killing the cell (Kjos, Nes et al. 2011). This directly supports the initial hypothesis of Chi during his PhD (Chi 2018), however, presence of the hypothesized YthA-GarKS complex has not been clearly defined. Thus, a different model has been developed, and we propose that YthA is part of a regulatory network and that it is somehow involved in the cellular envelope stress response system (CesSR), outlined below.

1.4 - The cell envelope stress response system in *L. lactis*

A previous transcriptomic approach to study the effects of stress in *L. lactis* indicated an involvement of *ythA* (Roces, Campelo et al. 2009). Additionally, studies have shown that a two-component system (TCS), designated CesSR, is upregulated when cells are subjected to bacteriocins that inhibits cell wall synthesis (Martinez, Zomer et al. 2007). In prokaryotic cells, TCSs are well-established cellular response mechanism involved in stimulus response, where the two components usually consist of a membrane-bound histidine kinase with a sensory function, and a response regulator that facilitates a cellular response following its activation by the cognate histidine kinase. Homologous systems of CesSR have been found in *Bacillus subtilis*, where the TCS LiaSR senses and induces genes necessary to resist cell wall-active antibiotics (Mascher, Zimmer et al. 2004), and in *Staphylococcus aureus,* VraSR functions in a similar way (Kuroda, Kuroda et al. 2003). Efforts to unravel this stress response mechanism in *L. lactis* IL1403 have resulted in a collaboration between LMG, Dr. Beatriz Martínez at Instituto de Productos Lácteos de Asturias (IPLA) in Spain and Dr. Saulius Kulakauskas at Institut National de la Recherche Agronomique (INRA) in France. A hypothetical working model has been established that incorporates our collective knowledge regarding the CesSR and its regulation in *L. lactis* IL1403 thus far. Presented here are the established parts of CesSR, as well as our hypothesized function of YthA and how it interacts with other members of CesSR. A list of the established and hypothesized constituents of CesSR is given in **Table 1.1**.

Table 1.1: Overview of proteins associated with CesSR, and their function. DFU = domain of unknown function. *Amino acid is abbreviated aa.

Name	Locus tag	Size*	Function	Regulation	Homologues
YthA	Llmg2164	154 aa	PspC domain-containing protein	*yth*-operon is	PspC
YthB	Llmg2163	67 aa	DUF-containing protein	thought to be	
YthC	-	249 aa	DUF-containing protein	regulated by CesR	
SpxB	Llmg1155	123 aa	G-protein associated signal transduction	CesR	
FtsH	Llmg0021	661 aa	ATP-dependent zinc metalloprotease		
OatA	Llmg2391	605 aa	Acetyltransferase	SpxB	
CesS	Llmg1649	332 aa	Sensor histidine kinase	CesR	BarA
CesR	Llmg1648	209 aa	DNA-binding response regulator	CesR	CitB, NarL

CesS is the histidine kinase in the TCS CesSR, and as such it functions to activate the regulator, CesR, by phosphorylation (Bhate, Molnar et al. 2015). YthA and CesS are both integral membrane proteins, with one and two transmembrane domains respectively, that both somehow may be involved in the sensory function of the cell when it comes to stress. We hypothesize that YthA, when fully functional, interacts with CesS and thereby hindering the phosphorylation and subsequent activation of CesR from being carried out. In the case of non-functional YthA, or if the cell is indeed under stress, the YthA-CesS-complex disassociates by an unknown mechanism. As the inner membrane bound zinc metalloprotease FtsH has been shown to have proteolytic activity against PspC domain-containing membrane proteins in *E. coli* and *Y. enterocolitica* (Singh and Darwin 2011), we hypothesize that the disassociation of the CesS-YthA complex likely happens due to proteolytic activity by FtsH. Indeed, *ftsH* coding for this protease is preceded by a CesR binding motif upstream of its promoter region, and has been shown to be involved in LAB stress response (Martinez, Zomer et al. 2007, Pinto, Kuipers et al. 2011)

The successful degradation of YthA is then thought to release CesS, which in turn becomes available to activate CesR. This DNA binding response regulator promotes the expression of key genes within CesSR, including *cesS, cesR, ythA, ftsH* and *spxB*, see **Figure 1.2** for a schematic overview. The G-protein-associated signal transduction protein SpxB has been linked to regulation of *oatA*, encoding the acetyltransferase OatA. This enzyme catalyses the acetylation of the 6´carbon of the N-acetylmuramic acid residue in PG as previously mentioned, resulting in increased resistance against hydrolysis (Veiga, Bulbarela-Sampieri et al. 2007).

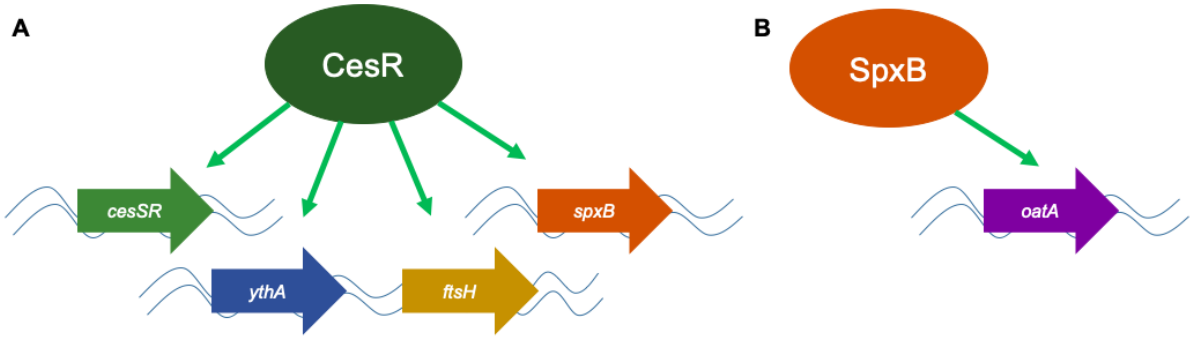

Figure 1.2: Simplified illustration of CesSR, incorporating already established constituents and their functions. **A** - CesR upregulates expression of several genes, including the *cesSR*-operon, *ythA*, *ftsH* and *spxB.* **B** - In turn, SpxB upregulates the expression of *oatA*, which facilitates the O-acetylation of PG (not shown)

1.5 - Aims to investigate the involvement of YthA in CesSR

This thesis is based on a selection of *L. lactis* IL1403 strains, all reported to have a different mutation in *ythA*. These strains have previously been isolated by Hai Chi during his work with his PhD thesis at LMG (Chi 2018). Mutations in *ythA* are hypothesized to contribute to an altered expression level of CesSR, ultimately resulting in a higher degree of acetylated PG in these mutant strains.

The coupling of the cytosolic constituents of CesSR, outlined in section 1.4 and illustrated in **Figure 1.2**, has already been established (Martinez, Zomer et al. 2007, Pinto, Kuipers et al. 2011). However, what role the PspC domain-containing membrane protein YthA is currently not yet understood. To investigate this, mutant strains of *L. lactis* IL1403 will be selected for expression analysis of genes associated with CesSR. This will reveal if the functionality of YthA is involved in the regulation of CesSR. This will be measured using quantitative PCR (qPCR) to relatively quantify the fold change in expression levels of the genes associated with CesSR. As such, the primary aims of this thesis are:

- To gain a better understanding of the mechanism of action and the resistance towards the three-peptide bacteriocin GarKS in *L. lactis* IL1403
- To understand how the PspC domain-containing protein YthA is involved in the transcriptional regulation of CesSR.

This will be done by first investigating a selection of *L. lactis* IL1403 strains, all reported to have a different mutation in *ythA*, and second, by exposing *L. lactis* IL1403 wild type to sublethal concentrations of the bacteriocin GarKS. This will help us answer questions such as:

- What phenotypes are displayed in *ythA*-mutants of *L. lactis* IL1403, and how does the mutation affect the robustness of the cells?
- How is the altered functionality of mutated YthA affecting the expression of genes associated with CesSR?
- How is the *yth*-operon and CesSR regulated in wild type *L. lactis* IL 1403 that has been exposed to sublethal doses of synthetic GarKS, and are they connected?

To give an overview of the general outline of the workflow in this thesis, the methods used to answer these questions are presented in the flowchart in **Figure 1.3**.

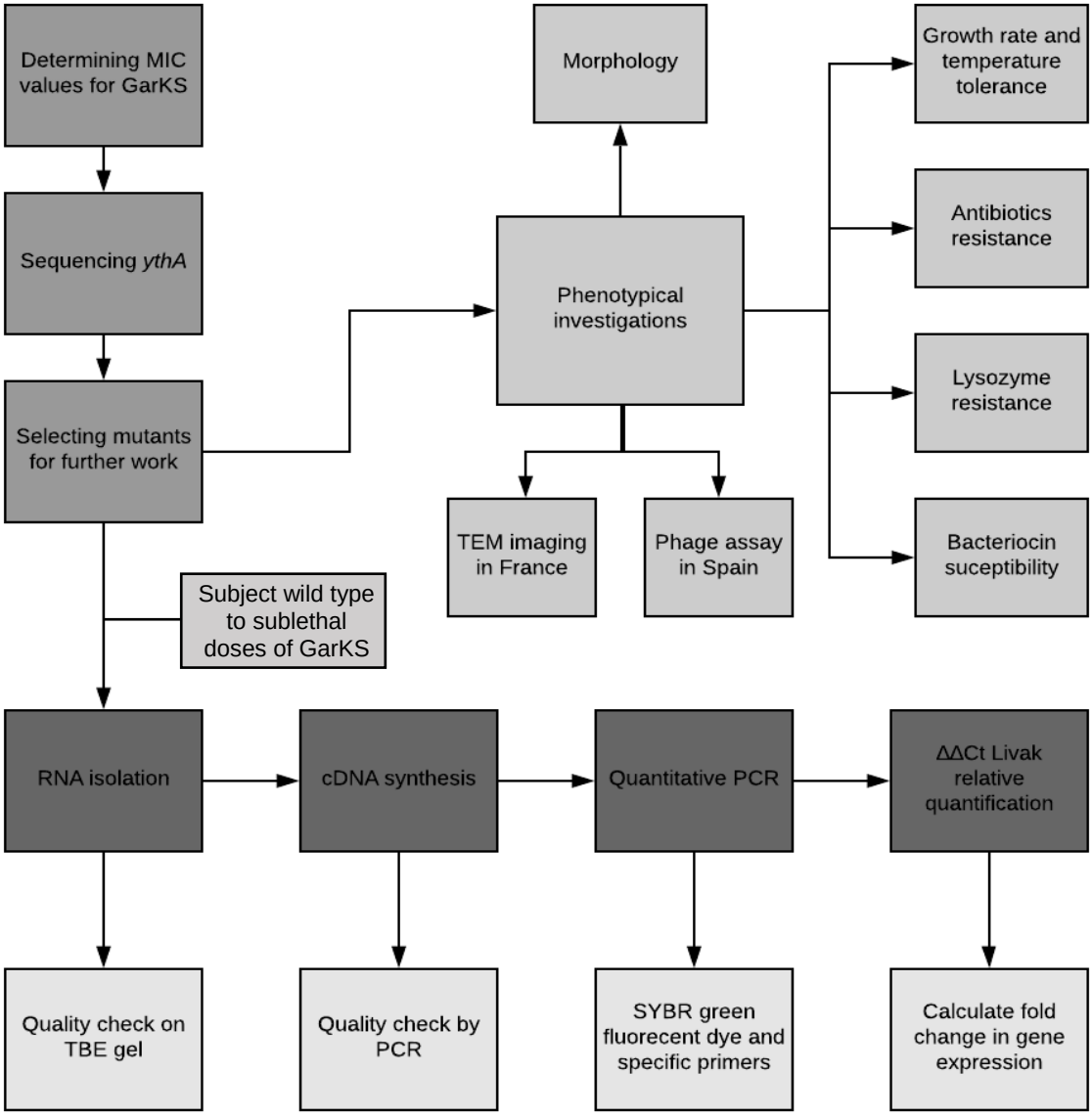

Figure 1.3: Outline of the workflow in this thesis. Strains of *L. lactis* IL1403 will be selected for further work based on their mutation in *ythA* and MIC value against GarKS. These strains will undergo several phenotypical tests to unravel the effects of these mutations. Ultimately, the main goal will be to quantify the expression levels of genes associated with CesSR in mutant strains, and in wild type exposed to sublethal doses of GarKS, to establish if *ythA* is somehow involved in this stress response.

2 - Materials and methods

2.1 - Cultivation of bacterial strains

All cultivation of *L. lactis* IL1403, and derivatives, was done in liquid GM17 medium at 30 °C in an incubation cabinet. See the Appendix, section A.3 for a full list of growth mediums and solutions used in this thesis. All work with live bacteria was performed in a sterile flow hood. Supplied strains of *L. lactis* IL1403 had been streaked out on GM17 agar plates, and single colonies from these plates were picked with a sterile toothpick and used to inoculate 5 ml of liquid overnight (ON) cultures. From each of these ON cultures, a frozen stock was made by mixing 500 µl of 45 % sterile glycerol (Sigma-Aldrich) with 1000 µl of ON culture in cryotubes. The frozen stocks were stored at - 80 °C and served as the base of all subsequent cultivation of the strains, performed in the following way:

A sterile toothpick was dipped in the still frozen stock and dropped into a new tube with 5 ml GM17. The tube was vortexed and incubated ON at 30 °C. The next day, the ON culture was diluted 100 times in a new tube with 5 ml of GM17 and incubated ON at 30 °C. This fresh ON culture was then used for all experimental purposes.

E. coli DH5-alpha was grown in Luria-Bertani (LB) broth, with 250 µg/ml of erythromycin as selection, at 37 °C and 200 rpm agitation. A 5 ml ON culture from a frozen stock was used to inoculate a 50 ml culture for harvesting.

2.2 - Minimum inhibitory concentration assay

In the first wells of a microtiter plate, (A1-H1), 10 µl of 0,3 mg/ml (0.1 mg/ml per peptide) of 98 % pure synthetic GarKS peptides (Pepmic Co., LTD, China) was added to 190 µl of GM17 and mixed thoroughly by pipetting several times. 100 µl of GM17 was added to all other wells that were going to be used. After mixing the contents of the first wells, 100 µl was transferred from the first well to the second well, which already contained 100 µl of GM17. This was repeated for each row of the plate to make a two-fold serial dilution of GarKS. Fresh ON culture was diluted 100 times to a total volume of 200 µl for all the wells. The plate was incubated at 30 °C in a sealed container with moisture provided in the form of a damp paper towel to prevent drying of the samples. The microtiter plate was read in a SPECTROstar Nano (BMG LABTECH) absorbance plate reader after 4 hours (early log-phase) and after 24 hours (well into stationary phase). The well with the highest concentration of GarKS that showed no growth was declared the minimum inhibitory concentration (MIC) value.

2.3 - Isolation of genomic DNA

Genomic DNA (gDNA), for use in PCR reactions, was isolated with the E.Z.N.A.® Plasmid DNA mini kit I (Omega Bio-Tek), modified for cellular lysis using bead beating. All subsequent isolations of gDNA were performed using this protocol.

- 0.5 g of < 106 µm acid washed glass beads (Sigma-Aldrich) was added to one FastPrep tube per sample.
- Cells were harvested by centrifuging 3 ml of fresh ON culture in an Eppendorf tube at 13.000 rpm for 1 minute.
- Cells were washed in 200 µl of TBS-buffer, then centrifuged at 13.000 rpm for 1 minute.
- The pellet was resuspended in 250 µl of ice cold Solution 1 with added RNase A (see manufacturers protocol), and the suspension was transferred to the FastPrep tube with glass beads.

- Cells were lysed in a MP Biomedical Fast prep 24 homogenizer, with three runs at 4 m/s for 20 seconds. The tubes were left on ice for 1 minute between each run.
- The FastPrep tubes were centrifuged for at 13.000 rpm for 1 minute, and the supernatant was transferred to a new Eppendorf tube.

The remaining steps are identical to the manufacturers protocol.

- 250 µl of Solution 2 was added and briefly mixed.
- 350 µl of Solution 3 was added and briefly mixed, followed by centrifugation at 13.000 rpm for 10 minutes.
- The supernatant was transferred to a mini prep column placed in a collection tube, and centrifuged at 13.000 rpm for 1 minute. Flow-through was discarded.
- 500 µl of HBC buffer diluted with isopropanol (see manufacturers protocol) was added to the column placed in a collection tube, and centrifuged at 13.000 rpm for 1 minute. Flow-through was discarded.
- 700 µl of DNA wash buffer diluted with ethanol (see manufacturers protocol) was added to the column placed in a collection tube, and centrifuged at 13.000 rpm for 1 minute. Flow-through was discarded, and this step was repeated once more
- The column was placed in a collection tube and dried by another centrifugation at 13.000 rpm for 2 minutes.
- The column was then placed in a new nuclease free Eppendorf tube, and 50 µl of pre-heated (60 °C) Elution buffer was added onto the center of the column. After an incubation at room temperature for 5 minutes, the column in the Eppendorf tube was centrifuged at 13.000 rpm for 1 minute, and isolated DNA was stored at - 20 °C.

DNA quality was checked by running the isolated gDNA on a 1 % TAE agarose gel, as described in section 2.4, as well as measuring the DNA concentration on a NanoDrop 2000 (Thermo Scientific).

2.4 - Polymerase chain reaction of selected genes

Primers used in the polymerase chain reactions (PCR) were designed using the following parameters. Each addition of adenosine or thymine increases the specific primer melting temperature (T_m) by 2 °C and each addition of guanine or cytosine, increases the T_m by 4 °C. The 3´ position of the primer should be a pyrimidine, and a high GC content near the 3´end is preferable. If possible, more than three consecutive repeats of a single nucleotide should be avoided. And total primer T_m should be approximately 62 - 64 °C.

Primers were checked *in silico* using the primer sequence as a query in a nucleotide Basic Local Alignment Search Tool (BLAST) search, to ensure specificity towards *L. lactis* IL1403. Primers were ordered from Invitrogen (Thermo Fisher Scientific). **Table A.2.1** in the Appendix, section A.2 contains a list of all primers used in the PCR reactions and the corresponding annealing temperature that was used.

All PCR reaction setups in this study followed the same protocol for making the master mix, listed in **Table 2.1**. Primers were dissolved in DEPC treated Milli-Q, to a final concentration of 100 µM. From this stock, 20 µl was aliquoted and diluted tenfold to a working solution of 10 µM for direct use in the master mix. Phusion® High-Fidelity DNA Polymerase (New England Biolabs (NEB)) was used in all PCR reactions.

Table 2.1: List of reagents used to make the PCR master mix for a 50 µl reaction. The same mix was used in all PCR reactions.

Reagent	Stock concentration	Final concentration	Volume per reaction
Buffer	5x	1x	10 µl
dNTP	10 mM	200 µM	1 µl
Forward Primer	10 µM	0.5 µM	2.5 µl
Reverse primer	10 µM	0.5 µM	2.5 µl
Phusion® Taq polymerase	2000 U/ml	1.0 U/ 50 µl	0.5 µl
DEPC treated Milli-Q water	-	-	Ad 50 µl

All PCR reactions were based on the same program, shown in **Table 2.2**, with a variable annealing temperature adjusted in accordance with the different T_m of the primers used. All PCR reactions were performed on a MyCycler™ thermal cycler (Bio-Rad). Regarding the amplification of *ythA* for sequencing, annealing temperature was set to 60 °C with a PCR run of 30 cycles. 2 µl of isolated gDNA was used as template.

The results of all PCR reactions were analysed on 1 % TAE agarose gel using 2 µl PeqGREEN (Peqlab) DNA/RNA dye per 50 ml gel. Purple loading Dye (NEB) was used when loading samples on the gel, and depending on the size of the amplicons, 5 µl of 100 base pair (bp) Ladder (NEB) or 1 kb Ladder (NEB) was used to estimate fragment size. All gels were run at 60 V for approximately 60 minutes.

Table 2.2: PCR program used on a MyCycler™ thermal cycler (Bio-Rad) for all PCR reactions. *Adjusted depending on the specific T_m of the primers used.

Step	Temperature	Duration	Cycles
Initial denaturation	98 °C	1 min	
Denaturation	98 °C	30 s	30 - 45
Annealing	41 - 66 °C*	30 s	
Elongation	72 °C	20 s/kb	
Final elongation	72 °C	2 min	
Hold	4 °C	∞	

2.5 - Sequencing of *ythA*

Following PCR amplification of *ythA*, the amplicons were purified using the NucleoSpin® Gel and PCR Clean-up (Macherey-Nagel) according to the manufacturers protocol. Concentrations of the purified amplicons were measured on a NanoDrop 2000 (Thermo Scientific) and diluted to within the range of 80 - 20 ng/µl in a nuclease free Eppendorf tube. The same primers used in the PCR reaction, see **Table A.2.1** in the Appendix, section A.2, were added to the purified amplicons for a final primer concentration of 2.5 nM, one primer per tube. The tubes were then sent to Eurofins genomics for sequencing.

Sequences were downloaded from the Eurofins Genomics website, and the corresponding chromatograms (in PDF format) were visually checked for any unambiguity in the sequence. The online bioinformatics tool Reverse Complement (Stothard 2000) (https://bioinformatics.org/sms/rev_comp.html) was used to generate a reverse complementary sequence from the revers sequencing reaction. The online multiple sequence alignment tool Clustal Omega (Madeira, Park et al. 2019) (https://www.ebi.ac.uk/Tools/msa/clustalo/) was then used to align the forward and reverse complement sequence. This consensus sequence was then used as a query in a nucleotide BLAST search.

2.6 - Growth rate and temperature tolerance

Fresh ON culture was diluted 100 times in liquid GM17 medium on a 96 well plate to a total volume of 300 µl, with five replicates per strain. The plate was then incubated in a Synergy H1 Hybrid reader (BioTek®) at 30 °C, 40 °C and 45 °C. The program was set up to shake the plate for three seconds followed by measuring OD_{600} at 10 minute intervals for 10 hours. The data from these incubations were then used to generate growth curves for all strains tested.

2.7 - Lysozyme susceptibility and multidrug resistance soft agar overlay assay

A widely-used technique for testing the level of resistance a strain of bacteria displays against different antimicrobial substances is the soft agar overlay assay (Hockett and Baltrus 2017). The principles are that fresh liquid ON culture is diluted in a liquid 0.7 % agar solution, mixed briefly and then poured on top of an agar plate, containing the same medium. The bacteria will then grow evenly inside the soft agar layer on top, thus forming a blanket of bacteria. Any exposure to antimicrobials on top of this layer will result in clear inhibition zones, and the radius of these zones provides a measure of how susceptible the bacteria are to the given antimicrobial agent.

5 ml of liquid GM17 0.7 % soft agar, cooled to 45 °C, was inoculated with 50 µl fresh ON culture, vortexed and directly poured out on a premade GM17 agar plate.

After hardening and drying, antimicrobial agents were applied on top of the soft agar layer. A list of antimicrobials and corresponding stock concentrations used in the soft agar assays are given in **Table 2.3**. 5 µl of each bacteriocin in a tenfold dilution series and 5 µl lysozyme in a twofold dilution series were applied on the surface of the soft agar. Antibiotic discs (Thermo Fisher Diagnostics) were placed carefully on the soft agar layer with a sterile tweezer and very gently pressed to ensure full contact.

Table 2.3: List of antimicrobial substances used in the soft agar assays, with their corresponding abbreviation used in this thesis and a simplified mechanism of action associated with the substance.

Name	Stock concentration	Abbreviation	Mechanism of action
Bacteriocins			
Garvicin KS	3.0 mg/ml	GarKS	Unknown
Lactococcin A	0.1 mg/ml	LcnA	Targeting the Mannose PTS
Micrococcin P1	1.8 mg/ml	MP1	Targeting the ribosome
LsbB	0.5 mg/ml	-	Targeting the RseP (in *Lactococcus*)
Nisin	0.45 mg/ml	-	Pore formation due to lipid II interactions
Antibiotics			
Penicillin G	10 U	P	Inhibits the crosslinking between NAG and NAM
Ampicillin	10 UG	Amp	Inhibits the crosslinking between NAG and NAM
Erythromycin	15 UG	E	Binds to the 50S subunit and inhibiting protein synthesis
Vancomycin	5 UG	Va	Inhibits the crosslinking between NAG and NAM
Ciprofloxacin	5 UG	Cip	Inhibition of DNA gyrase and topoisomerase IV thereby inhibiting DNA replication
Streptomycin	10 UG	S	Binds to the 16S subunit and inhibits protein synthesis
Enzymes			
Lysozyme	40 mg/ml		Hydrolysis of 1.4-beta-linkage between NAM and NAG in PG

2.8 - Bacteriophage plaque formation assay

The bacteriophage plaque assay was conducted at the Department of Technology and Biotechnology of Dairy Products, IPLA-CSIC Villaviciosa, Asturias in Spain. The assay was set up as described by Lopez-Gonzalez et al. (2018), without scoring plaque forming units for LMGT 3876, and only using presence or absence of inhibition halo. **(**Lopez-Gonzalez, Escobedo et al. 2018)

2.9 - Confocal and transmission electron microscopy

Fresh ON culture was diluted 100 times in 5 ml of GM17 and incubated at 30 °C for three hours. Two cultures were grown for each strain, one intended for phase contrast and one for fluorescent staining. Cells were harvested from 1 ml early log phase culture ($OD_{600} \approx 0,4$) by centrifugation at 13.000 rpm for 2 minutes, and then resuspended in 250 µl 1x PBS. Two different types of staining were used for imaging, the cell wall binding derivative of vancomycin modified with a fluorescent label, VanFL (Invitrogen), and the commonly used DNA binding fluorescent stain 4`.6-diamidino-2-phenylindole (DAPI).

For fluorescent staining, 1 µl of VanFL was added to the resuspended cells and incubated for 5 minutes. 0.5 µl of DAPI was then added, followed by incubation for another 5 minutes. The stained and unstained cells were mounted on a thin sheet of ultrapure agarose on a glass slide. Images were captured using a Zeiss AxioObserver confocal microscope with ZEN Blue software through a 100x phase contrast objective. The camera used to capture the images was ORCA-Flash 4.0 V2 Digital CMOS (Hamamatsu Photonics). A HPX 120 Illuminator (Zeiss) was used as the light source for the fluorescent microscopy. Filter Ex. wavelength for VanFL was set at 450 - 490 nm with 1.5 second exposure time. Analysis of the images taken were performed using MicrobeJ (Ducret, Quardokus et al. 2016) and subsequent plotting of the data were done in Rstudio using the *ggplot* package.

Transmission electron microscopy (TEM) was conducted by our colleagues at INRA in France. The work was performed by at MIMA2 MET, UMR 1313 *Génétique*

Animale et Biologie Intégrative (GABI), Equipe Plateformes, INRA, 78352 Jouy-en-Josas. The samples were prepared and the images captured as described in (Solopova, Formosa-Dague et al. 2016). The protocol used is included in the Appendix, section A.4.

2.10 - Preparation of ribonuclease free reagents and stock solutions

It is of the utmost importance that all reagents used in contact with RNA be nuclease free, and must therefore be prepared using diethyl pyrocarbonate (DEPC) treated Milli-Q™ water. DEPC covalently modifies the nuclease residues, especially the histidine, lysine, cysteine and tyrosine, resulting in loss of catalytic function. Autoclaving removes any residual DEPC, which can inhibit downstream enzymatic reactions (Huang, Leblanc et al. 1995). To ensure that all solutions used in the isolation and analysis of RNA were completely nuclease free, DEPC-treated Milli-Q water was made by adding 1 ml DEPC (Sigma-Aldrich) to 1000 ml Milli-Q water. This solution was left over night with vigorous stirring, then autoclaved twice for 15 minutes at 121 °C to ensure that any trace DEPC was neutralized. DEPC-treated water was then used in the preparation of all solutions needed for the isolation an analysis of RNA, see the Appendix, section A.3 for a full list of solutions used in this isolation process.

2.11 - Phenol:Cloroform extraction of total ribonucleic acids

Depending on the type of subsequent assays to be performed, a plethora of different methods for the isolation of nucleic acids exists. Nowadays most purposes can be fulfilled with the use of commercial kits that simplify the process. However, these kits are not always optimized for the smallest RNA fragments, and for gene expression studies such as the one performed in this thesis, a method that efficiently extracts fragments of all sizes is needed. Nucleic acid extraction using phenol mixed with chloroform in a 1:1 ratio represents just such a technique (Tan and Yiap 2013). The phenol:chloroform mixture is efficient at denaturing proteins, and as the mix and water is immiscible, the water soluble nucleic acids will be located in the aqueous phase while the denatured proteins have had their hydrophobic interior regions exposed and

thus will be located in the organic phase. This effectively separates the contents of lysed cells based on their solubility when the samples are centrifuged.

To obtain good quality RNA samples, vigilant use of a decontamination reagent on all work surfaces and equipment is necessary to neutralize any ribonucleases (RNases). RNases are ubiquitous and very stable nucleases that must be avoided whenever good quality RNA samples are needed. Contamination of the samples will result in degradation of the isolated RNA rendering the samples unusable in a gene expression study (Toni, Garcia et al. 2018).

An overview of sample preparation and the outline for this isolation is shown in **Figure 2.1.** All steps were carried out on ice, and all reagents were kept on ice before use in contact with isolated nucleic acids. To ensure no contamination of ribonucleases, RNase AWAY® (Molecular BioProducts) was used generously on all surfaces, pipettes and gloves during the isolation process.

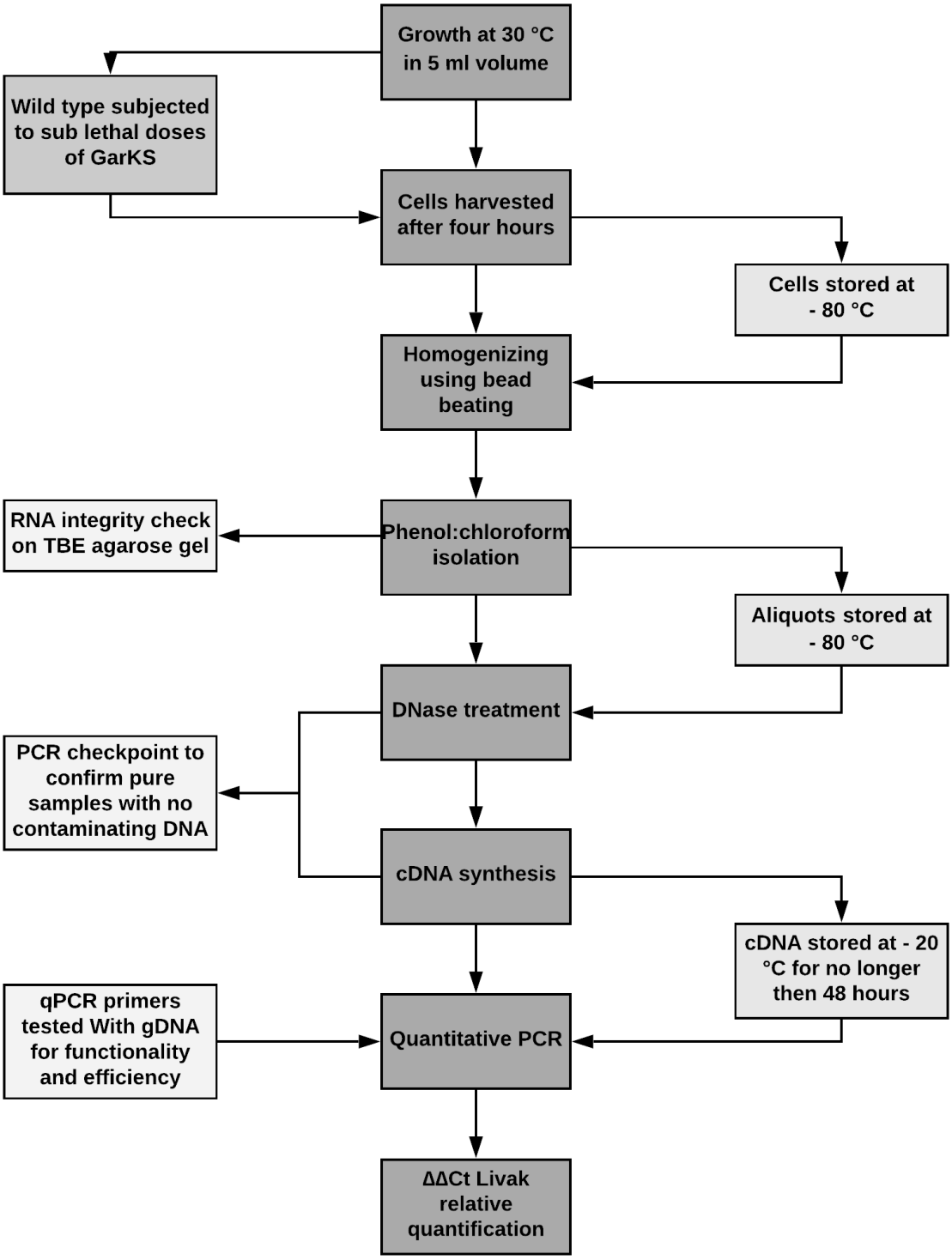

Figure 2.1: Flowchart outlining the RNA isolation process and subsequent qPCR based gene expression analysis. PCR checkpoints were conducted to test nucleic acid integrity and the absence of any unwanted nucleic acids in the RNA samples.

Cells were grown as previously described in section 2.1, in 5 ml culture volume for 4 hours at 30 °C and with 120 rpm agitation. Cell culture was poured in 15 ml Falcon tubes and centrifuged at 3220 x g and 4 °C for 10 minutes. Cells were washed with 5 ml of ice-cold TBS and then centrifuged at 3220 x g and 4 °C for an additional 10 minutes. After pouring of the supernatant, the pellet was frozen in liquid nitrogen, then stored at - 80 °C until the isolation process was performed using a modified protocol based on the works of (Aprianto, Slager et al. 2016) and (van der Meulen, de Jong et al. 2016).

- One FastPrep tube per sample was prepared with 0.5 g of < 106 µm acid washed glass beads (Sigma-Aldrich) + 50 µl of 10 % SDS + 500 µl of a 1:1 mixture of phenol (Sigma-Aldrich) and chloroform (Merck).
- Cells were thawed on ice and resuspended in 400 µl of 1 x TE buffer and added to the FastPrep tubes.
- Cells were lysed in a MP Biomedical Fast prep 24 homogenizer for 2 x 45 seconds, With 1 minute rest on ice between cycles.
- Tubes were centrifuged at 13.000 rpm for 10 minutes at 4 °C.
- Aqueous phase was transferred to a new nuclease free Eppendorf tube, and 500 µl chloroform was added, followed by gentle mixing by inversion of the tubes.
- Tubes were centrifuged at 13.000 rpm for 10 minutes at 4 °C, and aqueous phase was transferred to a new nuclease free Eppendorf tube.
- Nucleic acids were precipitated by adding 50 µl of 3 M Na-acetate + 1 ml of ice cold 100 % ethanol to each tube, followed by incubation for > 30 minutes* at - 20 °C. *Samples were left at - 20 °C ON for all ethanol precipitations in this protocol.
- Tubes were centrifuged at 13.000 rpm for 10 minutes at 4 °C, and without disturbing the pellet, the supernatant was pipetted off.
- The pellet was washed carefully with 1 ml of 70 % ice cold ethanol.
- Tubes were centrifuge at 13.000 rpm for 5 minutes at 4 °C, and the supernatant was decanted off.
- Tubes were quickly spun with a tabletop centrifuge, and any remaining ethanol was pipetted off. The pellet was air dried for 10 minutes.
- The pellet was resuspended in 35 µl DEPC treated MilliQ**, and 5 µl of DNase buffer (Thermo Scientific), 5 µl of DNase I (Thermo Scientific) and 5 µl of Ribolock

(Thermo/Fermentas) was added. This reaction mix was then incubated for 30 minutes at 37 °C.

**To avoid too high concentration of RNA/DNA, the pellet was resuspended in 350 µl and stored at - 80 °C. Aliquots of 35 µl were taken from this and used for the DNase treatment as described above.

- 450 µl of DEPC-treated Milli-Q water was added to each tube.
- 500 µl of phenol:chloroform mixture was added, followed by gentle mixing by inversion of the tubes.
- Tubes were centrifuged at 13.000 rpm for 10 min at 4 °C, and aqueous phase was transferred to a new nuclease free Eppendorf tube.
- RNA was precipitated by adding 50 µl of 3 M Na-acetate + 1 ml of ice cold 100 % ethanol to each tube, followed by incubation for > 30 minutes at - 20 °C.
- Tubes were centrifuged at 13.000 rpm for 10 minutes at 4 °C.
- The pellet was washed carefully with 1 ml of 70 % ice cold ethanol
- Tubes were centrifuge at 13.000 rpm for 5 minutes at 4 °C, and the supernatant was decanted off.
- Tubes were quickly spun with a tabletop centrifuge, and any remaining ethanol was pipetted off. The pellet was air dried for 10 minutes.
- The pellet was resuspended in 50 µl of 1x TE buffer and store at - 80 °C.

RNA concentrations were measured on a NanoDrop 2000 (Thermo Scientific), and by using the Qubit® RNA HS Assay kit with a Qubit® 2.0 fluorometer, according to the manufacturers protocol. RNA integrity was determined by running samples on a 1 % TBE agarose gel as previously described in section 2.3. A 45 cycle PCR reaction, with qPCR primers targeting *ythA*, shown in **Table A.2.2** in the Appendix, section A.2, was set up as previously described in section 2.4. One reaction with 2 µl of isolated total nucleic acids (TNA) before DNase treatment as template, and one reaction with 2 µl of isolated RNA as template. This was done to check if the isolation was successful and to ensure that the isolated RNA did not contain any contaminating DNA.

2.12 - Synthesis of complimentary DNA from isolated RNA

From isolated RNA, complimentary DNA (cDNA) was synthesized using Maxima First Strand cDNA Synthesis Kit for RT-qPCR (Thermo Scientific), according to the manufacturers protocol. RNA concentration was first measured using the Qubit® RNA HS kit on a Qubit® 2.0 fluorometer (Invitrogen) according to the manufacturers protocol. Isolated RNA was diluted and standardized in 20 ng/µl aliquots, and 5 µl of this was used as template in the reactions resulting in an amount of 100 ng of isolated RNA per cDNA synthesis reaction. After synthesis, the reaction mix was stored at - 20 °C for no longer than 48 hours before being used as a template in subsequent analyses.

2.13 - Relative quantification of gene expression using quantitative PCR

Real time quantitative PCR (qPCR) has become the gold standard of gene expression analysis since the initial study published in 1996 (Heid, Stevens et al. 1996). By isolating RNA, converting it to cDNA using the enzyme reverse transcriptase and then using qPCR for quantification of specific genes, it is possible to investigate at what level those genes were expressed when the cells were lysed. This process can be performed in one single reaction, referred to as reverse transcription-qPCR (RT-qPCR) or divided in two subsequent reactions, thus separating the reverse transcription and the amplification steps (Bustin, Benes et al. 2009). In this thesis, it was desirable to first synthesize cDNA that could be used in multiple runs using different primers without the need for multiplexing.

The principles of qPCR are the same as conventional PCR, however the data collection is not based on end-point analysis. Instead, a continuous or real time measurement of fluorescent signal is performed after each amplification step. This results in a value from the real-time instrument that correspond to where in the program fluorescent signal exceeds the background levels, referred to as the quantification cycle or threshold cycle (C_t) (Bustin, Benes et al. 2009). For the detection of amplification there are two main chemistries available, specific fluorescently labelled probes and unspecific fluorescent dyes, both with their own pros and cons (Kralik and

Ricchi 2017). SYBR™ green is one of the most commonly used dyes, as it preferentially intercalates with double stranded DNA (dsDNA) and is relatively safe and easy to use (Ponchel, Toomes et al. 2003). For the type of gene expression analysis performed in this thesis, fluorescent dyes offer a less complicated and less expensive alternative that is less specific than probe based assays. However, by designing primers that are highly specific for individual genes it is possible to achieve specificity with dye based assays.

There are also two main strategies when it comes to analysing the data from a qPCR reaction; absolute and relative quantification (DeCoste, Gadkar et al. 2011). Absolute quantification seeks to determine the true copy number of the specific gene of interest. This is made possible using external standards, DNA samples of known concentrations used to make a standard curve, with which the data of the test samples can be compared. Relative quantification on the other hand only indicates if the expression of a specific gene is upregulated or downregulated in mutant strains or in wild type exposed to some form of stimuli. With the use of an endogenous control in the form of housekeeping genes with a stable level of expression as a reference, it enables the calculation of fold change in the expression pattern of the test sample compared to a calibrator sample, usually untreated wild type. The relative quantification strategy referred to as the $\Delta\Delta C_t$ Livak method offers a convenient way of calculating fold change in expression levels in qPCR reactions where primer efficiency is relatively stable (Livak and Schmittgen 2001).

Using the same parameters previously described in section 2.4, primers for the qPCR reactions were designed to target the selected genes associated with CesSR. Two canonical reference genes were chosen; *gyrA,* encoding the DNA gyrase subunit A (Ulve, Monnet et al. 2008), and *tuf*, encoding the elongation factor Tu (Ruggirello, Dolci et al. 2014, Ballal, Veiga et al. 2015). Primer target-sequences were selected downstream of the start codon and in such a way that any known mutations were not included in the amplicon. For the qPCR primers, the target amplicon size was designed as close as possible to 205 bp, +/- 10 bp. The primer sequences were used as a query in a nucleotide BLAST search, to ensure specificity towards *L. lactis* IL1403.

The efficiency of the primers was tested using isolated gDNA from wild type *L. lactis* IL1403. Using the PowerUP™ SYBR™ Green Master Mix, a qPCR master mix was made for all the primers, with the reagents listed in **Table 2.4**

Table 2.4: List of reagents used in the making of the qPCR master mix, with 20 µl reaction volume. For testing of primer efficiency, 1 µl of gDNA isolated from wild type was used as template. For all sample runs 1 µl of ten times diluted cDNA synthesis reaction mix was used as template.

Reagent	Stock concentration	Final concentration	Volume per reaction
SYBR™ mix	2x	1x	10 µl
Forward Primer	10 µM	500 nM	1 µl
Reverse primer	10 µM	500 nM	1 µl
DEPC Milli-Q water	-	-	7 µl

A tenfold dilution series of isolated gDNA from *L. lactis* IL1403 wild type was made with final concentrations of 10 ng/µl, 1 ng/µl, 0.1 ng/µl and 0.01 ng/µl. 19 µl qPCR master mix followed by 1 µl template from the different concentrations of gDNA were added to the wells on a MicroAmp® Fast Optical 96-Well Reaction Plate With Barcode (0.1 ml) (Applied Biosystems), with four replicates per concentration per primer pair. 1 µl DEPC Milli-Q was used in a negative control for each primer. The plate was tightly sealed with an Optical Adhesive Cover (Applied Biosystems), then centrifuged briefly and kept on ice until reaction start. The qPCR program shown in **Table 2.5** was set up using the StepOne Software v2.3 accompanying the StepOnePlus™ Real-Time PCR System Thermal Cycling Block (Applied Biosystems). This setup allowed four primers to be tested on the same plate simultaneously, necessitating multiple runs.

Table 2.5: Program used on a StepOnePlus™ Real-Time PCR System Thermal Cycling Block (Applied Biosystems) for all qPCR reactions. The following settings were used on the instrument: Experiment type: Quantification - Comparative C_T, SYBR® green reagents, Standard ramp speed and 20 µl reaction volume. *Detection of fluorescent signal was performed at these steps.

Step	Ramp rate	Temperature	Duration	Cycles
UDG activation	-	50 °C	2 minutes	Hold
Dual-Lock™ DNA polymerase	-	95 °C	2 minutes	Hold
Denature	-	95 °C	15 s	40
Anneal/extend*	-	60 °C	1 minute	40
Melt curve step 1	1.6 °C/second	95 °C	15 seconds	-
Melt curve step 2	1.6 °C/second	60 °C	1 minute	-
Melt curve step 3* (dissociation)	0.15 °C/second	95 °C	15 s	-

The same master mix used to test the qPCR primers, seen in **Table 2.4**, and settings shown in **Table 2.5**, were used for all sample runs with cDNA as template. These samples were also run with four replicates of each sample, per primer pair. For the sample runs, 1 µl template, consisting of a 10 times diluted cDNA reaction mix after synthesis, was used in each well. One negative control with DEPC Milli-Q and one control of RNA without reverse transcription as template were included per primer pair in all reactions.

2.14 - Using the $\Delta\Delta C_t$ Livak method for relative quantification in expression levels

The Livak $\Delta\Delta C_t$ method was chosen for calculating the fold change in expression levels for the genes selected (Livak and Schmittgen 2001, Biosystems 2004). The principles of this method are to first normalize test sample C_t values to a reference gene with a stable level of expression despite difference in treatment. This allows offsetting of difference in efficiency during extraction, reverse transcription and other factors like pipetting irregularities that hinders samples from being comparative. Further, the normalized C_t values, ΔC_t, can be compared with other ΔC_t values. These $\Delta\Delta C_t$ values will then indicate any change in the expression between a test sample and the

calibrator sample, which is usually untreated wild type. A step by step guide to how calculations were done can be found in the Appendix, section A.1.

2.15 - RNA sequencing and transcriptome study

RNA samples from B1545, LMGT 3870 and LMGT 3876 were sent to the Norwegian High Throughput Sequencing Centre, Department of Medical Genetics at Oslo University Hospital, Ullevål. Samples were isolated using the same protocol as described in section 2.11, using commercial nuclease free water (Ambion®) to resuspend the isolated RNA in the last step, instead of DEPC TE buffer. Samples were sequenced using TruSeq stranded RNA sequencing (Illumina, Inc., San Diego, CA, USA).

The following work was performed by our resident bioinformatician. “Reads were mapped to the reference *L. lactis* IL1403 transcriptome downloaded from The European Nucleotide Archive (ENA) using the software rsem (RSEM: accurate transcript quantification from RNA-Seq data with or without a reference genome. Bo Li and Colin N Dewey. BMC Bioinformatics201112:323) (version 1.3.0). Fragments per kilobase million (FPKM) values were calculated and used for quantification of gene expression levels (Mortazavi, Williams et al. 2008).”

2.16 - Complement study

To make electro-competent cells, fresh ON culture of LMGT 3870, LMGT 3876 and wild type were diluted ten times in GM17 and grown at 30 °C until OD_{600} of approximately 0.3. 100 µl of this culture was then added in a dilution series of freshly made SGM17 and 1.0 - 2.0 % glycine. See the Appendix, section A.3 for a list of all solutions used in this experiment and **Table A.3.1** outlining the preparation of the dilution series of glycine in SGM17 medium. Cultures were incubated ON at 30 °C.

The culture in the dilution series with an OD_{600} between 0.3 - 0.4, after incubation ON, was placed on ice for 10 minutes before the cells were harvested by centrifugation at 5000 x g for 5 minutes at 4 °C. The cells were washed two times in 15 ml of ice cold 0.5 M sucrose. The pellet was then resuspended in 350 μl of 0.5 M sucrose with 10 % glycerol (Sigma-Aldrich), and 40 µl aliquots was taken out and stored at - 80 °C

Expression vector PMG36e , with already inserted *ythA*, one with a C-terminal flag tag and one with an N-terminal flag tag had been previously used in the work conducted by Hai Chi during his work on his PhD thesis (Chi 2018). These plasmids were therefore already available in frozen stocks. *E. coli* strains containing the plasmids with N-tag, C-tag and one strain containing the empty vector were grown as previously described in section 2.1. The HiSpeed® Plasmid Midi Kit (Qiagen) was used to isolate these plasmids according to the manufacturers protocol. The inserts in the vector were sequenced as previously described in section 2.5, using primers targeting the PMG36e backbone, see **Table A.2.1** in the Appendix, section A.2.

For electroporation of *L. lactis* IL1403*,* a Bio Rad gene pulser with 0.2 cm cuvettes were used. The instrument was set to 25 µF capacitance, 2.0 kV and 200 Ω. 4 μl of isolated plasmid was added to the 40 μl aliquots of competent cells, mixed briefly and transferred to the cuvette. Following pulsing, 700 µl of SGM17MC was added and mixed with the cells by careful pipetting. The solution was then transferred to an Eppendorf tube and incubated for 3 hours at 30 °C. 150 µl was then each plated on GM17 agar plates with two types of selection, 10 µg/ml and 25 µg/ml erythromycin, and incubated at 30 °C for three days.

Colonies were picked from each strain with a sterile toothpick and used to inoculate a 5 ml culture with 10 µg/ml erythromycin as selection. Frozen stocks of the strains were made by mixing 500 µl of 45 % sterile glycerol (Sigma-Aldrich) with 1000 µl of culture in cryotubes. The frozen stock was stored at - 80 °C and served as the base of subsequent cultivation of the strains.

2.17 - Repetitive element palindromic PCR

Repetitive element palindromic PCR (rep-PCR) is a fingerprinting method used to generate a genetic profile of different strains based on the amplification of variable repetitive elements in the genome of bacteria. This technique represents a fast and easy way to confirm the kinship of two or more strains. Using primers containing the inosine nucleotide, which can form Watson-Crick base pairs with any of the four bases adenine, thymine, guanine and cytosine (Watkins and SantaLucia 2005), fragments of different size will be amplified according to the varying polymorphisms in the genomes (Woods, Versalovic et al. 1993). When separating these fragments on an agarose gel, an identical pattern will emerge from clonal strains. Different subspecies could in theory give a different pattern, allowing distinction between even closely related strains.

A rep-PCR was performed on the two mutant strains LMGT 3870 and LMGT 3876, the wild type and a reference sample, B1627 (a strain of nisin producing *L. lactis*). gDNA was isolated as previously described in section 2.3. 5 µl of isolated gDNA was then used as template in 50 µl reaction volume using Phusion® Taq polymerase in the same setup as previously described in section 2.3. The PCR program was adjusted to the correct annealing temperature for the rep-primers, see **Table A.2.1** in the Appendix, section A.2, and the program was run for 40 cycles.

2.18 - Sequencing of the 16S rRNA gene

Samples were purified and sent to Eurofins genomics, and sequences were downloaded and analysed as previously described in section 2.5. Primers used in this sample preparation are given in **Table A.2.1** in the Appendix, section A.2.

3 - Results

3.1 - MIC values and sequencing of *ythA* in mutants revealed irregularities between what was previously reported

Although *ythA* had already been sequenced in LMGT 3870 and LMGT 3876, and MIC values for GarKS were available from previous work for all the strains that formed the basis of this work, it was decided that to ensure validity, the results needed to be reproduced. All mutant strains of *L. lactis* IL1403 were therefore tested on a microtiter plate to deduce the MIC values for GarKS.

The assay showed a range of MIC values for the different mutant strains, as seen in **Table 3.1.** Measured MIC values varied when comparing to what was previously reported for the strains (Chi 2018). Even though MIC values were presented in BU/ml the previous work and ng/µl in the present thesis, a simple comparison of the level of resistance can be inferred when comparing the fold ration between MIC for the wild type and for the mutants. There was no mention of how long the cells were grown in the presence of GarKS in the previous work (Chi 2018).

In the previous work, LMGT 3871 had the highest reported MIC value, but showed similar MIC values to several other strains when only regarding own results. Similar differences are the case for several of the other strains, as seen in **Table 3.1** under MIC values after 24 hours. The MIC assays were reproduced in three independent experiments and the results are based on average values.

Table 3.1: Overview of L. lactis mutant strains and wild type, with MIC values for GarKS after 4 hour and 24 hour incubations. Also listed is the mutation in the *ythA* gene and the amino acid consequence. The three columns on the left side of the table lists the reported MIC values for GarKS in BU/ml, reported mutation in the *ythA* gene and the resulting amino acid consequence. A reported MIC value of 5 BU/ml for the wild type corresponds to a mixture of 10 nM of each of the three GarKS peptides. When comparing own results to what was previously reported, several irregularities are uncovered.

Strain ID	MIC after 4 h ng/μl	MIC after 24 h ng/μl	Mutation	Consequence	Reported MIC (BU/ml)	Reported Mutation	Reported Consequence
Mutants							
LMGT 3870	0.625	1.25			80	GGG->GAG	G21E
LMGT 3871	0.625	1.25	GGG->GAG	G21E	160	TAT->CAT	Y55H
LMGT 3872	0.625	1.25	At position 62		80	TGG->TAG	W96*
LMGT 3873	0.625	1.25			40	GGG->GTG	G17V
LMGT 3874	0.625	1.25			80	GGG->GAG	G21E
LMGT 3875	1.25	5.0	Insert at position		40	GGG->GTG	G17V
LMGT 3876	1.25	5.0	410	K138*	80	AAG->TAG	K138*
LMGT 3878	1.25	5.0	TAAGACT		80	AAG->TAG	K138*
LMGT 3881	0.312	1.25			80	CGT->GTT	R110V
LMGT 3882	0.312	1.25			80	AAG->TAG	K138*
LMGT 3879	0.078	0.625			80	TGG->TAG	W96*
LMGT 3880	0.078	0.625	No mutation	None	80	TGG->TAG	W96*
Wild type							
B1545	0,078	0,625	-	-	5	-	-

The previously reported mutations in *ythA* are given in **Table 3.1**. These mutations also needed verification, necessitating the designing of new primers that could target the whole protein coding region of the gene. The newly designed primers for *ythA*, shown in **Table A.2.1** in the Appendix, section 2, were tested using gDNA from all strains. The resulting amplification of *ythA* can be seen in **Figure 3.1.**

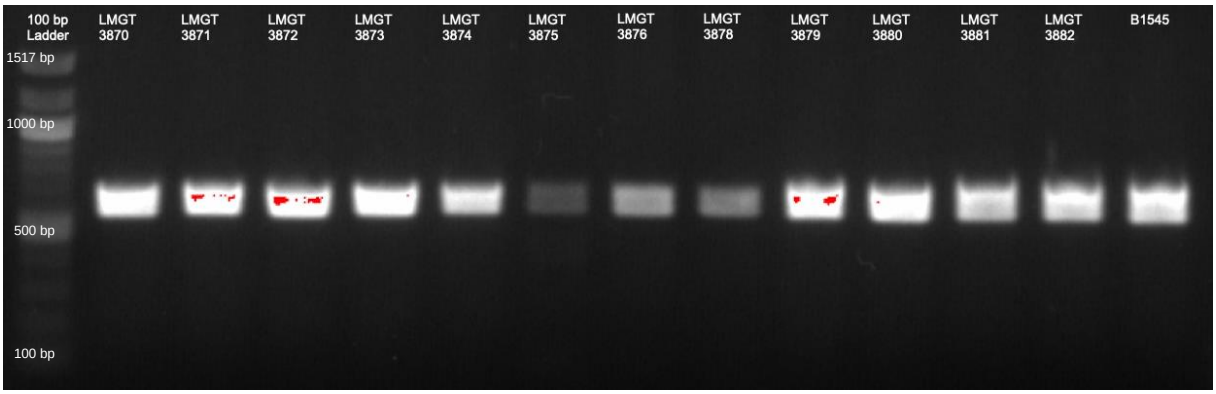

Figure 3.1: Gel image of preliminary PCR amplification, using *ythA*-primers specific for *L. lactis* IL1403. Expected amplicon size was 635 bp for wild type, B1545. It was noted that for LMGT 3875, LMGT 3876 and LMGT 3878, the amplification yielded bands of visibly lower intensity.

Sequencing of *ythA* uncovered more inconsistencies when regarding previous results. As seen in **Table 3.1**, only one of the strains tested had the reported mutation, LMGT 3870, with its substitution mutation GGG -> GAG at position 62 in the nucleotide sequence (Chi 2018). Two of the mutant strains, LMGT 3879 and LMGT 3880, appeared to have no mutation in *ythA*. For the strains LMGT 3876 and LMGT 3878, the reported substitution mutation, AAG->TAG, was not present. Instead, a duplication of the seven bp sequence TAAGACT was found at position 410 in the nucleotide sequence. However, for these two strains the amino acid consequence of the mutation was a truncation at position 138, as previously reported.

When using the sequence data as a query in a nucleotide BLAST search, all strains had the highest score with the genome of *L. lactis* IL1403. Note that the same was true for strains LMGT 3875, LMGT 3876 and LMGT 3878, the three strains that showed the highest MIC value for GarKS. **Figure 3.2** contains the results of a BLAST-search using the *ythA* sequence from LMGT 3876 as an example, with LMGT 3875 and LMGT 3878 yielding identical matches.

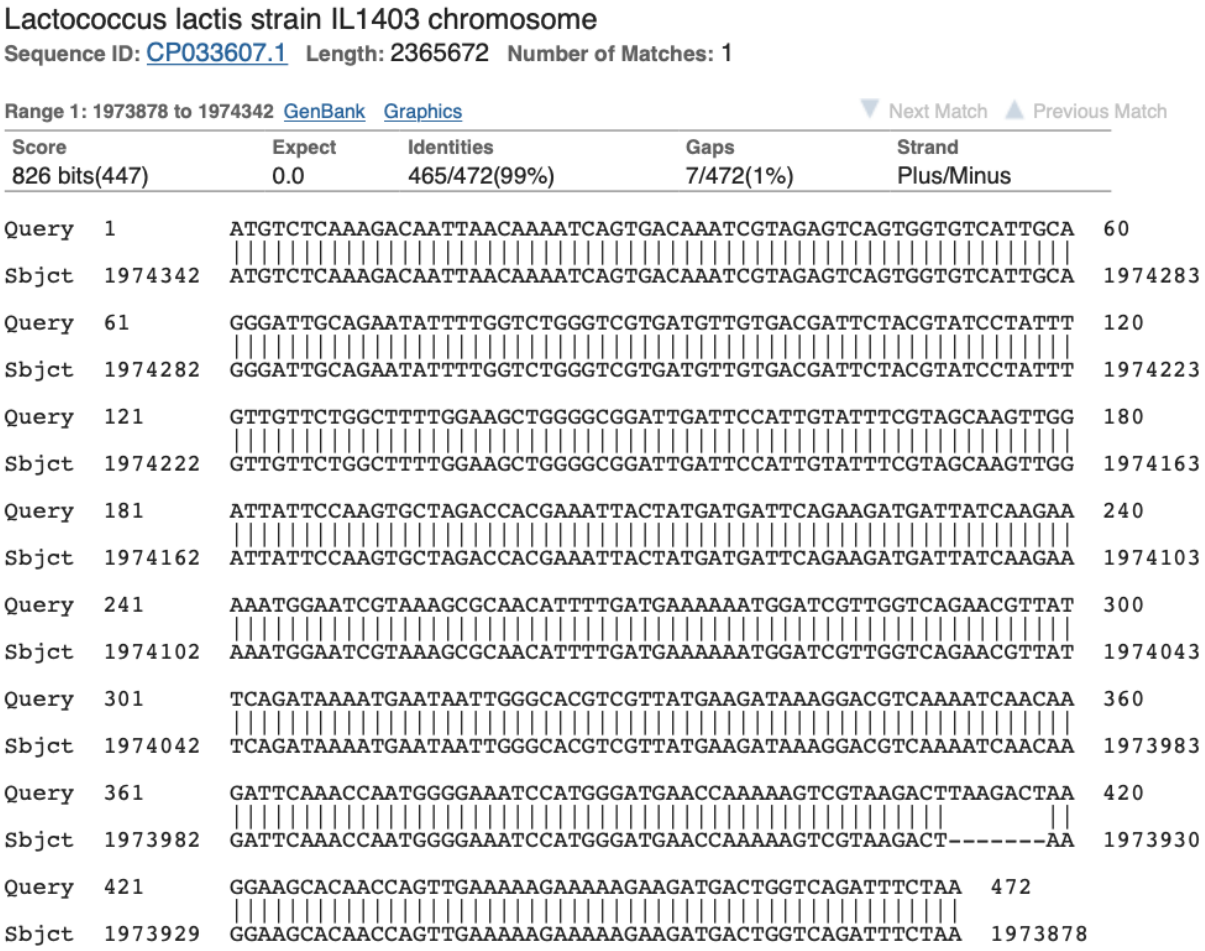

Figure 3.2: Alignment of LMGT 3876 *ythA*-sequence. Duplication of the seven bp sequence TAAGACT from position 411 - 418. All hits with a sequence identity >97 % was identified as *L. lactis ssp. lactis.*

Based on the MIC values and the results from the sequencing of *ythA*, two mutant strains were selected for further study. The intermediary resistant mutant LMGT 3870, with a substitution mutation GGG->GAG resulting in that the non-polar amino acid glycine is substituted with the charged amino acid glutamic acid, in position 21 of the peptide. This strain was selected as it was the only strain with the same mutation as previously reported, and it showed an intermediary level of resistance to GarKS. One of the mutants showing highest resistance to GarKS, LMGT 3876, was selected because of the K138* truncation mutation due to a sequence duplication. The wild type strain, B1545, was included as a comparative reference.

3.2 - Growth rate and temperature tolerance of *ythA* mutants deviated from wild type

As a standard preliminary phenotypical test for mutant strains, it was interesting to investigate if the mutations in *ythA* would influence the growth rate in any way. As expected, the growth of the truncated mutant LMGT 3876 deviated slightly from the wild type, displaying a somewhat slower growth rate, but being able to grow to a higher OD_{600} before reaching the stationary phase, as seen in **Figure 3.3.** LMGT 3870 also appeared to grow a little slower, however this mutant did not seem to be able to grow to any higher OD_{600} compared to the wild type.

It was decided to test if LMGT 3876 would display any resistance to higher temperatures then 30 °C, to investigate any difference in coping with stress in the form of heat shock. The temperatures 40 °C and 45 °C were arbitrarily chosen for subsequent incubations. From these experiments, it was revealed that LMGT 3876 not only grows faster at higher temperatures, but it can grow at temperatures that are deleterious to both LMGT 3870 and the wild type, as seen in **Figure 3.3.**

An additional experiment was set up to determine the oncentration of GarKS needed to induce a stress response in 5 ml cultures of wild type *L. lactis* IL1403, that would later be utilized in wild type cultures before RNA isolation. After incubation for 4 hours at 30 °C, OD_{600} was measured using an Ultrospec 10 Cell density meter (Amersham Biosciences) and growth was plotted as seen in **Figure 3.4**. The sublethal concentrations corresponding to 0.1 MIC and 0.5 MIC were chosen for the subsequent RNA isolation. 1 MIC corresponds to 0.078 ng/µl as previously deduced after 4 hour incubations, given in **Table 3.1**.

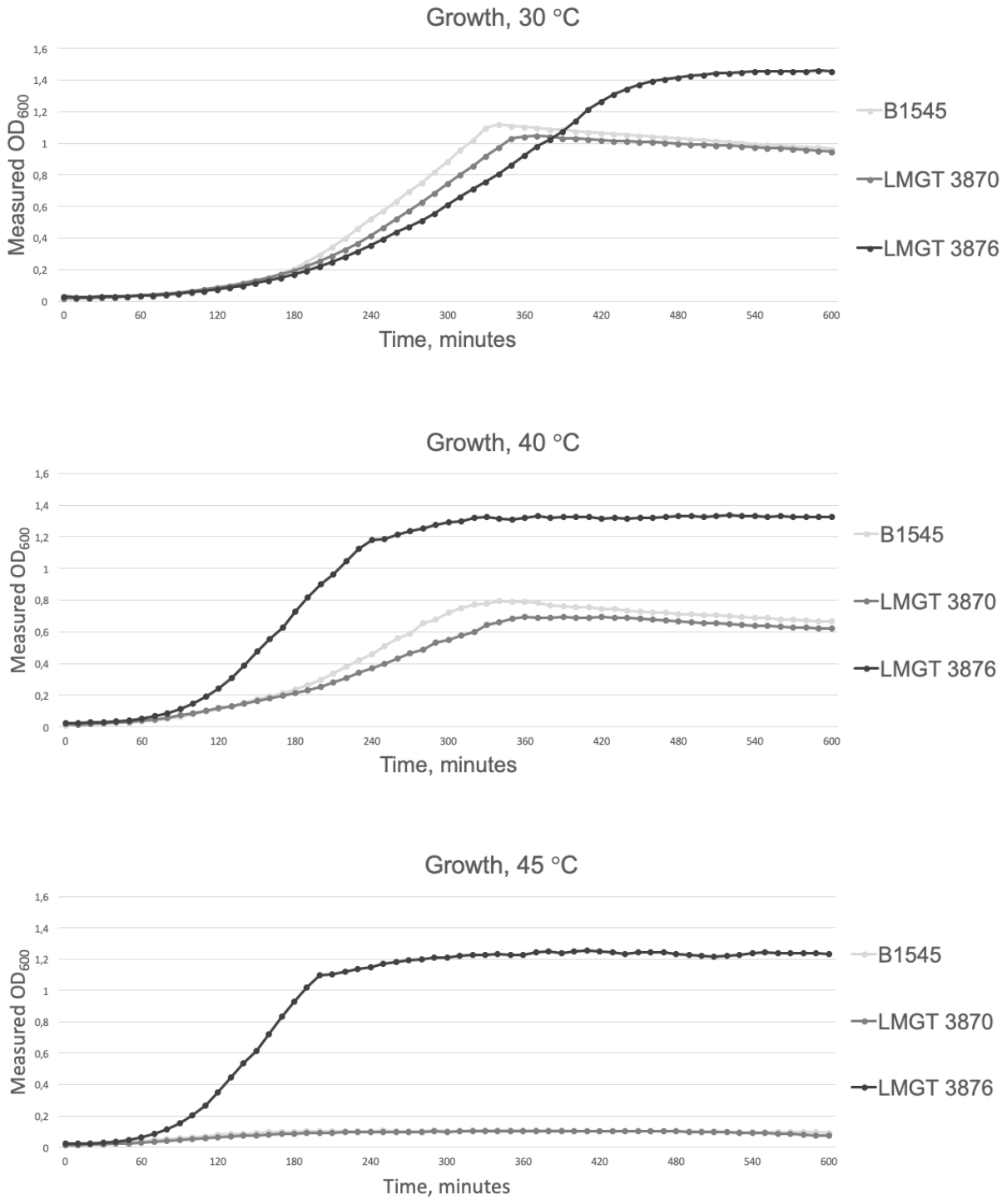

Figure 3.3: Growth curves for wild type, B1545, and the two mutants LMGT 3870 and LMGT 3876 when grown at three different temperatures, 30 °C, 40 °C and 45 °C. OD_{600} was measured every ten minutes for ten hours on a Synergy H1 Hybrid reader (BioTek®).

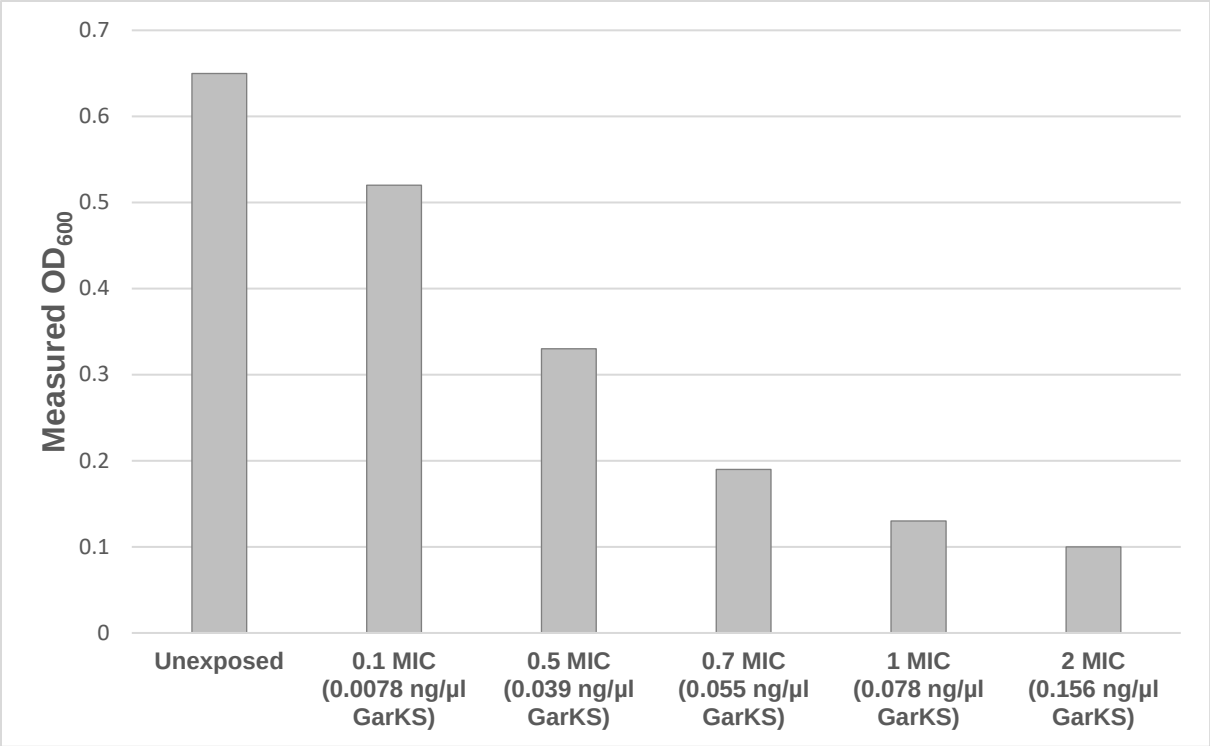

Figure 3.4: Growth of *L. lactis* IL1403 wild type when exposed to different sublethal doses of GarKS for 4 hours. Growth was performed in 5 ml culture volume and OD_{600} was measured using a Ultrospec 10 Cell density meter (Amersham Biosciences).

3.3 – *ythA* mutants showed an increased resistance to lysozyme, several different antibiotics and highly specific bacteriocins

As lysozyme resistance can be directly caused by acetylation of PG, increased resistance in the mutants could give an indication of whether the mutant possessed a higher degree of acetylated PG, thus indicating the upregulation of this process (Veiga, Bulbarela-Sampieri et al. 2007). Given the reported tendency for *L. lactis* strains with a mutation in *ythA* to show resistance to several different antibiotics as well as other types of antimicrobial agents (Wu, Liu et al. 2018) (personal communication, Dr. S. Kulakauskas), it was decided that LMGT 3870 and LMGT 3876 were to be tested using a selection of different antibiotics with different cellular targets. Additionally, it was reasonable to test these mutants against a variety of broad spectrum and highly specific bacteriocins, to further map the difference in phenotypes observed.

As was the case with the growth rate and temperature resistance, the mutant LMGT 3876 displayed extreme phenotypes against certain antimicrobials. The stock concentration of lysozyme was 40 mg/ml, and at this concentration LMGT 3876 showed no inhibition of growth, as seen in **Figure 3.5**. LMGT 3870 showed a marginally higher resistance to lysozyme, as the inhibition zones were slightly larger and a little more diffuse then for the wild type, which had clear inhibition zones.

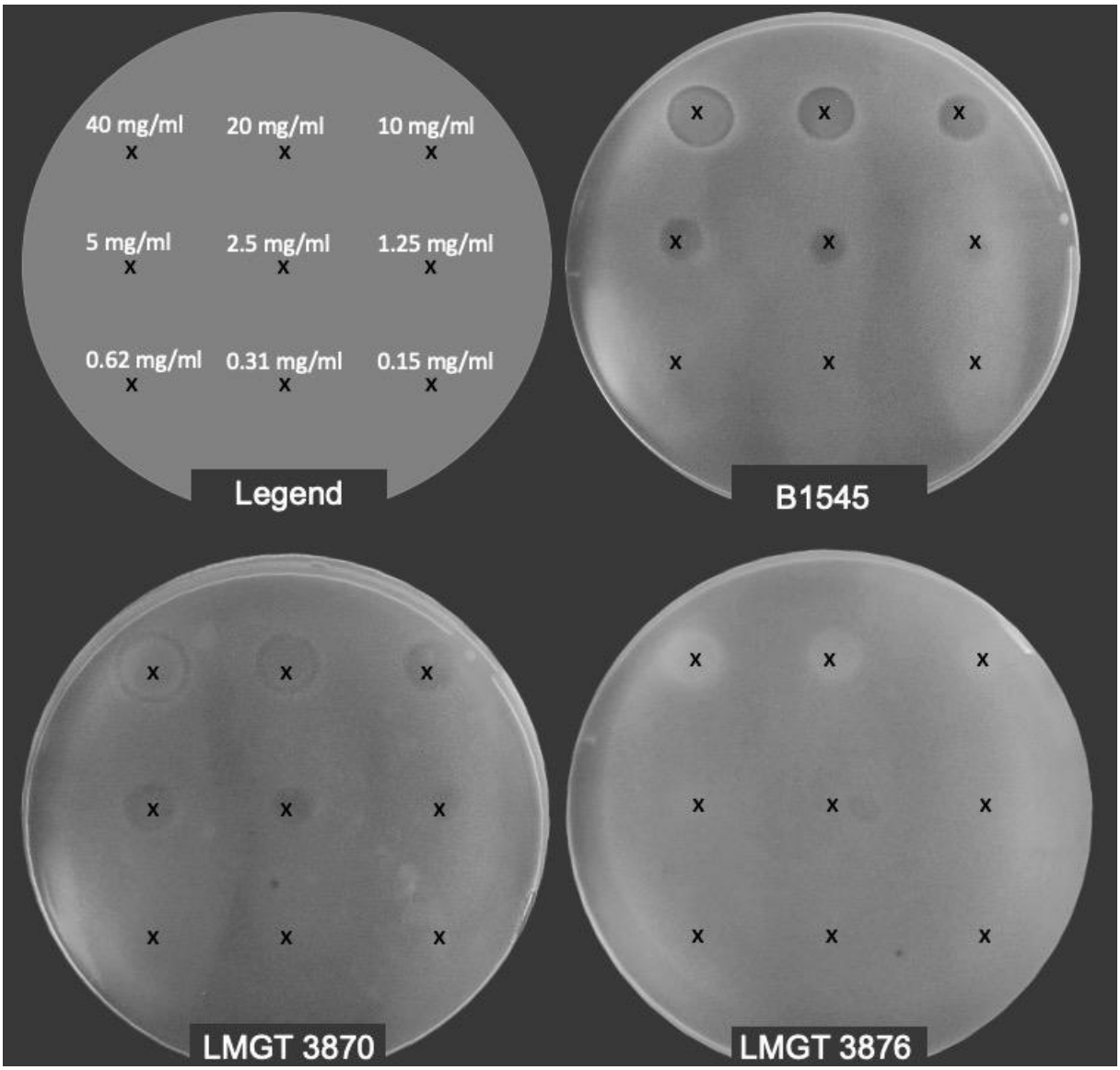

Figure 3.5: Images from the lysozyme susceptibility soft agar overlay assay for the wild type strain, B1545, and the two mutant strains LMGT 3870 and LMGT 3876. Any inhibition of growth is seen as a dark zone around the x. The diameter of the inhibition zone is negatively correlated with level of resistance. The legend indicates at what concentrations the lysozyme was applied to the soft agar layer, in a twofold dilution series. The highest concentration used was undiluted stock of 40 mg/ml freshly made lysozyme chloride from chicken egg white (Sigma-Aldrich). The volume applied was 5 µl for all spots

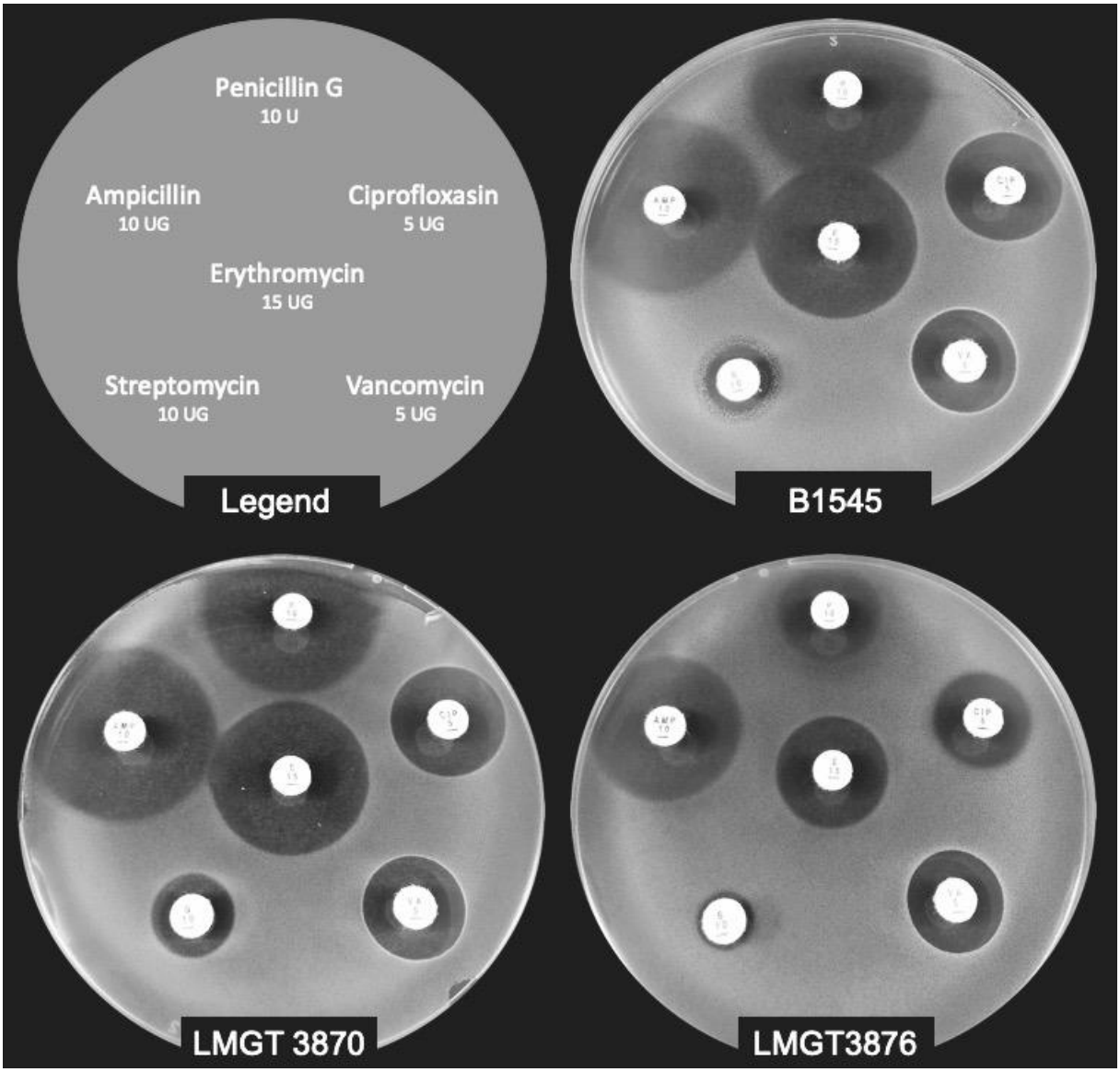

Figure 3.6: Images from the antibiotic susceptibility soft agar overlay assay for the wild type strain B1545, and the two mutant strains LMGT 3870 and LMGT 3876. Any inhibition of growth is seen as a dark zone around the discs. The diameter of the inhibition zone is negatively correlated with level of resistance. The legend indicates what type of antibiotic-disc (Thermo Fisher Diagnostics) was placed where on the soft agar layer, and what concentration they contain according to the manufacturer. The discs came from previously opened tubes that had been stored at - 20 °C for a period no longer than two months.

Again, LMGT 3876 showed an increased resistance towards all but one type of antibiotic, namely vancomycin, which appeared to be equally effective against all three strains, as seen in **Figure 3.6.** Most apparent is the increased resistance of LMGT 3876 towards penicillin G, as well as ampicillin and erythromycin. For easier comparison of the resistance levels of the strains, inhibition zone diameters were measured and color coded, as shown in **Table 3.2**. From this representation of the data, it becomes apparent that LMGT 3876 shows the most resistance towards all antibiotics tested.

Table 3.2: Measured diameter of inhibition zones for the antibiotic discs tested in the soft agar overlay assay. Each value range of 0.25 cm is given a colour code for easier visualisation of resistance levels. Darker shades of grey correspond to higher resistance.

High resistance			**Inhibition zones (cm)**					**Low resistance**
0.75 - 0.99	**1.00 - 1.24**	**1.25 -1.49**	**1.50 - 1.74**	**1.75 - 1.99**	**2.00 - 2.24**	**2.25 - 2.49**	**2.5 -2.74**	**2.75 -2.99**

	B1545	**LMGT 3870**	**LMGT 3876**
Antibiotics			
Penicillin G	*2.75 - 2.99*	*2.75 - 2.99*	*1.50 - 1.74*
Ampicillin	*2.75 - 2.99*	*2.75 - 2.99*	*2.25 - 2.49*
Erythromycin	*2.50 - 2.74*	*2.50 - 2.74*	*1.50 - 1.74*
Ciprofloxacin	*1.75 - 1.99*	*1.75 - 1.99*	*1.50 - 1.74*
Streptomycin	*1.25 - 1.49*	*1.00 - 1.24*	*0.75 - 0.99*
Vancomycin	*1.75 - 1.99*	*1.50 - 1.74*	*1.50 - 1.74*

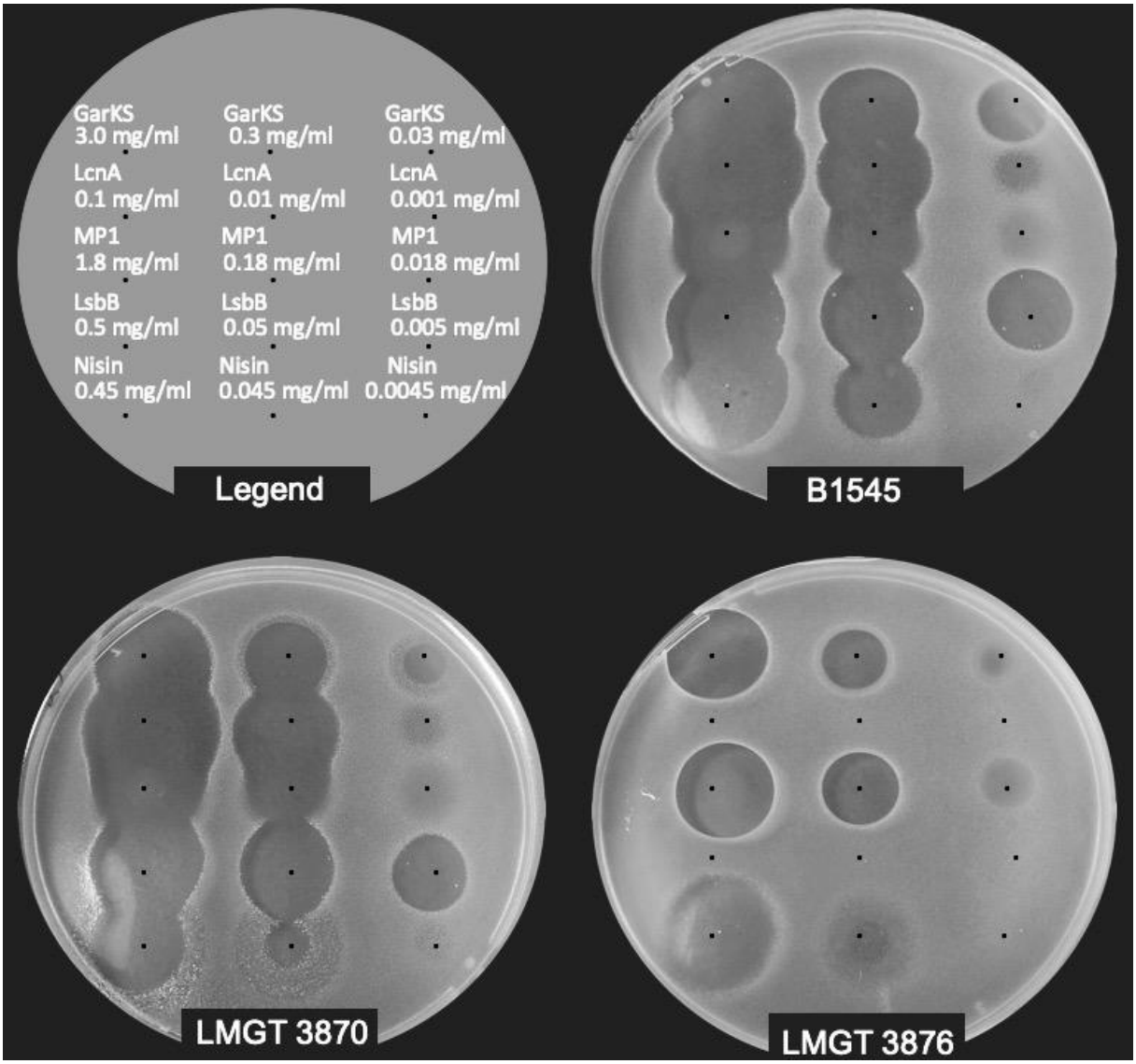

Figure 3.7: Images from the bacteriocin susceptibility soft agar overlay assay for the wild type strain B1545, and the two mutant strains LMGT 3870 and LMGT 3876. Any inhibition of growth is seen as a dark zone around the dot. The diameter of the inhibition zone is negatively correlated with level of resistance. The legend indicates where the different bacteriocins were applied to the soft agar, and at what concentration in a tenfold dilution series. The highest concentration used corresponds to undiluted stock, stored at - 20 °C. The volume applied was 5 µl for all spots.

Astonishingly, the bacteriocin susceptibility assay indicated that LMGT 3876 is completely resistant to the highly *L. lactis* specific LcnA and LsbB, which inhibits both LMGT 3870 and the wild type as seen in **Figure 3.7**. These results were confirmed by reproducing the exact same results on two separate occasions, both with two replicates. For the other bacteriocins that were tested, LMGT 3870 does show a slightly increased resistance compared to wild type, especially towards nisin.

To easier compare the resistance levels of the strains, inhibition zone diameters measured and color coded, as shown in **Table 3.3**. From this representation of the data, it becomes apparent that LMGT 3876 shows the highest degree of resistance to all bacteriocins that were tested.

Table 3.3: Measured diameter of inhibition zones of the bacteriocins tested in the soft agar assay. Each value range of 0.3 cm is given a colour code for easier visualisation of resistance levels. Darker shades of grey correspond to higher resistance.

High resistance			Inhibition zones (cm)					Low resistance
0.0 - 0.29	0.3 - 0.59	0.6 - 0.89	0.9 - 1.19	1.2 - 1.49	1.5 - 1.79	1.8 - 2.09	2.1 - 2.39	2.4 - 2.69

	B1545			LMGT 3870			LMGT 3876		
Bacteriocins	**Undiluted**	**10 x diluted**	**100 x diluted**	**Undiluted**	**10 x diluted**	**100 x diluted**	**Undiluted**	**10 x diluted**	**100 x diluted**
GarKS	*1.8 - 2.09*	*1.5 - 1.79*	*0.9 - 1.19*	*1.8 - 2.09*	*1.2 - 1.49*	*0.6 - 0.89*	*1.5 - 1.79*	*0.9 - 1.19*	*0.3 - 0.59*
LcnA	*2.1 - 2.39*	*1.8 - 2.09*	*0.6 - 0.89*	*2.1 - 2.39*	*1.8 - 2.09*	*0.6 - 0.89*	*0.0 - 0.29*	*0.0 - 0.29*	*0.0 - 0.29*
MP1	*1.5 - 1.79*	*1.2 - 1.49*	*0.6 - 0.89*	*1.8 - 2.09*	*1.2 - 1.49*	*0.6 - 0.89*	*1.2 - 1.49*	*1.2 - 1.49*	*0.6 - 0.89*
LsbB	*1.8 - 2.09*	*1.5 - 1.79*	*1.2 - 1.49*	*1.8 - 2.09*	*1.5 - 1.79*	*0.9 - 1.19*	*0.0 - 0.29*	*0.0 - 0.29*	*0.0 - 0.29*
Nisin	*1.8 - 2.09*	*1.2 - 1.49*	*0.3 - 0.59*	*1.2 - 1.49*	*0.6 - 0.89*	*0.3 - 0.59*	*1.2 - 1.49*	*0.6 - 0.89*	*0.0 - 0.29*

3.4 - Bacteriophage plaque formation assay showed no infection of LMGT 3876

The plaque formation assay, performed by our colleagues in Spain, indicated that LMGT 3876 appeared to be immune to all 11 phages tested in this assay. LMGT 3870 did not appear to have any increased resistance, on the contrary the opposite was observed for two of the phages, in that LMGT 3870 was more sensitive to phage *24* and phage *C2* compared to wild type B1545, as seen in **Figure 3.8**.

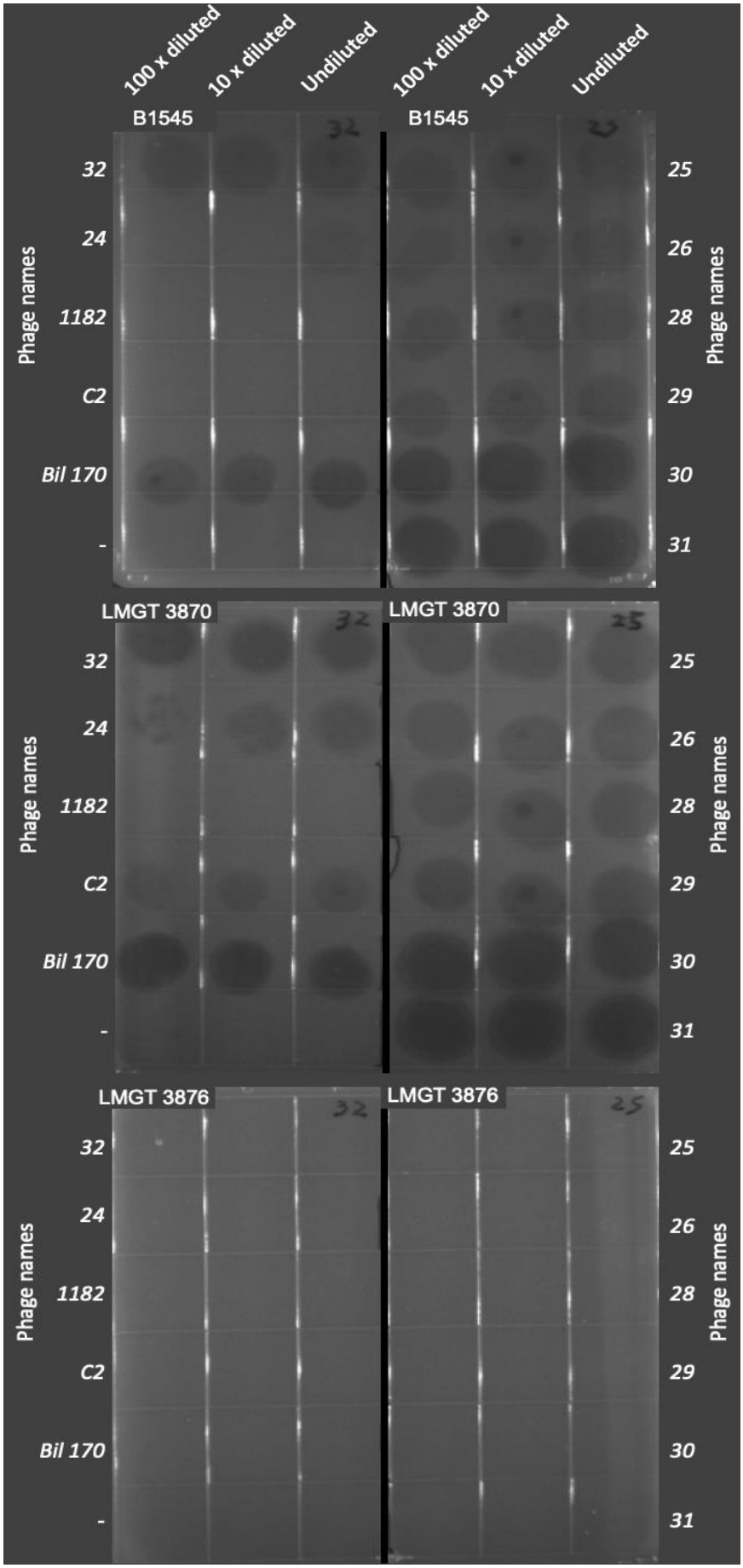

Figure 3.8: Images from the plaque formation assay performed by our colleagues in Spain, using the wild type strain B1545 and the two mutant strains LMGT 3870 and LMGT 3876. On each side of the central black line, three dilutions of the phages, marked at the top, were applied in a row, and the names of the phages applied can is seen on the left and right side of the plate. Clear zones appear dark and is a result of complete lysis of the cells. Turbid zones indicate temperate phages, which allows some cells to survive within the exposed area intact. The pages were spotted undiluted, 10 times diluted and 100 times diluted from stock isolated by enrichment with *L. lactis* IL1403. Note that the bottom row was left empty, and that phage 1182 did not infect the wild type due to an unknown error during the setup of the assay. Phage stocks had not been accurately titrated, but were all reported to be above 10^8 plaque forming units per ml.

3.5 - Cell wall thickness of LMGT 3876 differed significantly from the other two strains

As the results from the preliminary phenotypical tests indicated that the *ythA*-mutation in LMGT 3876 was severely affecting the robustness of the strain, an investigation of the cells morphology was deemed prudent. The images taken in-house using phase contrast microscopy, shown in **Figure 3.9**, did not show an obvious difference in cell size or shape. There was an observed difference in chain length when comparing the wild type to LMGT 3876 however. The wild type displayed growth as both diplococci and in longer chains. LMGT 3870 mostly displayed growth in longer chains while LMGT 3876 almost exclusively grew as diplococci.

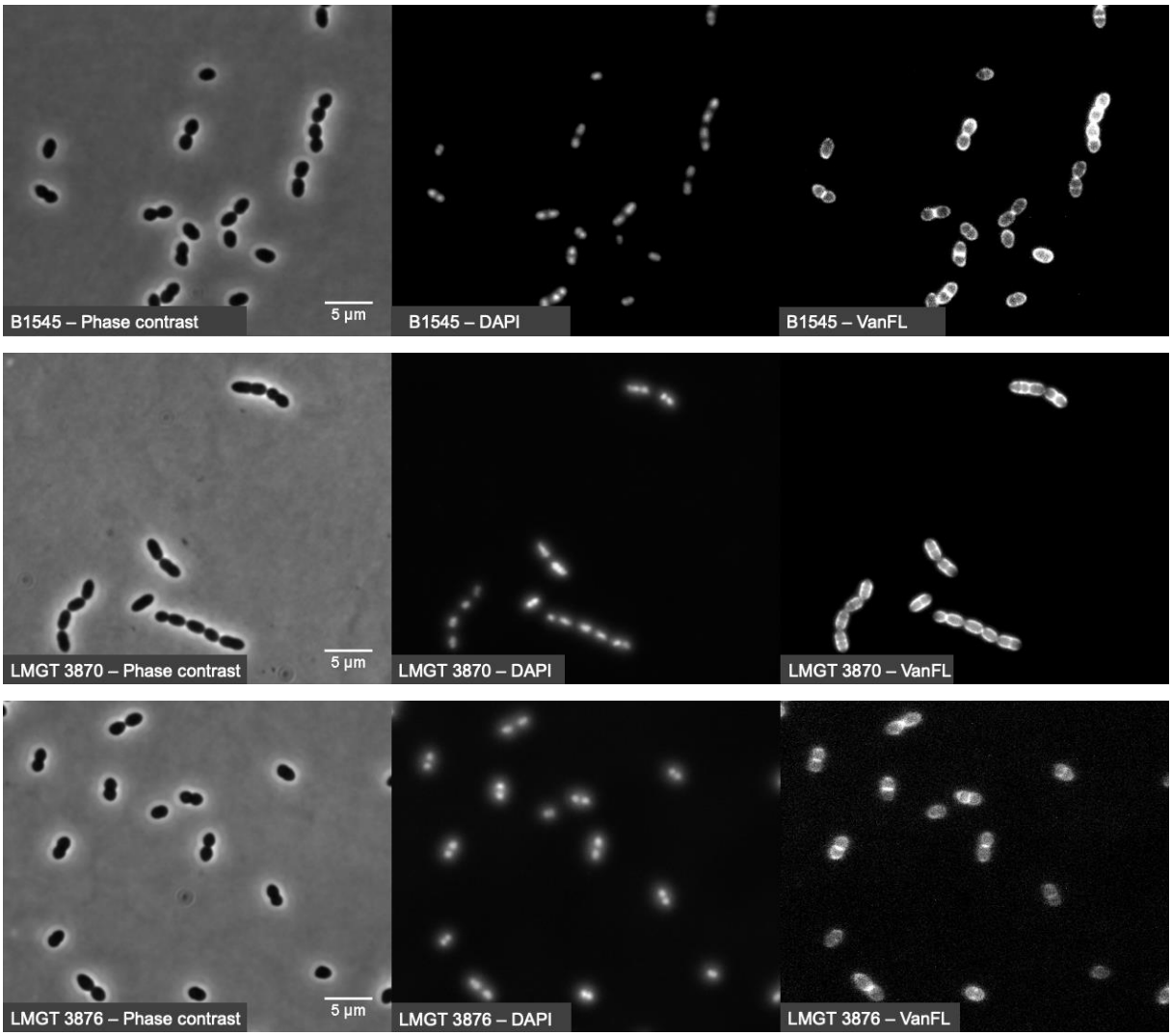

Figure 3.9: Confocal microscope images of *L. lactis* IL1403 wild type and mutant strains LMGT 3070 and LMGT 3876. Images were captured using phase contrast mode, staining with VanFL and by staining with DAPI. Scale bar = 5 µm.

Using the *ggplot* package in Rstudio, two box plots were made to visualize any difference in cell length and cell width. The plots shown in **Figure 3.10** indicate no differences in cell morphology, although LMGT 3870 appears to have slightly reduced widths then the two other strains.

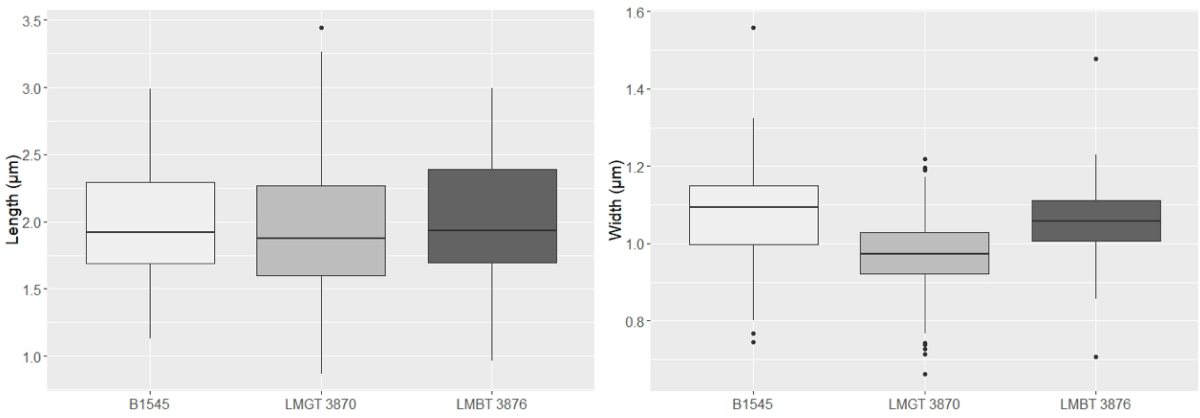

Figure 3.10: Average width and average length of the three strains that were imaged, B1545, LMGT 3870 and LMGT 3876. The median value of the measurements is marked by a horizontal line dividing the upper and lower 25 % quartile and potential outliers are represented as dots above and below the whiskers, corresponding to measurements lesser or greater then 1.5 times that of the lower and upper quartile respectively. Data was collected from a stack of four images taken from different areas of the same slides using the phase contrast setting on the microscope.

TEM images were sent to us from our colleagues at INRA in France. They uncovered some significant differences in morphology between the wild type and LMGT 3867. As seen in **Figure 3.11**, LMGT 3876 appeared to have a cell wall that was markedly thicker when compared to the wild type. For the mutant strain LMGT 3870, there did not appear to be any significant differences in morphology or cell wall thickness.

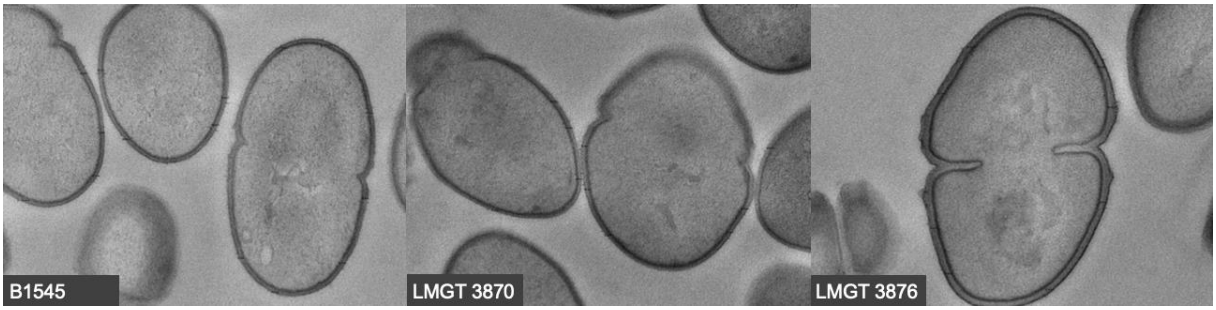

Figure 3.11: TEM-images taken at INRA, France, using a Hitachi HT7700 electron microscope operated at 80kV. The cell morphology differs significantly between the wild type strain B1545, and the mutant strain LMGT 3876, with a noticeable increase in cell wall thickness.

To more accurately quantify the differences, measurements were performed on the images taken of the cells by the technicians in France, and from that data, the plots seen in **Figure 3.12** were made. The cell wall thickness of LMGT 3876 differed from the wild type by a significant amount. Measurements of the width of the cells based on the TEM images also indicated that LMGT 3876 had a slightly wider morphology than the wild type or LMGT 3870.

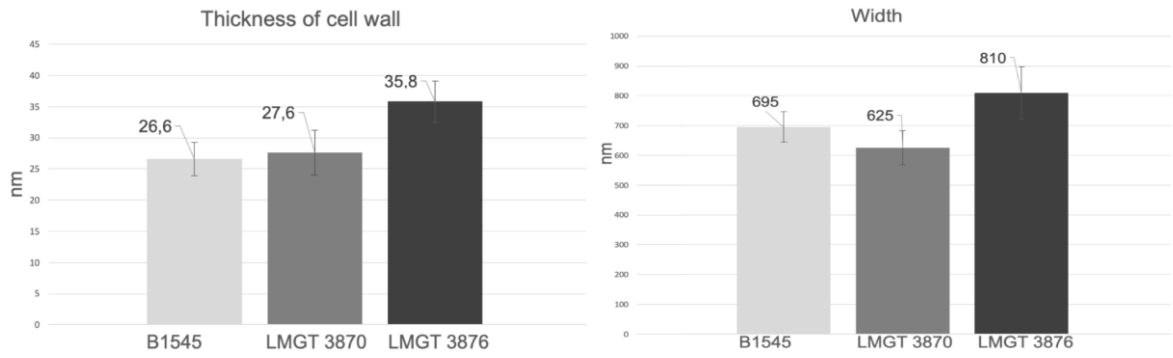

Figure 3.12: Comparison of variations in measured cell wall thickness and measured cell width for the wild type strain, LMGT 3870 and LMGT 3876. Measurements and plotting were done by our colleagues at INRA, France.

3.6 - Summary of the diverging phenotypes of mutant strain LMGT 3876

LMGT 3876 had so far displayed some remarkable phenotypical deviances from the wild type and the mutant LMGT 3870. For easier comparison of these diverging phenotypes, a summary of all results obtained so far is presented in **Table 3.4**.

Table 3.4: A summary of the genotype and phenotypes of the wild type strain and the two mutants LMGT 3870 and LMGT 3876, for a simple overview and easy comparison.

Phenotype	**B1545**	**LMGT 3870**	**LMGT 3876**
Consequence of mutation in *ythA*	-	G21E	K138*
Growth at different temperatures			
30 °C	Yes	Yes	Yes
40 °C	Reduced	Reduced	Yes
45 °C	No	No	Yes
MIC for GarKS	0.625 ng/µl	1.25 ng/µl	5.0 ng/µl
MIC for lysozyme	1.25 mg/ml	1.25 mg/ml	> 40 mg/ml
Resistance to antibiotics, diameter of inhibition zones			
Penicillin G	2.8 cm	2.6 cm	1.6 cm
Ampicillin	2.8 cm	2.8 cm	2.3 cm
Erythromycin	2.6 cm	2.5 cm	1.7 cm
Ciprofloxacin	1.8 cm	1.8 cm	1.5 cm
Streptomycin	1.3 cm	1.2 cm	0.8 cm
Vancomycin	1.6 cm	1.8 cm	1.6 cm
Resistance to bacteriocins, diameter of inhibition zones			
Garvicin KS	2.0 cm	2.0 cm	1.65 cm
Lactococcin	2.4 cm	2.35 cm	0.0 cm
Micrococcin	1.75 cm	1.85 cm	1.45 cm
LsbB	1.8 cm	1.8 cm	0.0 cm
Nisin	1.8 cm	1.45 cm	1.45 cm
Resistant to phages	24 and C2	C2	All
Average cell wall thickness	26.6 nm	27.6 nm	35.8 nm
Morphology, method of growth	Mixed	Longer chains	Diplococci

3.7 - Reverse transcription and qPCR to analyze transcriptional effects in GarKS resistant mutants and exposure to GarKS

To get further insights into the mechanisms of the GarKS resistant mutants, it was decided to perform transcription analysis to see if expression of CesSR was affected in the mutant strains. In addition, it was also decided to study the transcriptional effects *on L. lactis* IL1403 when they were exposed to sublethal concentration of GarKS, to see if this affected the CesSR pathway. In total, RNA was isolated from five samples: LMGT 3870, LMGT 3876, wild type B1545, wild type exposed to 0.1 MIC of GarKS and wild type exposed to 0.5 MIC of GarKS.

The optimized phenol:chloroform extraction proved very efficient at obtaining non-degraded RNA, and the amount of TNA isolated consequently exceeded 4000 ng/µl when measured by NanoDrop (data not shown), necessitating aliquots and dilutions to be made before DNase treatment. As seen in **Figure 3.13,** the absence of smears indicated no degradation of the RNA samples due to ribonuclease activity. Two clear bands, with an intensity ratio of approximately 1.6 - 2 to 1 for the largest fragment corresponds to the two most abundant RNA species, 23S and 16S respectively. As the samples were run on the gel without standardizing the concentrations, the bands for the two mutants LMGT 3870 and LMGT 3876 suggest lower yields of isolated RNA compared to the wild type (B1545). Indeed, this is the case when looking at the measured concentrations by the Qubit® assay, shown in **Table 3.5.** The same is observed for the samples where wild type was subjected to sublethal doses of GarKS, that resulted in lower OD_{600} compared to wild type, at the time of harvest (data not shown). A 100 bp ladder was used as reference, however this cannot be used to accurately deduce the fragment size of the RNA bands, as the ladder consists of dsDNA.

Table 3.5: Measured concentrations of RNA in all samples using the Qubit® RNA HS Assay kit with a Qubit® 2.0 fluorometer.

	LMGT 3870	**LMGT 3876**	**B1545**	**B1545 + 0.1 MIC**	**B1545 + 0.5 MIC**
Measured concentration	14.2 µg/ml	4.68 µg/ml	26.8 µg/ml	17.5 µg/ml	12.8 µg/ml

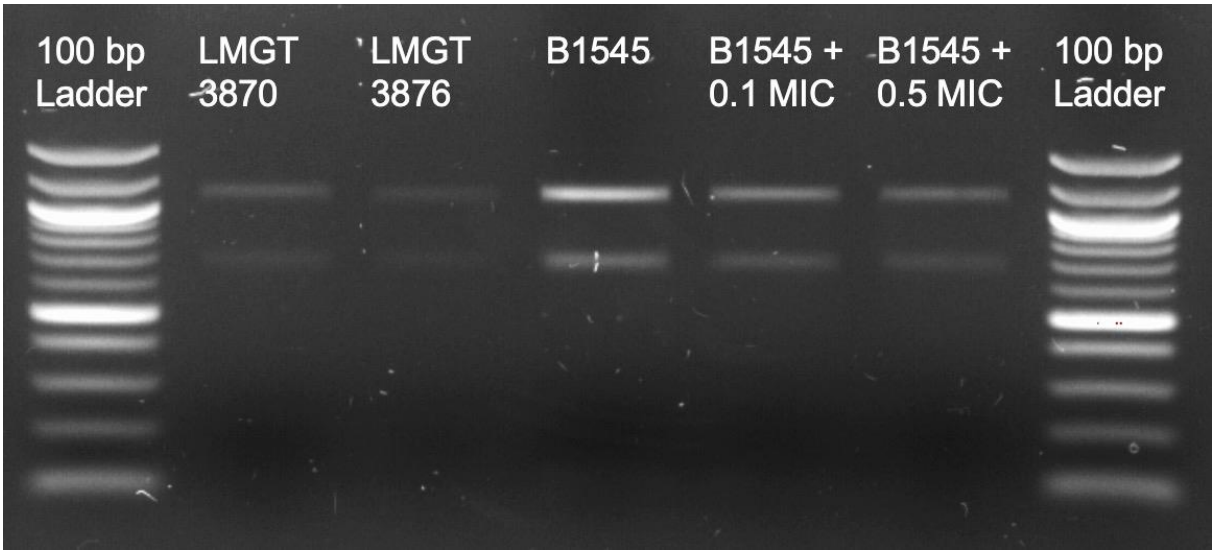

Figure 3.13: RNA integrity check on 1 % TBE agarose gel. Samples were not standardized before they were run on gel, and as such the mutant strains LMGT 3870 and LMGT 3876 show weaker bands of 23S and 16S. The RNA samples from the wild type cultures exposed to sublethal doses of GarKS, yielded visually weaker bands then the RNA sample from untreated wild type. 100 bp ladder cannot be used to estimate RNA fragment size, but was included for reference between individual gel-runs.

3.8 - Optimization of cDNA synthesis and verifying the absence of any contaminating DNA

When working with sensitive analysis methods as qPCR, it is of the utmost importance that the samples used as template are optimal for the reaction, as even tiny traces of contaminating DNA or inhibitory substances can significantly affect the results. Therefore, quality control steps that ensure template pureness and stability was given high priority. Preliminary PCR reactions, using isolated RNA after treatment with DNase as template and primers designed for the qPCR reaction, resulted in amplification of fragments of correct size (data not shown), indicating insufficient DNA degradation. This was thought to happen due to the high concentration of TNA that was isolated (> 4000 ng/µl). The reaction mix simply contained too much DNA for the DNase to degrade, also due to possible RNA-DNA hybrids forming to further prevent digestion of DNA.

However, using a tenfold dilution of the isolated TNA in the DNase reaction mix was successful, as subsequent PCR reactions using isolated RNA after DNase treatment as template along with primers designed for the qPCR reaction, see **Table A.2.2** in the Appendix, section A.2, gave no amplification after 45 cycles. After cDNA synthesis, amplification of fragments of the correct size was once again detectable, indicating a successful cDNA synthesis-reaction.

One example of these test results, using the primer targeting *ythA* can be seen in **Figure 3.14.** All other primers designed for the qPCR reactions were tested in this way using TNA, RNA and cDNA from wild type only (results not shown), which resulted in amplification of correct fragment size.

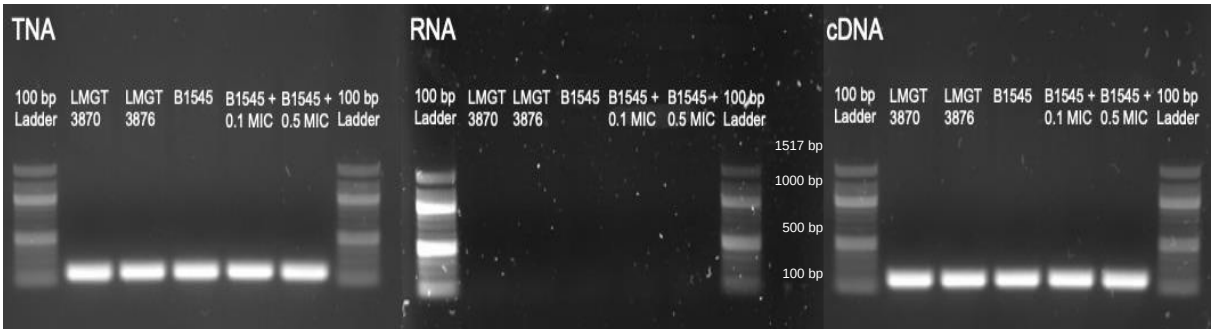

Figure 3.14: Three gel images showing the results of PCR using primers targeting *ythA* along with the different stages of RNA isolation as template. Expected amplicon size was approximately 200 bp. On the left, total nucleic acids isolated, before DNase treatment. In the middle, isolated RNA after DNase treatment. And on the right, cDNA synthesized from the RNA samples. The PCR reaction using RNA as template was run for 45 cycles, to ensure detection of even trace amounts of contaminating DNA

3.9 - Quantitative PCR for relative quantification of gene expressions using the $\Delta\Delta C_t$ Livak method for analysis

When using a relative quantification method to analyse qPCR data, primer efficiency is of high importance as the Livak method used for calculating fold change disregards actual primer efficiency and assumes 100 % efficiency in the reaction, i.e. a doubling of product per cycle (Livak and Schmittgen 2001). **Table A.2.2** in the Appendix, section A.2, contains sequences for all primers designed for the qPCR reactions. When tested with isolated gDNA from the wild type strain, they all gave satisfactory amplification within the range of concentrations tested, as seen in **Table 3.6**, all primers Melting curve analysis performed after each qPCR run yielded one peak per primer, indicating high primer specificity and no unspecific amplification (data not shown).

Table 3.6: List of primers and their efficiency when tested with wild type gDNA in a tenfold dilution series.

Primer target	Slope	R^2 - value	PCR efficiency (%)
ythA	- 3.38	0,999	97.77
ythB	- 3.39	0,999	97.42
ythC	- 3.45	0,999	95.04
ftsH	- 3.47	1,000	94.22
spxB	- 3.41	0,999	96.49
oatA	- 3.47	0,999	94.29
cesS	- 3.50	0,999	92.98
cesR	- 3.50	0,999	92.92
tuf	- 3.40	0,999	96.79
gyrA	- 3.32	0,999	99.98

The decision was made to use the housekeeping gene *tuf* as a reference, as this gene showed a more stable expression level in all the samples compared to the other housekeeping gene tested, *gyrA.* As the primer efficiencies for all primer pairs were within 5 % of the efficiencies of the *tuf* primers, the $\Delta\Delta C_t$ Livak method could be used to calculate the fold change in expression levels compared to the expression levels of the wild type. For a full overview of calculations performed with the data from the qPCR reactions, see Appendix, section A.1.

3.10 - *L. lactis* IL1403 wild type upregulate CesSR upon exposure to sublethal doses of GarKS

A cut off was set for calculated fold change values < 2. This was done to only emphasize sample runs that showed a significant upregulation of the genes. Fold-changes in expression of genes putatively involved in CesSR were determined in *L. lactis* wild type upon exposure to 0.1x MIC and 0.5x MIC GarKS relative to *L. lactis* wild type grown in the absence of GarKS, and the results are given in **Table 3.7**. In the samples of wild type exposed GarKS equivalent to 0.1 MIC, the only genes showing significant upregulations was the *yth-operon*, *spxB* and *oatA*. The other genes tested, *ftsH*, *cesS* and *cesR,* all show a slight upregulation, but the fold change fails to exceed the cut off value. In the samples of wild type exposed GarKS equivalent to 0.5 MIC, a significant upregulation of all genes associated with CesSR, apart from *ftsH,* was observed. This general trend of higher upregulation in samples exposed to higher dose of GarKS is observed is noteworthy.

Table 3.7: Calculated fold change in expression levels of genes tested for the mutant LMGT 3870, and the two samples of wild type subjected to sublethal doses of GarKS. Expression is presented as a range of calculated fold difference +/- standard deviation. A cut off was decided for fold change values < 2. Fold changes > 2 are highlighted in bold.

Gene	**Fold change in expression levels compared to wild type**		
	LMGT 3870	**B1545 + 0.1 MIC**	**B1545 + 0.5 MIC**
ythA	*0.60 - 0.70*	***2.02 - 2.31***	***3.61 - 4.35***
ythB	*0.69 - 0.80*	***2.59 - 2.95***	***3.57 - 4.68***
ythC	*0.84 - 0.97*	***2.51 - 2.89***	***3.42 - 4.27***
ftsH	*0.83 - 0.95*	*1.11 - 1.42*	*1.63 - 1.88*
spxB	*1.06 - 1.21*	***2.33 - 2.81***	***3.75 - 4.37***
oatA	*1.00 - 1.17*	***3.44 - 4.38***	***5.00 - 5.72***
cesS	*0.53 - 0.59*	*1.49 - 1.67*	***1.77 - 2.03***
cesR	*0.54 - 0.66*	*1.28 - 1.52*	***2.01 - 2.26***

3.11 - Transcriptional analysis of LMGT 3870 indicated downregulation of CesSR

Comparison of transcription of CesSR-related genes in LMGT 3870 relative to the wild type, indicated no upregulation, as none of the genes tested showed a fold-change > 2. On the contrary, calculated fold change indicate downregulation for most of the genes targeted in the qPCR sample runs. Note that *cesS* and *cesR* show a near halved level of expression compared to untreated wild type, shown in **Table 3.7**.

3.12 - Transcriptional analysis of LMGT 3876 did not give any result

Synthesized cDNA from LMGT 3876 did not result in any amplification in the qPCR sample runs. It was first thought that this was due to difficulties extracting RNA without contamination form inhibitory substances. This was debunked by running a PCR with 16S primers using Isolated RNA from LMGT 3876 along with isolated gDNA from wild type. This would reveal if the isolated RNA contained any inhibitory substances that could interfere with the amplification of 16S rRNA gene from the gDNA. This was not the case (results not shown), and it was concluded that cDNA synthesis was not being inhibited by any substances in the isolated RNA from LMGT3876, and that the problem must lie elsewhere. Further testing of the primers was conducted to see if there was any amplification of LMGT 3876 cDNA using Phusion® Taq polymerase in a 40 cycle reaction. The results of this investigation are included in the Appendix, section A.5.

To get further insights into the transcriptional differences, it was decided to perform RNA sequencing for each of the mutant strains and for the wild type. The number of reads generated (150 bp, paired end) was 7.456.208 for LMGT 3870, 6.909.980 for LMGT 3876 and 6.761.128 for the wild type. Only the results for the same genes that were selected for qPCR are included here. No reads from LMGT 3876 mapped to the reference genome of *L. lactis* IL1403. Shown in **Figure 3.15** is the fragments per kilobase million (FPKM) -values from LMGT 3870 and wild type B1545. These values indicate low levels of basal transcription and no significant regulation, except for cesR. This gene has a FPKM value over three times higher in LMGT 3870 compared to wild type. Surprisingly, no reads were mapped to *ythB* in any of the samples. Note that CesSR-associated genes are transcribed at a generally low level.

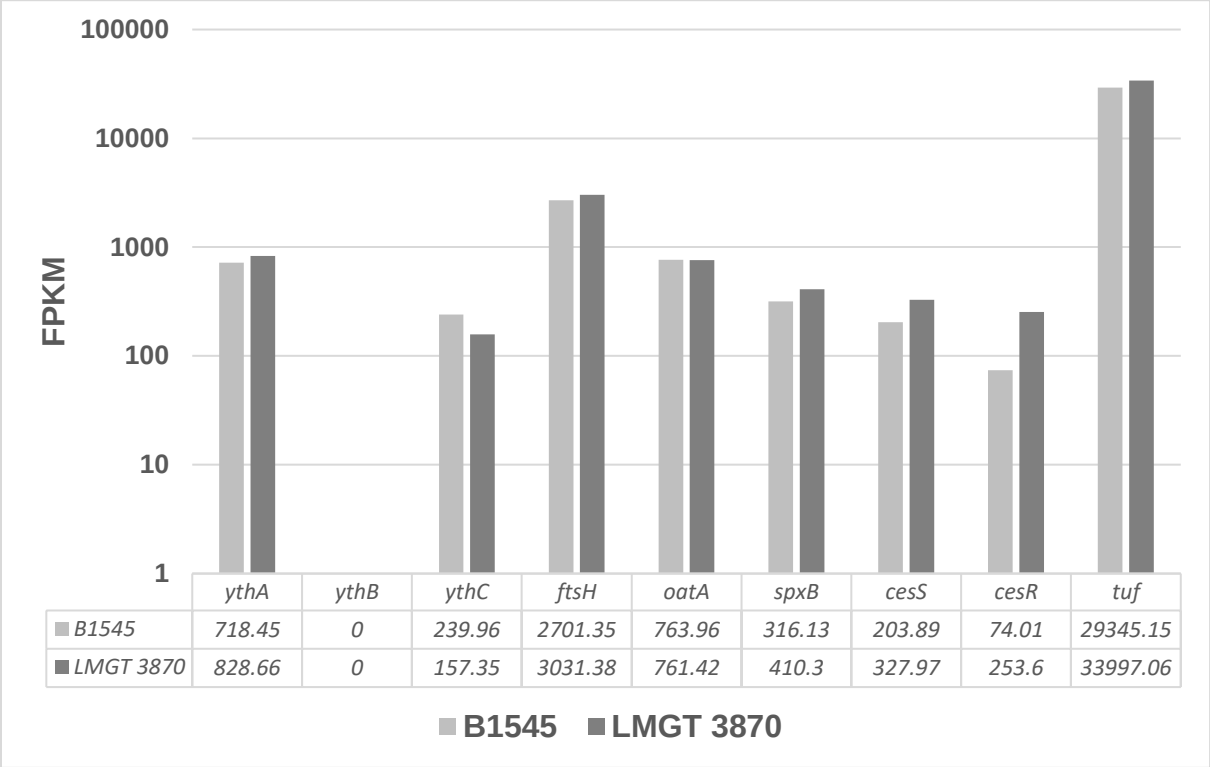

	ythA	ythB	ythC	ftsH	oatA	spxB	cesS	cesR	tuf
B1545	718.45	0	239.96	2701.35	763.96	316.13	203.89	74.01	29345.15
LMGT 3870	828.66	0	157.35	3031.38	761.42	410.3	327.97	253.6	33997.06

Figure 3.15: FPKM values for LMGT 3870 and wild type, B1545. FPKM values have been standardized and are directly comparable, where higher values indicate a higher level of expression. FPKM values are plotted on a logarithmic y-axis.

3.13 - Complementing LMGT 3870 did not result in reversion of phenotype

To confirm that the observed phenotype in a mutant is in fact caused by a mutation in a specific gene, a useful approach is to complement the mutant for that same gene. Accordingly, a fully functional copy of the gene is inserted into the mutant, thus restoring the function of that gene in the cell. The mutant can then be tested under the same conditions used to discover the mutant phenotypes. If the phenotype reverts to one that resembles the wild type, it can then be inferred that the mutation was the cause of the observed phenotype. Alternatively, inserting the gene in an expression vector for highly upregulated expression is also interesting, to see if high levels of the gene product affects the phenotype in other ways.

LMGT 3876 proved difficult to transform with the conventional protocol involving growth of lactococci in glycine-containing medium. Strangely, LMGT 3876 showed resistance to high concentrations of glycine, thus making it difficult to obtain competent cells. As a result, several attempts to transform this strain were unsuccessful. LMGT 3870 and the wild type were successfully transformed with a plasmid containing *ythA* with an N-terminal flag tag and with a plasmid containing *ythA* with a C-terminal flag tag. The empty plasmid was also successfully transformed into wild type and LMGT 3870. When subjected to the same phenotypical tests however, the complemented LMGT 3870 did not display any reversion in phenotype, except for slightly slower growth rate (data not shown). Still, there was no difference when comparing complemented LMGT 3870 with LMGT 3870 transformed with empty vector.

3.14 - DNA fingerprinting reveals a possible contamination of the LMGT 3876 stock

The results of the phenotypical tests continually hinted at a possible problem with contamination of the LMGT 3876 strain. Especially when the results of the work being done externally in Spain and France were sent to us. It was deemed unlikely that these extreme differences in phenotypes could be attributed to a single mutation. Using qPCR to quantify gene expression changes in LMGT 3876 had also been unsuccessful, and making the strain competent was not achieved. So, to investigate whether the results hitherto obtained were sound, or if they stemmed from some form of contamination, a repetitive extra genic palindromic-PRC (rep-PCR) was performed.

As seen in **Figure 3.16**, the amplification of wild type and LMGT 3870 gDNA gave near identical patterns, indicating that they are derived from the same subspecies. Also, when comparing to another *L. lactis* reference strain (B1627), some bands are identical, some are absent and some appear to deviate in size from the wild type and LMGT 3870. However, LMGT 3876 showed a distinctly different pattern that did not match any of the other strains at all.

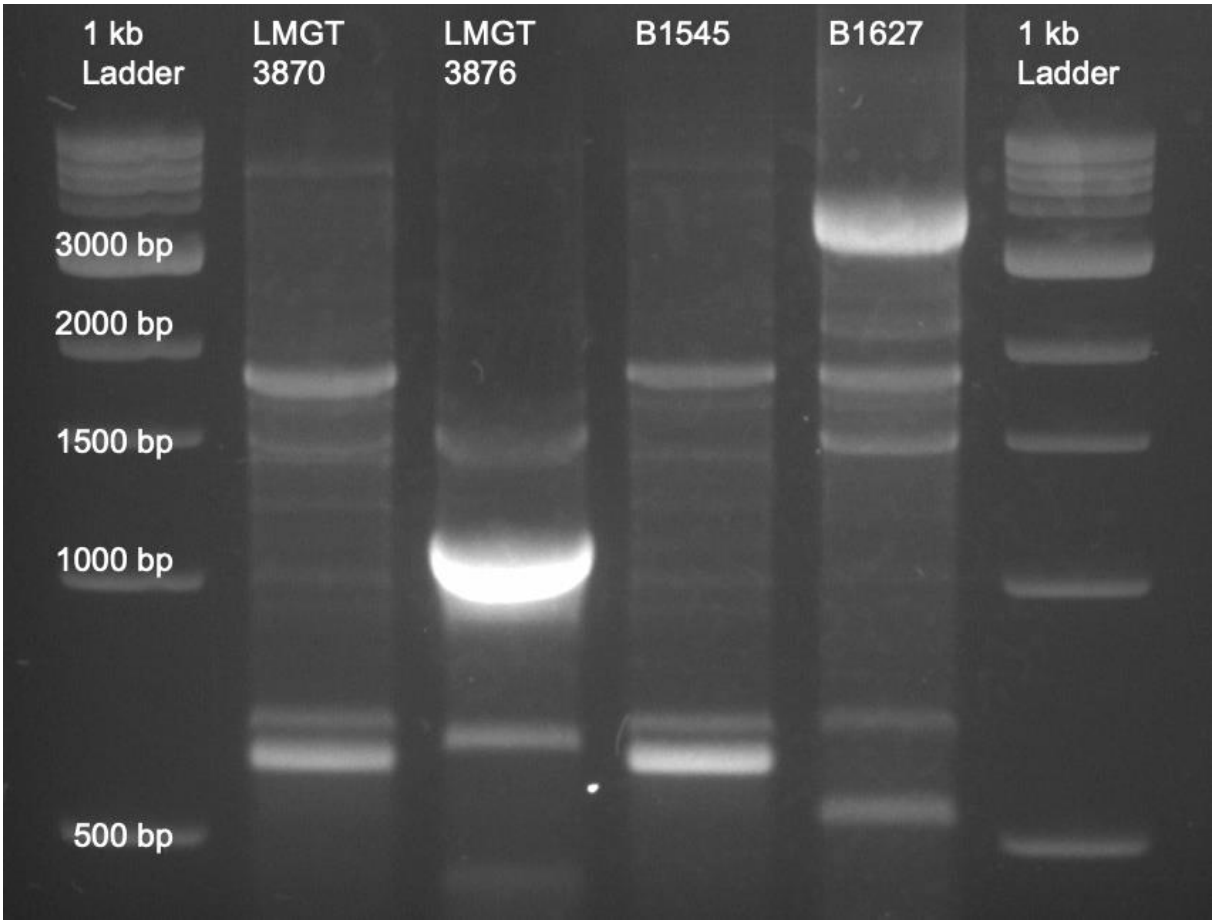

Figure 3.16: Amplified fragments following the rep-PCR. 10 µl PCR product was run on a 1.5 % TAE gel at 60 V for 1 hour. A nisin-producing strain of *L. lactis*, B1627, was used as a reference. 1 kb ladder (NEB) was used as a marker.

3.15 - Sequencing of the 16S rRNA gene confirms a systemic contamination of LMGT 3876

Continuing the verification that the strains where of the same species, it was decided that the 16S rRNA gene for all strains were to be sequenced. The results were conclusive in that the strain LMGT 3876 was identified as *Enterococcus faecium*, and not *L. lactis* IL1403. The same was the case for strains LMGT 3875 and LMGT 3878, which were included in the sequencing for investigative purposes. Further inquiry revealed a systemic contamination of *E. faecium*, not only in the frozen stock from which all subsequent cultivation of LMGT 3876 was performed, but also in the permanent storage where LMG keeps the strains. It also appeared that the cultures in the stocks were pure *E. faecium*, and not primarily *L. lactis* IL1403 contaminated by *E. faecium,* as the sequences was of good quality and yielded one consensus sequence, as seen in **Figure 3.17**.

Enterococcus faecium strain APR 210 16S ribosomal RNA gene, partial sequence
Sequence ID: HM481246.1 Length: 1320 Number of Matches: 1

Range 1: 19 to 1121 GenBank Graphics ▼ Next Match

Score	Expect	Identities	Gaps	Strand
2032 bits(1100)	0.0	1102/1103(99%)	0/1103(0%)	Plus/Plus

```
Query  1     TGCTCACCGGAAAGAGGAGTGGCGAACGGGTGAGTAACACGTGGGTAACCTGCCCATCAG  60
             ||||||||||||||| ||||||||||||||||||||||||||||||||||||||||||||
Sbjct  19    TGCTCACCGGAAAGAAGAGTGGCGAACGGGTGAGTAACACGTGGGTAACCTGCCCATCAG  78

Query  61    AAGGGGATAACACTTGGAAACAGGTGCTAATACCGTATAACAATCGAAACCGCATGGTTT  120
             ||||||||||||||||||||||||||||||||||||||||||||||||||||||||||||
Sbjct  79    AAGGGGATAACACTTGGAAACAGGTGCTAATACCGTATAACAATCGAAACCGCATGGTTT  138

Query  121   TGATTTGAAAGGCGCTTTCGGGTGTCGCTGATGGATGGACCCGCGGTGCATTAGCTAGTT  180
             ||||||||||||||||||||||||||||||||||||||||||||||||||||||||||||
Sbjct  139   TGATTTGAAAGGCGCTTTCGGGTGTCGCTGATGGATGGACCCGCGGTGCATTAGCTAGTT  198

Query  181   GGTGAGGTAACGGCTCACCAAGGCCACGATGCATAGCCGACCTGAGAGGGTGATCGGCCA  240
             ||||||||||||||||||||||||||||||||||||||||||||||||||||||||||||
Sbjct  199   GGTGAGGTAACGGCTCACCAAGGCCACGATGCATAGCCGACCTGAGAGGGTGATCGGCCA  258

Query  241   CATTGGGACTGAGACACGGCCCAAACTCCTACGGGAGGCAGCAGTAGGGAATCTTCGGCA  300
             ||||||||||||||||||||||||||||||||||||||||||||||||||||||||||||
Sbjct  259   CATTGGGACTGAGACACGGCCCAAACTCCTACGGGAGGCAGCAGTAGGGAATCTTCGGCA  318

Query  301   ATGGACGAAAGTCTGACCGAGCAACGCCGCGTGAGTGAAGAAGGTTTTCGGATCGTAAAA  360
             ||||||||||||||||||||||||||||||||||||||||||||||||||||||||||||
Sbjct  319   ATGGACGAAAGTCTGACCGAGCAACGCCGCGTGAGTGAAGAAGGTTTTCGGATCGTAAAA  378

Query  361   CTCTGTTGTTAGAGAAGAACAAGGATGAGAGTAACTGTTCATCCCTTGACGGTATCTAAC  420
             ||||||||||||||||||||||||||||||||||||||||||||||||||||||||||||
Sbjct  379   CTCTGTTGTTAGAGAAGAACAAGGATGAGAGTAACTGTTCATCCCTTGACGGTATCTAAC  438

Query  421   CAGAAAGCCACGGCTAACTACGTGCCAGCAGCCGCGGTAATACGTAGGTGGCAAGCGTTG  480
             ||||||||||||||||||||||||||||||||||||||||||||||||||||||||||||
Sbjct  439   CAGAAAGCCACGGCTAACTACGTGCCAGCAGCCGCGGTAATACGTAGGTGGCAAGCGTTG  498

Query  481   TCCGGATTTATTGGGCGTAAAGCGAGCGCAGGCGGTTTCTTAAGTCTGATGTGAAAGCCC  540
             ||||||||||||||||||||||||||||||||||||||||||||||||||||||||||||
Sbjct  499   TCCGGATTTATTGGGCGTAAAGCGAGCGCAGGCGGTTTCTTAAGTCTGATGTGAAAGCCC  558

Query  541   CCGGCTCAACCGGGGAGGGTCATTGGAAACTGGGAGACTTGAGTGCAGAAGAGGAGAGTG  600
             ||||||||||||||||||||||||||||||||||||||||||||||||||||||||||||
Sbjct  559   CCGGCTCAACCGGGGAGGGTCATTGGAAACTGGGAGACTTGAGTGCAGAAGAGGAGAGTG  618

Query  601   GAATTCCATGTGTAGCGGTGAAATGCGTAGATATATGGAGGAACACCAGTGGCGAAGGCG  660
             ||||||||||||||||||||||||||||||||||||||||||||||||||||||||||||
Sbjct  619   GAATTCCATGTGTAGCGGTGAAATGCGTAGATATATGGAGGAACACCAGTGGCGAAGGCG  678

Query  661   GCTCTCTGGTCTGTAACTGACGCTGAGGCTCGAAAGCGTGGGGAGCAAACAGGATTAGAT  720
             ||||||||||||||||||||||||||||||||||||||||||||||||||||||||||||
Sbjct  679   GCTCTCTGGTCTGTAACTGACGCTGAGGCTCGAAAGCGTGGGGAGCAAACAGGATTAGAT  738

Query  721   ACCCTGGTAGTCCACGCCGTAAACGATGAGTGCTAAGTGTTGGAGGGTTTCCGCCCTTCA  780
             ||||||||||||||||||||||||||||||||||||||||||||||||||||||||||||
Sbjct  739   ACCCTGGTAGTCCACGCCGTAAACGATGAGTGCTAAGTGTTGGAGGGTTTCCGCCCTTCA  798

Query  781   GTGCTGCAGCTAACGCATTAAGCACTCCGCCTGGGGAGTACGACCGCAAGGTTGAAACTC  840
             ||||||||||||||||||||||||||||||||||||||||||||||||||||||||||||
Sbjct  799   GTGCTGCAGCTAACGCATTAAGCACTCCGCCTGGGGAGTACGACCGCAAGGTTGAAACTC  858

Query  841   AAAGGAATTGACGGGGGCCCGCACAAGCGGTGGAGCATGTGGTTTAATTCGAAGCAACGC  900
             ||||||||||||||||||||||||||||||||||||||||||||||||||||||||||||
Sbjct  859   AAAGGAATTGACGGGGGCCCGCACAAGCGGTGGAGCATGTGGTTTAATTCGAAGCAACGC  918

Query  901   GAAGAACCTTACCAGGTCTTGACATCCTTTGACCACTCTAGAGATAGAGCTTCCCCTTCG  960
             ||||||||||||||||||||||||||||||||||||||||||||||||||||||||||||
Sbjct  919   GAAGAACCTTACCAGGTCTTGACATCCTTTGACCACTCTAGAGATAGAGCTTCCCCTTCG  978

Query  961   GGGGCAAAGTGACAGGTGGTGCATGGTTGTCGTCAGCTCGTGTCGTGAGATGTTGGGTTA  1020
             ||||||||||||||||||||||||||||||||||||||||||||||||||||||||||||
Sbjct  979   GGGGCAAAGTGACAGGTGGTGCATGGTTGTCGTCAGCTCGTGTCGTGAGATGTTGGGTTA  1038

Query  1021  AGTCCCGCAACGAGCGCAACCCTTATTGTTAGTTGCCATCATTCAGTTGGGCACTCTAGC  1080
             ||||||||||||||||||||||||||||||||||||||||||||||||||||||||||||
Sbjct  1039  AGTCCCGCAACGAGCGCAACCCTTATTGTTAGTTGCCATCATTCAGTTGGGCACTCTAGC  1098

Query  1081  AAGACTGCCGGTGACAAACCGGA  1103
             |||||||||||||||||||||||
Sbjct  1099  AAGACTGCCGGTGACAAACCGGA  1121
```

Figure 3.17: BLAST search results of LMGT 3876 16S rRNA sequence, generating hits with >99 % match with *E. faecium.* Strains LMGT 3875 and LMGT 3878 gave identical matches.

4 - Discussion

4.1 - Contamination of LMGT 3876 invalidates the results of the phenotypic assays

Initially, when considering the phenotypes displayed in the selected *L. lactis* IL1403 mutant LMGT 3876, it appeared that the frameshift mutation resulting in the K138* truncation of YthA resulted in several extreme phenotypes when compared to the wild type. As collection of data from the phenotypical assays progressed, two possible explanations seemed likely. Either this mutation somehow induces constitutive activation of the cell envelope stress response pathway, resulting in such extensive modification of the cell wall as to make LMGT 3876 extremely robust. Or another possible explanation, that in hindsight seems more likely, was that the phenotypes observed could stem from some form of contamination. As the preliminary sequencing of *ythA* indicated that these strains were indeed *L. lactis* IL1403, as seen in **Figure 3.2,** the latter was deemed unlikely. Indeed, in the case of LMGT 3870 and LMGT 3876, repeated sequencing of *ythA* matched that which was previously reported, with identical amino acid consequences of the mutations. As such it was determined early in the process that the work with the three selected strains were to continue, as no other phenotypical tests had been performed yet that indicated a possible contamination.

After collection of data and discussing our findings with our colleagues in Spain and France, a more thorough investigation was conducted. Not surprisingly, the preliminary fingerprinting of the strains strongly suggested that LMGT 3876 was not a derivative of wild type *L. lactis* IL1403. After sequencing the 16S rRNA gene it was indeed confirmed that LMGT 3876 was *E. faecium,* as seen in **Figure 3.17**. In this thesis, *ythA* from LMGT 3876 was sequenced two times, independently and on separate occasions. When taking into consideration that this gave a 99 % match, (100 % match was not possible due to the mutation) to *L. lactis* IL1403, as shown in **Figure 3.2**, the reason as to how this could occur is not immediately apparent. From these

results, it seemed that the LMGT 3867 frozen stock contained only *E. faecium* when sequencing the 16S rRNA gene, and only *L. lactis* IL1403 when sequencing *ythA*. It is still unknown how the initial amplification and sequencing of the *L. lactis ythA* gene variant from this stock was possible.

Upon further investigation, it was revealed that three of the frozen stocks provided at the start of this work was *E. faecium* and not *L. lactis* IL1403. The three strains that initially showed the highest MIC for GarKS, LMGT 3875, LMGT 3876 and LMGT 3878, as shown in **Table 3.1**, were also identified as *E. faecium.* This effectively nullifies the comparative results for LMGT 3876 in this thesis, both the increased resistance to bacteriocins and antibiotics as well as the difference in cell wall thickness. The seemingly extreme heat tolerance can easily be explained, as *E. faecium* has an optimal temperature for growth at around 45 °C. The phage plaque assay also makes much more sense, since all the phages tested were specific for *L. lactis.* This contamination also explains the unsuccessful attempts to quantify gene expression using primers that were designed to be specific for *L. lactis* IL1403, evidenced by the highly unspecific amplification achieved in **Figure A.5.1 i**n the Appendix, section 5.

4.2 - Stress induces upregulation of key genes in the cell envelope stress response system, as well as the *yth*-operon

Two main arguments can be made from the gene expression analysis. Firstly, sublethal doses of GarKS affects the expression of all the genes associated with CesSR, as well as the genes in the *yth*-operon. This can be seen in **Table 3.7**, where the wild type strain exposed to sublethal doses of GarKS shows a significant upregulation of all genes, apart from *ftsH*. This protease is indeed upregulated, but the level of upregulation does not exceed the threshold set at > 2-fold change. Other studies reveal a similar, lower degree of upregulation of FtsH that can be attributed to the need for a highly specific and precise stress response (Pinto, Kuipers et al. 2011, Guo and Gross 2014). If indeed FtsH degrades YthA and further activates the stress response, a level of regulation that is disproportionate to the stress factor may be detrimental for the cell due to exhaustion of energy supplies (Gur, Biran et al. 2011).

Secondly, there seemed to be a correlation between the amount of GarKS the cells were subjected to and the level of upregulation. However, the range that was tested was limited in that the wild type was only exposed to two doses, equivalent to 0.1 and 0.5 times the wild type MIC-value of GarKS. Further experimentation with a wider range of sublethal doses could enforce the notion of this correlation, as the present results indicate a response that is proportional to the level of stress. For wild type exposed to 0.5 MIC, relatively high upregulation was found for several genes, most notably for *spxB*, *oatA* and the *yth*-operon. This data further indicates the involvement of the YthA in the CesSR pathway in cells under stress and is compatible with our hypothesized model.

The intermediary mutant LMGT 3870 on the other hand, did not show any significant upregulation of the genes associated with CesSR. On the contrary, as shown in **Table 3.7**, most of the genes appeared to be downregulated, with a fold change value < 1. Indeed, the central genes of the TCS, *cesS* and *cesR,* appear to be expressed at near half the level of untreated wild type, suggesting that CesR is not activated by the histidine kinase CesS. If this is directly due to the mutation in YthA is not yet clear. Regarding the transcriptome analysis, even levels of expression in LMGT 3870 and wild type, suggests no activation of CesSR as a result of the mutation in *ythA*. Some inconsistencies between the qPCR results and transcriptome analysis are observed. As shown in **Figure 3.15**, only CesR appears to be significantly upregulated, conversely to the indicated downregulation from the qPCR results. RNA-sequencing indicates that the transcription levels of genes associated with CesSR are generally very low. Therefore, it would be intuitive to assume that small variations in expression, and sample variations introduced during handling, will result in large differences when analysed with qPCR.

The observed downregulation of CesSR was unexpected in LMGT 3870, as this mutant shows increased resistance to GarKS, as well as slightly increased resistance to other antimicrobials. This was thought to stem from an upregulation of CesSR, and without this regulation, the increased resistance shown in LMGT 3870 becomes difficult to explain by our working model. However, the substitution mutation in *ythA* causes the small non-polar amino acid glycine to be replaced by the larger and charged amino acid glutamic acid. This could have a substantial effect on the shape and

function of YthA. The observed downregulation could be a consequence of this mutation, which may alter the binding affinity of YthA to FtsH or to CesS, resulting in lower activation of CesSR in LMGT 3870 than in wild type.

It should be noted that the C_t values of the reference gene *tuf* were similar in all samples, except for LMGT3870, where the fluorescent signal exceeded the threshold more than one cycle earlier than in the other samples, as shown in **Table A.1.1** in the Appendix, section A.1. RNA-sequencing further indicated that *tuf* has an approximately 1.15 times higher FPKM value in LMGT 3870 compared to wild type, as seen in **Figure 3.15**. This could affect the calculations performed with the Livak method, and may explain the downregulation of CesSR that is indicated by the qPCR results. However, the calculations using the Livak method should be adequately valid when taking the individual genes associated standard deviations into consideration.

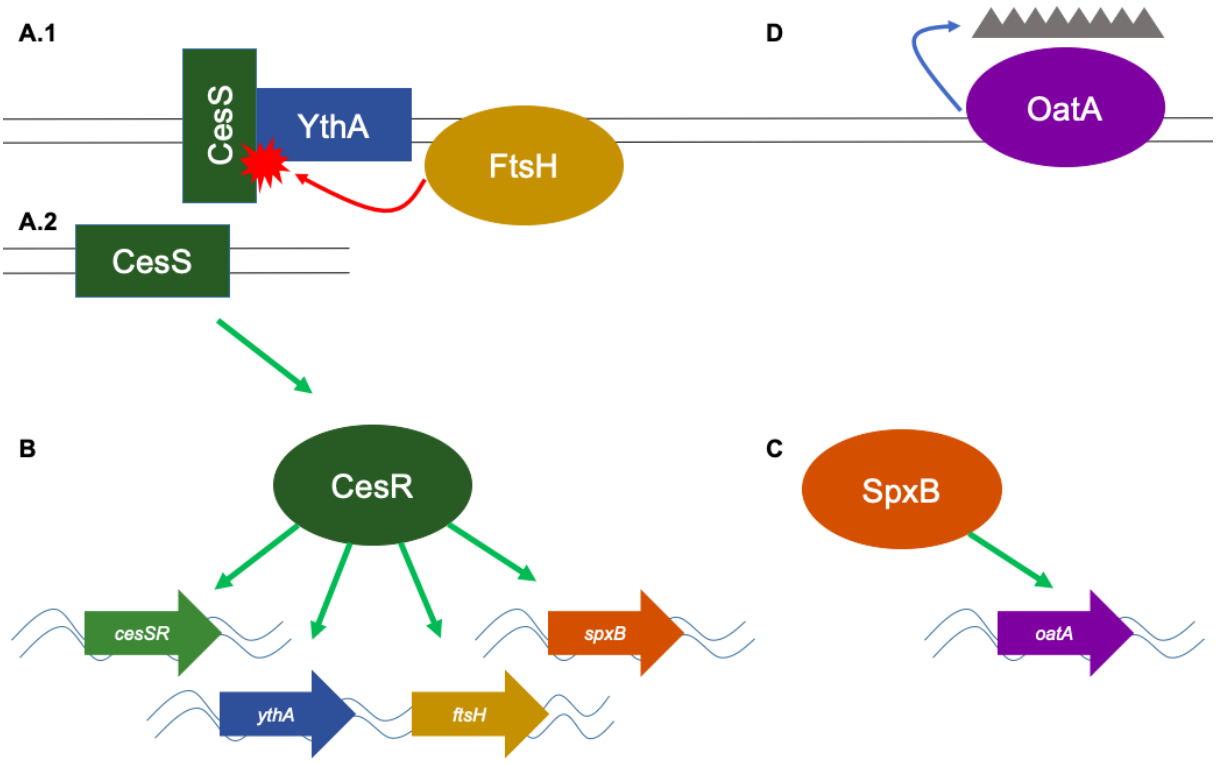

Figure 4.1: Illustration of hypothesized mechanism of CesSR, updated after considering qPCR data, in which the role of YthA is incorporated. YthB and YthC is not included in the model as their functions are unknown. **A.1** - As a result of an external stress factor, YthA is targeted for degredation by the membrane anchored protease FtsH. **A.2** - When the CesS-antagonist YthA is degraded, the still membrane bound CesS becomes able to activate the response regulator CesR. **B** - CesR facilitates the transcription of *cesSR,* resulting in a positive feedback loop, as well as *ythA, ftsH* and *spxB.* **C** - SpxB facilitates the transcription of *oatA.* **D** - OatA catalyses the acetylation of PG, illustrated as grey spikes.

Based on these new data acquired by qPCR of wild type subjected to sublethal doses of GarKS, an updated version of the working model can be inferred, as illustrated in **Figure 4.1**. We propose that the interaction between one or more of the Yth-proteins (YthA, YthB, YthC) and CesS effectively sequesters CesS from interacting with CesR. As YthA is the only Yth-protein that contains the PspC-domain, this is the candidate we hypothesize functions as an antagonist of CesSR, and therefor YthB and YthC are not included in the current model. Upon sensing external stress factors, the YthA-CesS somehow dissociates, possibly due to proteolysis by the membrane anchored protease FtsH, resulting in the activation CesSR. Indeed, uncomplexed PspC is digested by FtsH in both *Y. enterocolitica* and *E. coli* (Singh and Darwin 2011), and this may be the case with the PspC-homologue YthA in *L. lactis* IL1403. They hypothesized that specifically uncomplexed PspC could be deleterious to the cell, as no other phage shock protein undergoes digestion by FtsH. This indicates that FtsH functions as a "clean-up" mechanism after PspC has disassociated from other proteins during stress response in *Y. enterocolitica* and *E. coli*. If this is the case in *L. lactis* IL1403 as well, it raises the question of how FtsH is activated.

As indicated by our present working model, the following three alternatives seem likely, shown in **Figure 4.2**. Either CesS is involved in sensing stress factors which result in direct disassociation from YthA, allowing FtsH to digest any uncomplexed YthA in the membrane. Or, external stress factors are not sensed by CesS directly, rather elsewhere by an unknown mechanism, thus activating FtsH-dependant degradation of YthA in complex with CesS. Alternatively, CesS could somehow be involved in the facilitation of FtsH-dependant degradation of YthA while still in complex with CesS, perhaps by conformational changes in the CesS-YthA induced by an external stress factor. This is an interesting point for future efforts to fully understand the involvement of YthA in the stress response mechanism CesSR.

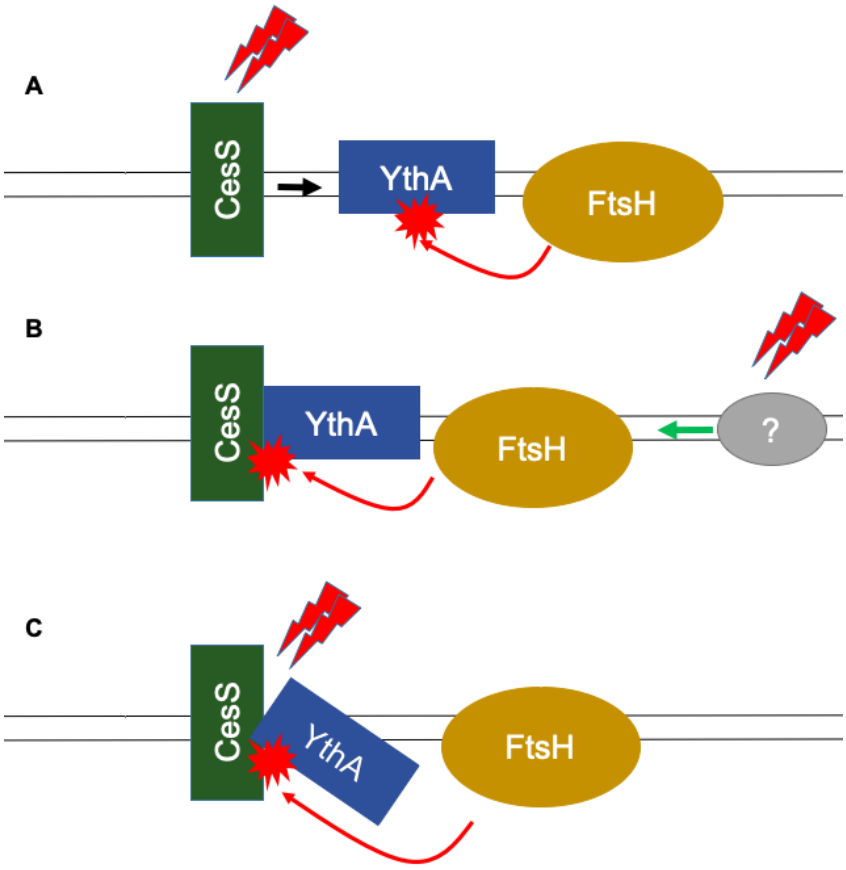

Figure 4.2: Illustration of three hypothesized mechanisms of how CesS-YthA is involved in the sensing of stress. **A** - CesS senses stress factors, illustrated as red lightning bolts, which result in direct disassociation from YthA, allowing FtsH to digest uncomplexed YthA. **B** - Stress factors are sensed by an unknown mechanism, which activates FtsH-dependant degradation of YthA in complex with CesS. **C** - CesS senses stress factors which activates FtsH-dependant degradation of YthA while still in complex with CesS.

4.3 - Concluding remarks and suggested further work

A substantial amount of work in this thesis was dedicated to unravelling the inexplicable results stemming from the contaminated frozen stocks. It would be preferential to perform the gene expression analysis using a *L. lactis* IL1403 strain with loss-of-function mutation in *ythA*, as was intended in this thesis. This would further our understanding of how the phenotype of increased resistance to lysozyme and GarKS affects the expression of CesSR. In the case of lysozyme resistant mutants, it would be intuitive to assume that *spxB* and *oatA* would show a significant upregulation, as these genes has previously been linked to lysozyme resistance in *L. lactis* (Veiga, Bulbarela-Sampieri et al. 2007). It would also be interesting to see if there is a direct correlation between the concentration of the sublethal dose of GarKS and upregulation of CesSR, by subjecting cells to a wider range of GarKS-concentrations. This would give us important information needed to unravel the exact mechanisms that is operating in the cell membrane when sensing stress, and to further deduce how GarKS affects the cells.

Subsequent experiments should also focus on further investigations of the role the Yth-proteins play in the stress response, specifically to find out what other proteins they interact with. If indeed YthA is the substrate of the protease FtsH, as is the case with homologue PspC in *E. coli* and Y*. enterocolitica* (Singh and Darwin 2011), this could be investigated by a technique called substrate trapping (Arends, Thomanek et al. 2016). This technique aims to isolate the targeted enzyme-substrate complex in its transition state. This is achieved by changing the residues within the active site of the enzyme by site-directed mutagenesis in such a way that the binding affinity of the enzyme to its substrate is not lost, while at the same time rendering the catalytic site inert. The transition state complex can then be isolated by a variety of techniques, for example by immunoprecipitation (Blanchetot, Chagnon et al. 2005).

Lastly, as is the case in many similar signalling cascades in bacteria, the complexity of CesSR and the involvement of YthA may still elude us, and unidentified constituents of the stress response mechanism may yet be unknown and uncharacterized. YthA could have multiple binding partners, including YthB and YthC, or function in an entirely different manner than what is hypothesized in this thesis. A full transcriptomic analysis could serve to identify other potentially interesting candidates for further study. However, the involvement of CesSR and YthA in the stress response of *L. lactis* IL1403 subjected to sublethal concentrations of GarKS, seems to be of importance, and should serve as a basis for further studies.

References

Alvarez-Sieiro, P., M. Montalban-Lopez, D. Mu and O. P. Kuipers (2016). "Bacteriocins of lactic acid bacteria: extending the family." Appl Microbiol Biotechnol **100**(7): 2939-2951.

Aprianto, R., J. Slager, S. Holsappel and J. W. Veening (2016). "Time-resolved dual RNA-seq reveals extensive rewiring of lung epithelial and pneumococcal transcriptomes during early infection." Genome Biol **17**(1): 198.

Arends, J., N. Thomanek, K. Kuhlmann, K. Marcus and F. Narberhaus (2016). "In vivo trapping of FtsH substrates by label-free quantitative proteomics." Proteomics **16**(24): 3161-3172.

Aubry, C., C. Goulard, M. A. Nahori, N. Cayet, J. Decalf, M. Sachse, I. G. Boneca, P. Cossart and O. Dussurget (2011). "OatA, a Peptidoglycan O-Acetyltransferase Involved in Listeria monocytogenes Immune Escape, Is Critical for Virulence." Journal of Infectious Diseases **204**(5): 731-740.

Ballal, S. A., P. Veiga, K. Fenn, M. Michaud, J. H. Kim, C. A. Gallini, J. N. Glickman, G. Quere, P. Garault, C. Beal, M. Derrien, P. Courtin, S. Kulakauskas, M. P. Chapot-Chartier, J. van Hylckama Vlieg and W. S. Garrett (2015). "Host lysozyme-mediated lysis of Lactococcus lactis facilitates delivery of colitis-attenuating superoxide dismutase to inflamed colons." Proc Natl Acad Sci U S A **112**(25): 7803-7808.

Bera, A., S. Herbert, A. Jakob, W. Vollmer and F. Gotz (2005). "Why are pathogenic staphylococci so lysozyme resistant? The peptidoglycan O-acetyltransferase OatA is the major determinant for lysozyme resistance of Staphylococcus aureus." Molecular Microbiology **55**(3): 778-787.

Bhate, M. P., K. S. Molnar, M. Goulian and W. F. DeGrado (2015). "Signal transduction in histidine kinases: insights from new structures." Structure **23**(6): 981-994.

Biosystems, A. (2004). Guide to Performing Relative Quantitation of Gene Expression Using Real-Time Quantitative PCR.

Blanchetot, C., M. Chagnon, N. Dube, M. Halle and M. L. Tremblay (2005). "Substrate-trapping techniques in the identification of cellular PTP targets." Methods **35**(1): 44-53.

Boor, K. J. (2006). "Bacterial stress responses: What doesn't kill them can make them stronger." Plos Biology **4**(1): 18-20.

Braat, H., P. Rottiers, D. W. Hommes, N. Huyghebaert, E. Remaut, J. P. Remon, S. J. van Deventer, S. Neirynck, M. P. Peppelenbosch and L. Steidler (2006). "A phase I trial with transgenic bacteria expressing interleukin-10 in Crohn's disease." Clin Gastroenterol Hepatol **4**(6): 754-759.

Bustin, S. A., V. Benes, J. A. Garson, J. Hellemans, J. Huggett, M. Kubista, R. Mueller, T. Nolan, M. W. Pfaffl, G. L. Shipley, J. Vandesompele and C. T. Wittwer (2009). "The MIQE guidelines: minimum information for publication of quantitative real-time PCR experiments." Clin Chem **55**(4): 611-622.

Cassini, A., L. D. Hogberg, D. Plachouras, A. Quattrocchi, A. Hoxha, G. S. Simonsen, M. Colomb-Cotinat, M. E. Kretzschmar, B. Devleesschauwer, M. Cecchini, D. A. Ouakrim, T. C. Oliveira, M. J. Struelens, C. Suetens, D. L. Monnet and A. M. R. C. G. Burden of (2019). "Attributable deaths and disability-adjusted life-years caused by infections with antibiotic-resistant bacteria in the EU and the European Economic Area in 2015: a population-level modelling analysis." Lancet Infect Dis **19**(1): 56-66.

Chapot-Chartier, M. P. and S. Kulakauskas (2014). "Cell wall structure and function in lactic acid bacteria." Microb Cell Fact **13 Suppl 1**: S9.

Chi, H. (2018). Garvicin KS, a bacteriocin with wide inhibitory spectrum and potential application PhD, Norwegian University of Life Siences.

Chikindas, M. L., R. Weeks, D. Drider, V. A. Chistyakov and L. M. Dicks (2018). "Functions and emerging applications of bacteriocins." Curr Opin Biotechnol **49**: 23-28.

Clardy, J., M. A. Fischbach and C. R. Currie (2009). "The natural history of antibiotics." Curr Biol **19**(11): R437-441.

Clarke, A. J. and C. Dupont (1992). "O-acetylated peptidoglycan: its occurrence, pathobiological significance, and biosynthesis." Can J Microbiol **38**(2): 85-91.

Corr, S. C., Y. Li, C. U. Riedel, P. W. O'Toole, C. Hill and C. G. M. Gahan (2007). "Bacteriocin production as a mechanism for the antfinfective activity of Lactobacillus salivarius UCC118." Proceedings of the National Academy of Sciences of the United States of America **104**(18): 7617-7621.

Darwin, A. J. (2007). "Regulation of the phage-shock-protein stress response in Yersinia enterocolitica." Genus Yersinia: From Genomics to Function **603**: 167-177.

DeCoste, N. J., V. J. Gadkar and M. Filion (2011). "Relative and absolute quantitative real-time PCR-based quantifications of hcnC and phlD gene transcripts in natural soil spiked with Pseudomonas sp. strain LBUM300." Appl Environ Microbiol **77**(1): 41-47.

Diep, D. B., M. Skaugen, Z. Salehian, H. Holo and I. F. Nes (2007). "Common mechanisms of target cell recognition and immunity for class II bacteriocins." Proc Natl Acad Sci U S A **104**(7): 2384-2389.

Ducret, A., E. M. Quardokus and Y. V. Brun (2016). "MicrobeJ, a tool for high throughput bacterial cell detection and quantitative analysis." Nat Microbiol **1**(7): 16077.

Egan, K., D. Field, M. C. Rea, R. P. Ross, C. Hill and P. D. Cotter (2016). "Bacteriocins: Novel Solutions to Age Old Spore-Related Problems?" Front Microbiol **7**: 461.

Fallico, V., R. P. Ross, G. F. Fitzgerald and O. McAuliffe (2011). "Genetic response to bacteriophage infection in Lactococcus lactis reveals a four-strand approach involving induction of membrane stress proteins, D-alanylation of the cell wall, maintenance of proton motive force, and energy conservation." J Virol **85**(22): 12032-12042.

Flores-Kim, J. and A. J. Darwin (2012). "Phage Shock Protein C (PspC) of Yersinia enterocolitica Is a Polytopic Membrane Protein with Implications for Regulation of the Psp Stress Response." Journal of Bacteriology **194**(23): 6548-6559.

Ghodhbane, H., S. Elaidi, J. M. Sabatier, S. Achour, J. Benhmida and I. Regaya (2015). "Bacteriocins active against multi-resistant gram negative bacteria implicated in nosocomial infections." Infect Disord Drug Targets **15**(1): 2-12.

Guo, M. S. and C. A. Gross (2014). "Stress-induced remodeling of the bacterial proteome." Curr Biol **24**(10): R424-434.

Gur, E., D. Biran and E. Z. Ron (2011). "Regulated proteolysis in Gram-negative bacteria--how and when?" Nat Rev Microbiol **9**(12): 839-848.

Hassan, M., M. Kjos, I. F. Nes, D. B. Diep and F. Lotfipour (2012). "Natural antimicrobial peptides from bacteria: characteristics and potential applications to fight against antibiotic resistance." J Appl Microbiol **113**(4): 723-736.

Heid, C. A., J. Stevens, K. J. Livak and P. M. Williams (1996). "Real time quantitative PCR." Genome Res **6**(10): 986-994.

Hockett, K. L. and D. A. Baltrus (2017). "Use of the Soft-agar Overlay Technique to Screen for Bacterially Produced Inhibitory Compounds." Jove-Journal of Visualized Experiments(119).

Huang, Y. H., P. Leblanc, V. Apostolou, B. Stewart and R. B. Moreland (1995). "Comparison of Milli-Q PF Plus water to DEPC-treated water in the preparation and analysis of RNA." Biotechniques **19**(4): 656-661.

Kikuchi, M., Y. Yamamoto, Y. Taniyama, K. Ishimaru, W. Yoshikawa, Y. Kaisho and M. Ikehara (1988). "Secretion in yeast of human lysozymes with different specific activities created by replacing valine-110 with proline by site-directed mutagenesis." Proc Natl Acad Sci U S A **85**(24): 9411-9415.

Kjos, M., I. F. Nes and D. B. Diep (2009). "Class II one-peptide bacteriocins target a phylogenetically defined subgroup of mannose phosphotransferase systems on sensitive cells." Microbiology **155**(Pt 9): 2949-2961.

Kjos, M., I. F. Nes and D. B. Diep (2011). "Mechanisms of resistance to bacteriocins targeting the mannose phosphotransferase system." Appl Environ Microbiol **77**(10): 3335-3342.

Kleerebezem, M., W. Crielaard and J. Tommassen (1996). "Involvement of stress protein PspA (phage shock protein A) of Escherichia coli in maintenance of the protonmotive force under stress conditions." Embo Journal **15**(1): 162-171.

Kralik, P. and M. Ricchi (2017). "A Basic Guide to Real Time PCR in Microbial Diagnostics: Definitions, Parameters, and Everything." Front Microbiol **8**: 108.

Kumariya, R., A. K. Garsa, Y. S. Rajput, S. K. Sood, N. Akhtar and S. Patel (2019). "Bacteriocins: Classification, synthesis, mechanism of action and resistance development in food spoilage causing bacteria." Microbial Pathogenesis **128**: 171-177.

Kuroda, M., H. Kuroda, T. Oshima, F. Takeuchi, H. Mori and K. Hiramatsu (2003). "Two-component system VraSR positively modulates the regulation of cell-wall biosynthesis pathway in Staphylococcus aureus." Molecular Microbiology **49**(3): 807-821.

Levison, M. E. and J. H. Levison (2009). "Pharmacokinetics and pharmacodynamics of antibacterial agents." Infect Dis Clin North Am **23**(4): 791-815, vii.

Liu, T., K. Y. Wang, J. Wang, D. F. Chen, X. L. Huang, P. Ouyang, Y. Geng, Y. He, Y. Zhou and J. Min (2016). "Genome Sequence of the Fish Pathogen Yersinia ruckeri SC09 Provides Insights into Niche Adaptation and Pathogenic Mechanism." International Journal of Molecular Sciences **17**(4).

Livak, K. J. and T. D. Schmittgen (2001). "Analysis of relative gene expression data using real-time quantitative PCR and the 2(T)(-Delta Delta C) method." Methods **25**(4): 402-408.

Lopez-Gonzalez, M. J., S. Escobedo, A. Rodriguez, A. R. Neves, T. Janzen and B. Martinez (2018). "Adaptive Evolution of Industrial Lactococcus lactis Under Cell Envelope Stress Provides Phenotypic Diversity." Frontiers in Microbiology **9**.

Madeira, F., Y. M. Park, J. Lee, N. Buso, T. Gur, N. Madhusoodanan, P. Basutkar, A. R. N. Tivey, S. C. Potter, R. D. Finn and R. Lopez (2019). "The EMBL-EBI search and sequence analysis tools APIs in 2019." Nucleic Acids Res.

Martinez, B., T. Bottiger, T. Schneider, A. Rodriguez, H. G. Sahl and I. Wiedemann (2008). "Specific interaction of the unmodified bacteriocin Lactococcin 972 with the cell wall precursor lipid II." Appl Environ Microbiol **74**(15): 4666-4670.

Martinez, B., A. L. Zomer, A. Rodriguez, J. Kok and O. P. Kuipers (2007). "Cell envelope stress induced by the bacteriocin Lcn972 is sensed by the lactococcal two-component system CesSR." Molecular Microbiology **64**(2): 473-486.

Martinez, R. C. R., V. O. Alvarenga, M. Thomazini, C. S. Favaro-Trindade and A. D. Sant'Ana (2016). "Assessment of the inhibitory effect of free and encapsulated commercial nisin (Nisaplin (R)), tested alone and in combination, on Listeria monocytogenes and Bacillus cereus in refrigerated milk." Lwt-Food Science and Technology **68**: 67-75.

Mascher, T., S. L. Zimmer, T. A. Smith and J. D. Helmann (2004). "Antibiotic-inducible promoter regulated by the cell envelope stress-sensing two-component system LiaRS of Bacillus subtilis." Antimicrobial Agents and Chemotherapy **48**(8): 2888-2896.

Mathur, H., D. Field, M. C. Rea, P. D. Cotter, C. Hill and R. P. Ross (2017). "Bacteriocin-Antimicrobial Synergy: A Medical and Food Perspective." Front Microbiol **8**: 1205.

Miljkovic, M., G. Uzelac, N. Mirkovic, G. Devescovi, D. B. Diep, V. Venturi and M. Kojic (2016). "LsbB Bacteriocin Interacts with the Third Transmembrane Domain of the YvjB Receptor." Appl Environ Microbiol **82**(17): 5364-5374.

Mortazavi, A., B. A. Williams, K. McCue, L. Schaeffer and B. Wold (2008). "Mapping and quantifying mammalian transcriptomes by RNA-Seq." Nat Methods **5**(7): 621-628.

Oscariz, J. C. and A. G. Pisabarro (2001). "Classification and mode of action of membrane-active bacteriocins produced by gram-positive bacteria." Int Microbiol **4**(1): 13-19.

Ovchinnikov, K. V., H. Chi, I. Mehmeti, H. Holo, I. F. Nes and D. B. Diep (2016). "Novel Group of Leaderless Multipeptide Bacteriocins from Gram-Positive Bacteria." Appl Environ Microbiol **82**(17): 5216-5224.

Perez, R. H., T. Zendo and K. Sonomoto (2014). "Novel bacteriocins from lactic acid bacteria (LAB): various structures and applications." Microb Cell Fact **13 Suppl 1**: S3.

Pfeffer, J. M., H. Strating, J. T. Weadge and A. J. Clarke (2006). "Peptidoglycan O acetylation and autolysin profile of Enterococcus faecalis in the viable but nonculturable state." J Bacteriol **188**(3): 902-908.

Pinto, J. P., O. P. Kuipers, R. K. Marreddy, B. Poolman and J. Kok (2011). "Efficient overproduction of membrane proteins in Lactococcus lactis requires the cell envelope stress sensor/regulator couple CesSR." PLoS One **6**(7): e21873.

Ponchel, F., C. Toomes, K. Bransfield, F. T. Leong, S. H. Douglas, S. L. Field, S. M. Bell, V. Combaret, A. Puisieux, A. J. Mighell, P. A. Robinson, C. F. Inglehearn, J. D. Isaacs and A. F. Markham (2003). "Real-time PCR based on SYBR-Green I fluorescence: an alternative to the TaqMan assay for a relative quantification of gene rearrangements, gene amplifications and micro gene deletions." BMC Biotechnol **3**: 18.

Riley, M. A. and J. E. Wertz (2002). "Bacteriocins: evolution, ecology, and application." Annu Rev Microbiol **56**: 117-137.

Roces, C., A. B. Campelo, P. Veiga, J. P. Pinto, A. Rodriguez and B. Martinez (2009). "Contribution of the CesR-regulated genes llmg0169 and llmg2164-2163 to Lactococcus lactis fitness." Int J Food Microbiol **133**(3): 279-285.

Ruggirello, M., P. Dolci and L. Cocolin (2014). "Detection and viability of Lactococcus lactis throughout cheese ripening." PLoS One **9**(12): e114280.

Silva, C. C. G., S. P. M. Silva and S. C. Ribeiro (2018). "Application of Bacteriocins and Protective Cultures in Dairy Food Preservation." Front Microbiol **9**: 594.

Singh, S. and A. J. Darwin (2011). "FtsH-Dependent Degradation of Phage Shock Protein C in Yersinia enterocolitica and Escherichia coli." Journal of Bacteriology **193**(23): 6436-6442.

Solopova, A., C. Formosa-Dague, P. Courtin, S. Furlan, P. Veiga, C. Pechoux, J. Armalyte, M. Sadauskas, J. Kok, P. Hols, Y. F. Dufrene, O. P. Kuipers, M. P. Chapot-Chartier and S. Kulakauskas (2016). "Regulation of Cell Wall Plasticity by Nucleotide Metabolism in Lactococcus lactis." J Biol Chem **291**(21): 11323-11336.

Song, A. A., L. L. A. In, S. H. E. Lim and R. A. Rahim (2017). "Erratum to: A review on Lactococcus lactis: from food to factory." Microb Cell Fact **16**(1): 139.

Stothard, P. (2000). "The sequence manipulation suite: JavaScript programs for analyzing and formatting protein and DNA sequences." Biotechniques **28**(6): 1102, 1104.

Tagg, J. R., A. S. Dajani and L. W. Wannamaker (1976). "Bacteriocins of gram-positive bacteria." Bacteriol Rev **40**(3): 722-756.

Tan, S. C. and B. C. Yiap (2013). "DNA, RNA, and Protein Extraction: The Past and the Present (vol 2009, 574398, 2009)." Biomed Research International.

Telke, A. A., K. V. Ovchinnikov, K. S. Vuoristo, G. Mathiesen, T. Thorstensen and D. B. Diep (2019). "Over 2000-Fold Increased Production of the Leaderless Bacteriocin Garvicin KS by Increasing Gene Dose and Optimization of Culture Conditions." Front Microbiol **10**: 389.

Toni, L. S., A. M. Garcia, D. A. Jeffrey, X. Jiang, B. L. Stauffer, S. D. Miyamoto and C. C. Sucharov (2018). "Optimization of phenol-chloroform RNA extraction." MethodsX **5**: 599-608.

Ulve, V. M., C. Monnet, F. Valence, J. Fauquant, H. Falentin and S. Lortal (2008). "RNA extraction from cheese for analysis of in situ gene expression of Lactococcus lactis." J Appl Microbiol **105**(5): 1327-1333.

van der Meulen, S. B., A. de Jong and J. Kok (2016). "Transcriptome landscape of Lactococcus lactis reveals many novel RNAs including a small regulatory RNA involved in carbon uptake and metabolism." RNA Biol **13**(3): 353-366.

Veiga, P., C. Bulbarela-Sampieri, S. Furlan, A. Maisons, M. P. Chapot-Chartier, M. Erkelenz, P. Mervelet, P. Noirot, D. Frees, O. P. Kuipers, J. Kok, A. Gruss, G. Buist and S.

Kulakauskas (2007). "SpxB regulates O-acetylation-dependent resistance of Lactococcus lactis peptidoglycan to hydrolysis." J Biol Chem **282**(27): 19342-19354.

Vollmer, W., D. Blanot and M. A. de Pedro (2008). "Peptidoglycan structure and architecture." FEMS Microbiol Rev **32**(2): 149-167.

Watkins, N. E., Jr. and J. SantaLucia, Jr. (2005). "Nearest-neighbor thermodynamics of deoxyinosine pairs in DNA duplexes." Nucleic Acids Res **33**(19): 6258-6267.

Woods, C. R., J. Versalovic, T. Koeuth and J. R. Lupski (1993). "Whole-cell repetitive element sequence-based polymerase chain reaction allows rapid assessment of clonal relationships of bacterial isolates." J Clin Microbiol **31**(7): 1927-1931.

World Health Organization (2014). Antimicrobial resistance : global report on surveillance. Geneva, Switzerland, World Health Organization.

Wu, H., J. Liu, S. Miao, Y. Zhao, H. Zhu, M. Qiao, P. E. J. Saris and J. Qiao (2018). "Contribution of YthA, a PspC Family Transcriptional Regulator of Lactococcus lactis F44 Acid Tolerance and Nisin Yield: a Transcriptomic Approach." Appl Environ Microbiol **84**(6).

Yadav, A. K., A. Espaillat and F. Cava (2018). "Bacterial Strategies to Preserve Cell Wall Integrity Against Environmental Threats." Front Microbiol **9**: 2064.

Yang, S. C., C. H. Lin, C. T. Sung and J. Y. Fang (2014). "Corrigendum: Antibacterial activities of bacteriocins: application in foods and pharmaceuticals." Front Microbiol **5**: 683.

Yocum, R. R., J. R. Rasmussen and J. L. Strominger (1980). "The mechanism of action of penicillin. Penicillin acylates the active site of Bacillus stearothermophilus D-alanine carboxypeptidase." J Biol Chem **255**(9): 3977-3986.

Zhu, M. L. and X. F. Dai (2018). "High Salt Cross-Protects Escherichia coli from Antibiotic Treatment through Increasing Efflux Pump Expression (vol 3, e00095-18, 2018)." Msphere **3**(3).

Appendix

A.1 - Calculations of fold change values from qPCR runs

From the qPCR sample runs, the StepOne Software v2.3 calculated mean C_t values from the four replicates as well as the mean standard deviation (SD), shown in **Table A.1.1**, along with calculated variance. These values were used in the calculations outlined below.

Table A.1.1: Raw data from the qPCR sample runs showing mean C_t values from four replicates, mean standard deviation from the same replicates and variance. Mean C_t values and mean standard deviation was calculated by the software. *Values for the reference gene *gyrA* is included but was not used in any calculations due to unstable levels of transcription.

Mean C_t values

	ythA	***ythB***	***ythC***	***ftsH***	***spxB***	***oatA***	***cesS***	***cesR***	***tuf***	***gyrA****
B1545	*24,7110*	*23,2513*	*23,5578*	*20,7943*	*22,8364*	*25,7837*	*23,5641*	*22,5400*	*18,9810*	*18,0036*
LMGT 3870	*23,8289*	*22,1787*	*22,1979*	*19,4554*	*21,1480*	*24,1637*	*22,9084*	*21,7800*	*17,4803*	*16,7819*
B1545 + 0.1 MIC	*23,5633*	*21,7488*	*22,0899*	*20,4311*	*21,4449*	*23,7907*	*22,8660*	*22,0240*	*18,9438*	*17,5365*
B1545 + 0.5 MIC	*22,6674*	*21,1609*	*21,5665*	*19,9260*	*20,7628*	*23,3050*	*22,5812*	*21,3923*	*18,9237*	*16,8288*

Mean standard deviation

	ythA	***ythB***	***ythC***	***ftsH***	***spxB***	***oatA***	***cesS***	***cesR***	***tuf***	***gyrA****
B1545	*0,0417*	*0,0510*	*0,1131*	*0,0981*	*0,0356*	*0,1168*	*0,0634*	*0,1184*	*0,0619*	*0,1262*
LMGT 3870	*0,0900*	*0,0879*	*0,0823*	*0,0779*	*0,0680*	*0,0887*	*0,0498*	*0,1310*	*0,1913*	*0,1250*
B1545 + 0.1 MIC	*0,0750*	*0,0701*	*0,0798*	*0,1707*	*0,1186*	*0,1639*	*0,0499*	*0,1088*	*0,0315*	*0,0442*
B1545 + 0.5 MIC	*0,1211*	*0,1858*	*0,1482*	*0,0832*	*0,0908*	*0,0743*	*0,0758*	*0,0588*	*0,2078*	*0,1127*

Variance (SD^2)

	ythA	***ythB***	***ythC***	***ftsH***	***spxB***	***oatA***	***cesS***	***cesR***	***tuf***	***gyrA****
B1545	*0,0017*	*0,0026*	*0,0128*	*0,0096*	*0,0013*	*0,0136*	*0,0040*	*0,0140*	*0,0038*	*0,0159*
LMGT 3870	*0,0081*	*0,0077*	*0,0068*	*0,0061*	*0,0046*	*0,0079*	*0,0025*	*0,0172*	*0,0366*	*0,0156*
B1545 + 0.1 MIC	*0,0056*	*0,0049*	*0,0064*	*0,0291*	*0,0141*	*0,0269*	*0,0025*	*0,0118*	*0,0010*	*0,0020*
B1545 + 0.5 MIC	*0,0147*	*0,0345*	*0,0220*	*0,0069*	*0,0082*	*0,0055*	*0,0057*	*0,0035*	*0,0432*	*0,0127*

The process of calculating relative fold change in expression levels using the Livak method can be divided into three steps:

First the C_t value of the target gene must be normalized to the C_t value of the reference gene, resulting in a ΔC_t value for each test sample (LMGT 3870, B1545 +0.1 MIC and B1545 +0.5 MIC) and the calibrator sample (untreated wild type). Using the C_t values from **Table A.1.1**, the C_t value of the reference gene, *tuf,* was subtracted from the individual C_t values of the target genes for each sample. This results in a ΔC_t value for all target genes in all samples, shown in **Table A.1.2,** section 1. Associated SD for each value is shown in **Table A.1.2,** section 2.

Second the ΔC_t value of the test sample must be normalized to the ΔC_t of the calibrator sample, resulting in a $\Delta\Delta C_t$ value. Using the ΔC_t values from **Table A.1.2,** section 1, the individual ΔC_t values of the test samples were subtracted from the ΔC_t value of the calibrator sample. This results in a $\Delta\Delta C_t$ value for all test samples, calculated values can be seen in **Table A.1.2,** section 3.

The third step is then to calculate the fold difference in expression between the test sample and the calibrator. This was done by first calculating the interval of $\Delta\Delta C_t$ values that results from subtracting and adding the associated SD. The $\Delta\Delta C_t$ values minus associated SD are shown in **Table A.1.2**, section 4, and the $\Delta\Delta C_t$ values plus associated SD are shown in **Table A.1.2**, section 5. The negative of these $\Delta\Delta C_t$ values +/- associated SD was then squared to give an interval of fold change in the expression level of each gene compared to the wild type, given in **Table 3.7** in the Results.

Table A.1.2: Calculations of the fold change in expression for the genes tested, using the housekeeping gene *tuf* as a reference. Values from **Table A.1.1** in appendix section A.1 was used in these calculations.

Section 1	**ΔC_t values** (C_t value for target gene - C_t value for reference gene)							
	ythA	***ythB***	***ythC***	***ftsH***	***spxB***	***oatA***	***cesS***	***cesR***
ΔCt (B1545)	*5,7299*	*4,2703*	*4,5767*	*1,8133*	*3,8554*	*6,8026*	*4,5830*	*3,5590*
ΔCt (LMGT 3870)	*6,3486*	*4,6984*	*4,7177*	*1,9751*	*3,6678*	*6,6835*	*5,4282*	*4,2997*
ΔCt (B1545 + 0.1 MIC)	*4,6195*	*2,8049*	*3,1460*	*1,4873*	*2,5011*	*4,8469*	*3,9222*	*3,0802*
ΔCt (B1545 + 0.5 MIC)	*3,7437*	*2,2373*	*2,6428*	*1,0023*	*1,8392*	*4,3814*	*3,6575*	*2,4686*

Section 2	**Associated standard deviation** ((SD (target gene) - SD (*tuf*))^0.5)							
	ythA	***ythB***	***ythC***	***ftsH***	***spxB***	***oatA***	***cesS***	***cesR***
ΔC_t B1545	*0,0746*	*0,0802*	*0,1289*	*0,1160*	*0,0714*	*0,1321*	*0,0886*	*0,1336*
ΔC_t LMGT 3870	*0,1092*	*0,1075*	*0,1030*	*0,0995*	*0,0919*	*0,1081*	*0,0795*	*0,1449*
ΔC_t B1545 + 0.1 MIC	*0,0972*	*0,0935*	*0,1010*	*0,1815*	*0,1338*	*0,1752*	*0,0795*	*0,1252*
ΔC_t B1545 + 0.5 MIC	*0,1360*	*0,1958*	*0,1606*	*0,1037*	*0,1099*	*0,0967*	*0,0979*	*0,0854*

Section 3	**$\Delta\Delta C_t$ values** (ΔC_t (sample) - ΔC_t (B1545))							
	ythA	***ythB***	***ythC***	***ftsH***	***spxB***	***oatA***	***cesS***	***cesR***
$\Delta\Delta C_t$ (LMGT 3870)	*0,6187*	*0,4281*	*0,1409*	*0,1619*	*-0,1876*	*-0,1192*	*0,8452*	*0,7407*
$\Delta\Delta C_t$ (B1545 + 0.1 MIC)	*-1,1104*	*-1,4654*	*-1,4307*	*-0,3260*	*-1,3543*	*-1,9558*	*-0,6608*	*-0,4788*
$\Delta\Delta C_t$ (B1545 + 0.5 MIC)	*-1,9862*	*-2,0330*	*-1,9339*	*-0,8110*	*-2,0162*	*-2,4213*	*-0,9255*	*-1,0904*

Section 4	**$\Delta\Delta C_t$ values - standard deviation**							
	ythA	***ythB***	***ythC***	***ftsH***	***spxB***	***oatA***	***cesS***	***cesR***
$\Delta\Delta C_t$ (LMGT 3870)	*0,5095*	*0,3206*	*0,0379*	*0,0624*	*-0,2795*	*-0,2273*	*0,7657*	*0,5958*
$\Delta\Delta C_t$ (B1545 + 0.1 MIC)	*-1,2077*	*-1,5589*	*-1,5317*	*-0,5075*	*-1,4881*	*-2,1310*	*-0,7403*	*-0,6040*
$\Delta\Delta C_t$ (B1545 + 0.5 MIC)	*-2,1222*	*-2,2288*	*-2,0945*	*-0,9147*	*-2,1260*	*-2,5180*	*-1,0234*	*-1,1758*

Section 5	**$\Delta\Delta C_t$ values + standard deviation**							
	ythA	***ythB***	***ythC***	***ftsH***	***spxB***	***oatA***	***cesS***	***cesR***
$\Delta\Delta C_t$ (LMGT 3870)	*0,7278*	*0,5356*	*0,2439*	*0,2613*	*-0,0957*	*-0,0111*	*0,9246*	*0,8856*
$\Delta\Delta C_t$ (B1545 + 0.1 MIC)	*-1,0132*	*-1,3719*	*-1,3297*	*-0,1444*	*-1,2205*	*-1,7805*	*-0,5813*	*-0,3537*
$\Delta\Delta C_t$ (B1545 + 0.5 MIC)	*-1,8503*	*-1,8372*	*-1,7734*	*-0,7073*	*-1,9063*	*-2,3246*	*-0,8277*	*-1,0050*

A.2 - Primers used in PCR reactions

Table A.2.1: Sequences of the forward and reverse primers used in PCR reactions. Also listed are the expected amplicon size as well as T_m used in the PCR program. *For empty plasmid as size varies according to insert in vector. **I = Inosine. ***Fragment size of *ythA* from wild type *L. lactis* IL 1403.

Target	Sequence forward	Sequence reverse	Amplicon length	T_m
16S	5´ - TAACACATGCAAGTCGAACG - 3´	5´ - ACGGGCGGTGTGTRC - 3´	1356 bp	58 °C
PMG36e	5´- GGTCGATCGAATTCGGTCCTC -3´	5´ - ATAAGCAAAAGGCAGCTGATCTC - 3´	405 bp*	60 °C
ythA	5´- GTGATTGCGAGTCTATTGATGAC-3´	5´ - ATATAGGAGGCCAGTTTTTGGTC - 3´	635 bp***	60 °C
REP	5´- IIIICGICGICATCIGGC -3´**	5´ - ICGICTTATCIGGCCTAC - 3´**	Variable	41 °C

Table A.2.2: Sequences of the forward and reverse primers designed for the qPCR reactions. Also listed are the expected amplicon size for each primer pair and the specific T_m calculated when designing them.

Target	Sequence forward	Sequence reverse	Amplicon length	T_m
ythA	5´ - GGGCGGATTGATTCCATTGTA - 3´	5´ - ATCTTCATAACGACGTGCCCA - 3´	196 bp	62 °C
ythB	5´ - AAACTCTGAAAAGATCAAGTAGCA - 3´	5´ - AACCTTGTGACGGTGTCATC - 3´	192 bp	64 °C
ythC	5´ - GTAATGATGGCACGAATTCAGA - 3´	5´ - ACCAAGCCCAAACTTTCTGGT - 3´	202 bp	62 °C
ftsH	5´ - CAAGGATATCCAAAATGCAGCT - 3´	5´ - AGCACGAGATTTACCGAAGGA - 3´	205 bp	62 °C
spxB	5´ - CTGAGTGCGTTACCAGTTGGT - 3´	5´ - GCTCCGTCGAAATTTGATCCA - 3´	204 bp	64 °C
oatA	5´ - CTTTATGCCTGCTCAAGGGAC - 3´	5´ - CAAGTACCTTAGCTTCAGCGA - 3´	213 bp	64 °C
cesS	5´ - CTGAATCTCCTGAATTACAAGCT - 3´	5´ - AAATTTGGTGTCGAACCAGCA - 3´	211 bp	64 °C
cesR	5´ - CGAAGTGGTTGGTGAAGCTG - 3´	5´ - TCCAGCAGCTAAAGCCGGA - 3´	211 bp	62 °C
tuf	5´ - CCACAAACTCGTGAACACATC - 3´	5´ - GTGGTTCACCGTTCAAAGCA - 3´	211 bp	62 °C
gyrA	5´ - TTGGTTCAATGGACGGTGAC - 3´	5´ - CCCAACGGCAATCCCTGTG - 3´	206 bp	62 °C

A.3 - Growth media and solutions

M17 broth

Made by dissolving 36.15 g of M17 powder (Formedium™) in Milli-Q water and bringing final volume to 1000 ml. The solution was then autoclaved.

40 % Glucose

Made by dissolving 40 g of glucose (VWR chemicals) in Milli-Q water and bringing final volume to 100 ml. The solution was then autoclaved.

GM17

Made by adding 10 ml of sterile 40 % glucose (VWR chemicals) to 1000 ml M17 broth.

LB broth

Made by dissolving 10 g of Tryptone (Oxoid), 5 g of Yeast extract (Oxoid) and 10 g of Sodium Chloride (VWR Chemicals) in Milli-Q water and bringing final volume to 1000 ml. The solution was then autoclaved.

GM17 agar plates

Made by adding 7.5 g of UltraPure™ agarose (Invitrogen) to 500 ml of M17 broth. The solution was then autoclaved, before adding 5 ml sterile 40 % glucose, along with appropriate selection if needed, with magnetic stirring. Approximately 25 ml was poured in each petri dish in a sterile flow hood and stored at 4 °C in a sealed plastic bag until use.

GM17 soft agar

Made by adding 0.8 g of UltraPure™ agarose (Invitrogen) to 100 ml of M17 broth. The solution was then autoclaved, before adding 1 ml of sterile 40 % glucose.

10 x TBE

Made by dissolving 108 g of Trizma® base (Sigma-Aldrich), 55 g of boric acid (Merck) and 9.3 g of EDTA (Merck) in Milli-Q water and bringing final volume to 1000 ml.

1 x PBS

Made by dissolving 8.0 g of NaCl (VWR Chemicals), 0.2 g of KCl (Merck), 1.44 g of Na_2HPO_4 (VWR Chemicals) and 0.24 g of KH_2PO_4 (Merck) in Milli-Q water. pH was adjusted to 7.4 with HCL (VWR Chemicals), before bringing final volume to 1000 ml.

Phenol:chloroform mixture

Made by adding equal parts of phenol (Sigma-Aldrich) and chloroform (Merck). The solution was stored at room temperature with the flask covered with aluminium foil.

3 M Sodium acetate

Made by dissolving 24.6 g of Sodium Acetate (Sigma-Aldrich) in DEPC-treated Milli-Q water and bringing final volume to 100 ml. The solution was then autoclaved.

TE buffer

Made by mixing 1 ml of 1 M Trisma® base* (Merck) and 0.1 ml of 1 M EDTA** (Sigma-Aldrich) and bringing final volume to 100 ml using DEPC-treated Milli-Q water.
*1 M Trisma® base was made dissolved 1.21 g in DEPC-treated Milli-Q water and bringing final volume to 10 ml.
**1 M EDTA was made dissolved 2.92 g in DEPC-treated Milli-Q water and bringing final volume to 10 ml.

1 M Sucrose

Made by dissolving 342.3 g of sucrose (Sigma-Aldrich) in Milli-Q water and bringing final volume to 1000 ml. The solution was then autoclaved.

SGM17

Made by adding equal parts of 2 x GM17 and 1 M sucrose.

SGM17MC

Made by adding equal parts of 2 x GM17 and 1 M sucrose, then adding 200 µl of 2 M $MgCl_2$* and 200 µl of 200 mM $CaCl_2$**. Milli-Q water was added to a final volume of 20 ml.

*2 M $MgCl_2$ was made by dissolving 40.66 g of $MgCl_2$ (Sigma-Aldrich) in Milli-Q water and bringing final volume to 100 ml.

**200 mM $CaCl_2$ was made by dissolving 2.22 g $CaCl_2$ (Merch) in Milli-Q water and bringing final volume to 100 ml.

Table A.3.1: Dilution series of glycine used to generate competent cells for electroporation.

Glycine concentration (%)	SGM17 (ml)	20 % glycine (µl)
1.0	*9.5*	*500*
1.2	*9.4*	*600*
1.4	*9.3*	*700*
1.6	*9.2*	*800*
1.8	*9.1*	*900*
2.0	*9.0*	*1000*

A.4 - Protocol for TEM imaging

This work was performed by our colleagues at INRA, France. As such the protocol is included here in the appendix, based on their previous work (Solopova, Formosa-Dague et al. 2016).

Transmission electron microscopy - Pellets of bacteria were fixed using 2 % glutaraldehyde in 0.1 M Na cacodylate buffer pH 7.2, for 3 hours at RT. Samples were contrasted with Oolong Tea Extract (OTE) 0.5% in cacodylate buffer, fixed with 1% osmium tetroxide that contained 1.5% potassium cyanoferrate, gradually dehydrated in ethanol (30% to 100%), substituted gradually in a mixture of propylene oxide-epon, and embedded in Epon (Delta microscopie, Labège, France). Thin (70 nm) sections were collected onto 200 mesh copper grids, and counterstained with lead citrate. Grids were examined using a Hitachi HT7700 electron microscope operated at 80kV (Elexience, France). Images were acquired with a charge-coupled device camera (AMT).

A.5 - Testing qPCR primers with gDNA from LMGT 3876

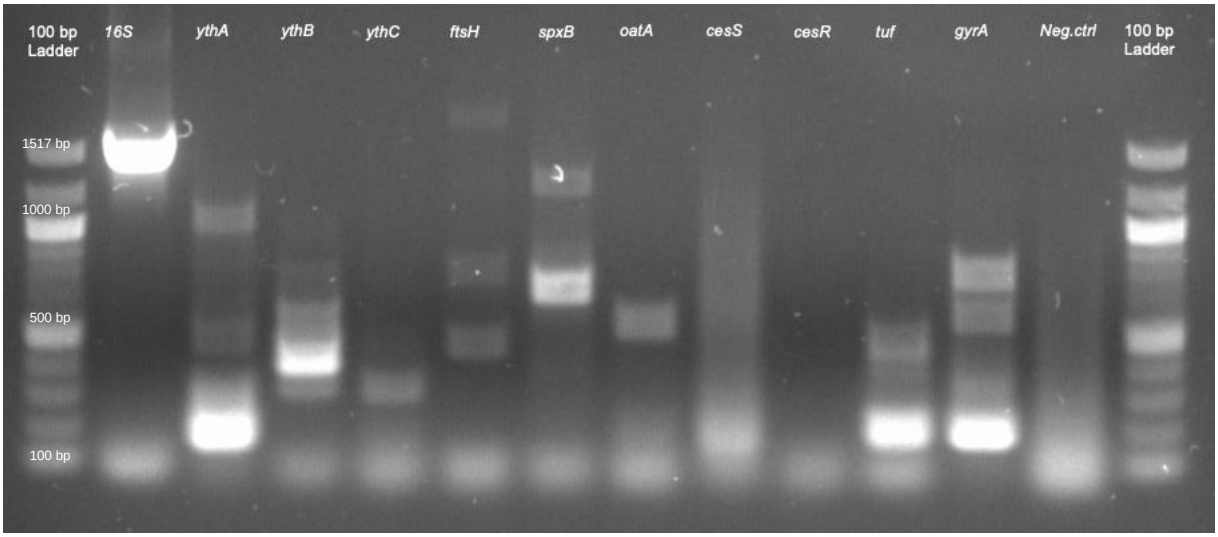

Figure A.5.1: Results of PCR with LMGT 3876 gDNA as template, using all the different qPCR primers and the 16S rRNA primers as a positive control. Sporadic and highly unspecific amplification explains problems encountered during qPCR sample runs. Negative control was run without primers. A 100 bp DNA ladder (NEB) was used as a reference, all amplicons were expected to be in approximately 200 bp.

A.6 - Sequence data

Sequence of *ythA* in wild type and the two mutants investigated in this study.

> B1545_*ythA*_forward (Wild type)

ATGTCTCAAAGACAATTAACAAAATCAGTGACAAATCGTAGAGTCAGTGGTGTCATTGCAGGGATT
GCAGAATATTTTGGTCTGGGTCGTGATGTTGTGACGATTCTACGTATCCTATTTGTTGTTCTGGCT
TTTGGAAGCTGGGGCGGATTGATTCCATTGTATTTCGTAGCAAGTTGGATTATTCCAAGTGCTAG
ACCACGAAATTACTATGATGATTCAGAAGATGATTATCAAGAAAAATGGAATCGTAAAGCGCAACA
TTTTGATGAAAAAATGGATCGTTGGTCAGAACGTTATTCAGATAAAATGAATAATTGGGCACGTCG
TTATGAAGATAAAGGACGTCAAAATCAACAAGATTCAAACCAATGGGGAAATCCATGGGATGAAC
CAAAAAGTCGTAAGACTAAGGAAGCACAACCAGTTGAAAAAGAAAAAGAAGATGACTGGTCAGAT
TTC

> LMGT_3870_*ythA*_forward (Substitution mutation marked in gray)

ATGTCTCAAAGACAATTAACAAAATCAGTGACAAATCGTAGAGTCAGTGGTGTCATTGCAGAGATT
GCAGAATATTTTGGTCTGGGTCGTGATGTTGTGACGATTCTACGTATCCTATTTGTTGTTCTGGCT
TTTGGAAGCTGGGGCGGATTGATTCCATTGTATTTCGTAGCAAGTTGGATTATTCCAAGTGCTAG
ACCACGAAATTACTATGATGATTCAGAAGATGATTATCAAGAAAAATGGAATCGTAAAGCGCAACA
TTTTGATGAAAAAATGGATCGTTGGTCAGAACGTTATTCAGATAAAATGAATAATTGGGCACGTCG
TTATGAAGATAAAGGACGTCAAAATCAACAAGATTCAAACCAATGGGGAAATCCATGGGATGAAC
CAAAAAGTCGTAAGACTAAGGAAGCACAACCAGTTGAAAAAGAAAAAGAAGATGACTGGTCAGAT
TTC

> LMGT_3876_*ythA*_forward (Sequence duplication marked in Grey)

ATGTCTCAAAGACAATTAACAAAATCAGTGACAAATCGTAGAGTCAGTGGTGTCATTGCAGGGATT
GCAGAATATTTTGGTCTGGGTCGTGATGTTGTGACGATTCTACGTATCCTATTTGTTGTTCTGGCT
TTTGGAAGCTGGGGCGGATTGATTCCATTGTATTTCGTAGCAAGTTGGATTATTCCAAGTGCTAG
ACCACGAAATTACTATGATGATTCAGAAGATGATTATCAAGAAAAATGGAATCGTAAAGCGCAACA
TTTTGATGAAAAAATGGATCGTTGGTCAGAACGTTATTCAGATAAAATGAATAATTGGGCACGTCG
TTATGAAGATAAAGGACGTCAAAATCAACAAGATTCAAACCAATGGGGAAATCCATGGGATGAAC
CAAAAAGTCGTAAGACTTAAGACTAAGGAAGCACAACCAGTTGAAAAAGAAAAAGAAGATGACTG
GTCAGATTTC

Protein sequences of the three peptides that make up the bacteriocin GarKS, as ordered from (Pepmic Co., LTD, China)

GakA - 34 amino acid residues

MGAIIKAGAKIVGKGVLGGGASWLGWNVGEKIWK

GakB - 34 amino acid residues

MGAIIKAGAKIIGKGLLGGAAGGATYGGLKKIFG

GakC - 32 amino acid residues

MGAIIKAGAKIVGKGALTGGGVWLAEKLFGGK

Norges miljø- og biovitenskapelige universitet
Noregs miljø- og biovitskapelege universitet
Norwegian University of Life Sciences

Postboks 5003
NO-1432 Ås
Norway